FROM NONRADIATING SOURCES TO DIRECTIONALLY INVISIBLE OBJECTS

by

Elisa Hurwitz

A dissertation submitted to the faculty of
The University of North Carolina at Charlotte
in partial fulfillment of the requirements
for the degree of Doctor of Philosophy in
Optical Science and Engineering

Charlotte

2017

Approved by:

_____
Dr. Greg Gbur

_____
Dr. Thomas Suleski

_____
Dr. Michael Fiddy

_____
Dr. Shaozhong Deng

ABSTRACT

ELISA HURWITZ. From nonradiating sources to directionally invisible objects.
(Under the direction of DR. GREG GBUR)

The goal of this dissertation is to extend the understanding of invisible objects, in particular nonradiating sources and directional nonscattering scatterers. First, variations of null-field nonradiating sources are derived from Maxwell's equations. Next, it is shown how to design a nonscattering scatterer by applying the boundary conditions for nonradiating sources to the scalar wave equation, referred to here as the "field cloak method." This technique is used to demonstrate directionally invisible scatterers for an incident field with one direction of incidence, and the influence of symmetry on the directionality is explored. This technique, when applied to the scalar wave equation, is extended to show that a directionally invisible object may be invisible for multiple directions of incidence simultaneously. This opens the door to the creation of optically switchable, directionally invisible objects which could be implemented in couplers and other novel optical devices. Next, a version of the "field cloak method" is extended to the Maxwell's electro-magnetic vector equations, allowing more flexibility in the variety of directionally invisible objects that can be designed. This thesis concludes with examples of such objects and future applications.

ACKNOWLEDGMENTS

Many people have contributed directly and indirectly to the success of this work. First, of all I would like to thank my advisor Dr. Greg Gbur giving me the chance to do my doctoral work under him. I appreciate very much the opportunity to study invisibility and how he very patiently advised me on how to solve problems from a theoretical perspective; without his guidance none of the work in this thesis would have come to fruition.

I also would like to thank my office mate Matt Smith for listening attentively while I explained to him my approach to writing some of the algorithms, so that I could find my flaws. He claimed he could easily be replaced by a cardboard cut-out of himself, but it really helped me to explain those subjects to the living version of himself. My group mate W. Scott Raburn also helped me thoroughly understand the electromagnetic wave equation for the general scattering case. We also had many fruitful discussions about simulating the general electromagnetic vector case, and I am certain that it might have taken me much longer to find the errors in my code without our discussions. Of course all of us enjoyed many hot chocolates and lunches together.

I also would like to thank my family for their support. My husband, Dr. Stephen Thomas Russell, always encouraged me and tried to do everything within his power to make my life easier. I also thank my daughter, Ana, for constantly entertaining me and forcing me to take breaks. I would like to thank my parents, Nilse Quercia Hurwitz and Dr. William Eliot Hurwitz, for their support and ensuring that I fre-

quently visit classical music concerts and operas to take breaks. Had my parents not sent me to such rigorous schools in my youth, I may not have had the discipline and the versatility to look at this problem from different perspectives. I also would thank my close friends Katalin Hardi and Dr. Robert Hardi for their advice and support.

I never would have been able to begin this work without the help of Dr. Angela Davies, and the remaining members of the Department of Optical Science and Engineering admission's committee, Dr. Boreman, Dr. Tsinghua Her, and Dr. Farahi, for accepting me into this program on short notice and Dr. Katherine Hall-Hertel for helping to facilitate the transfer. I would like to thank the Graduate School for supporting me with the GASP scholarship for 5 years of the program.

Without the care of Dr. Karen Blackwelder from the UNC Charlotte Student Health Center, I might have been forced to drop out of this program. She did her best restore my health as quickly as possible whenever I caught something. My classmates in the optics program and other inhabitants of Grigg Hall were great company and, naturally, another source of moral support. These include Nassim Habibi, Ravil Bikmetov, Mahsa Farsad, Farzaneh Abolamali, Gelareh Babbaie, Zahrah Hosseini, Jason Marmon, Babar Hussain, Kyle, and Nitish Chandra.

I also would like to thank the UNC Charlotte Facilities staff for keeping the building and, especially, my office impeccably clean. They were extremely friendly, helpful, and cheerful, and generous. Thank you for the many invitations to lunch. Special thanks to Rochelle Marrow, Lila Bonilla, Marcos Gutierrez, and Gladys Baquero. I will miss all of you very much!

TABLE OF CONTENTS

LIST OF FIGURES

CHAPTER 1: INTRODUCTION

1.1 Overview

Invisibility has been a subject of science fiction throughout the ages, but only in the last century has it also developed into a science. Whereas most invisibility theories begin by manipulating material parameters, here, we approach the invisibility problem by building on the monochromatic theory of nonradiating sources described by the wave equation to develop a new theory of nonscattering scatterers. Section 1.3 reviews Maxwell's equations, upon which all theories presented here are based. In Chapter 2, variations of null-field nonradiating sources are derived from Maxwell's equations, building on Ehrenfest's 1910 invisibility theory. These types of nonradiating sources cannot be designed using transformation optics, and, therefore, this thesis extends the theory of invisible objects. In Chapter 3, scalar scattering theory is reviewed, and the figures of merit are introduced. One connection between the source equations and the scattering equations is introduced in the scalar domain and developed for the electromagnetic case, resulting in new scattering equations for the fields other than the electric field. In Chapter 4, a new method, "field cloak method," developed by Greg Gbur is derived, demonstrating how to design a nonscattering scatterer by applying the boundary conditions for nonradiating sources to the scalar wave equation. This technique is used to demonstrate directionally invisible scatterers

for an incident field with one direction of incidence, and the influence of symmetry on the directionality is explored. The origin of directional invisibility is revealed through a proof. In Chapter 5, this technique when applied to the scalar wave equation is extended to show that a directionally invisible object may be invisible for multiple directions of incidence simultaneously. This opens the door to the design of optically switchable, directionally invisible objects which could be implemented in couplers and other novel optical devices. In Chapter 6, a version of the "field cloak method" is extended to the Maxwell's electro-magnetic vector equations, and this allows more flexibility in the variety of directionally invisible objects that can exist. This thesis concludes with examples of such objects and future applications.

1.2 Historical Background

Invisibility has fascinated humans since antiquity and has usually been a quality attributed to gods, ghosts, and superheros in a variety of literature. The advances in science in the 19^{th} century laid the foundations for understanding certain light-matter interactions. Specifically, the following discoveries were particularly instrumental, namely, that light is an electro-magnetic wave which may be described by Maxwell's equations, the discovery of the periodic table dividing matter into atomic elements, the observation of atomic spectra and their mathematical characterization by the Lyman and Balmer series. However, late in the 19^{th} century, scientists were still struggling to understand atomic structure. In 1897 J.J. Thomson discovered that the ray emitted by the cathode ray tube was a stream of negatively charged particles that were subatomic, and these were called electrons [40]. Consequently he assumed

that the atom must be charge-neutral and must have an equal number of positively charged particles. The discovery of electrons sparked a flurry of new models of the atom that now included both positive and negative charge [45, 65, 51]. Because of experiments with the cathode ray tube, it was known that accelerating electrons must radiate energy. In 1904 Arnold Sommerfeld introduced the idea of the rigid extended electron [62, 63]. But none of the atomic models proposed until 1910 accounted for the frequency of emitted radiation [39], nor could they explain how accelerating electrons would not eventually collapse after radiating all the energy they possessed [28, 40]. To reconcile charge neutrality and the existence of accelerating electrons in the atom, research into the possibility of nonradiating, extended charge distributions began. The first exposition of how to design a nonradiating extended charge distribution was in 1910 by Paul Ehrenfest. In Chapter 2 we explain Ehrenfest's theory and extend his work. Such nonradiating extended charge distributions became part of the first class of invisible objects, known as nonradiating sources, primary sources that do not radiate energy outside of their domain of support. There is an excellent review of the history of such nonradiating sources here [27], and we will now summarize the main discoveries and the evolution from such sources to nonscattering scatterers, which is the focus of this review [28].

Shortly after Ehrenfest's discovery, Niels Bohr eclipsed all other models with his model of the atom in 1913 [56], building on Planck's radiation law, Rutherford's experiment demonstrating that atoms consist of a heavy nucleus surrounded by a volume of free space [59], and Einstein's exposition of the photon nature of light. Planck's radiation law in 1900 showed that light is emitted and absorbed by discrete

energy quanta, called *photons* by Einstein in 1905, when he demonstrated that they are proportional to frequency in his photoelectric effect experiment. Bohr postulated that these energy quanta may only exist in specific stationary orbits, and electrons could suddenly appear in a higher orbit during energy absorption via a quantum leap, or emit radiation when they fell from a higher orbit to a lower orbit. Bohr's atom was electrically neutral unless disturbed by an energy exchange. While this theory explained the stability of atoms, it did not explain why these electrons did not radiate energy while accelerating in a stationary orbit. In 1925 Louis DeBroglie introduced the idea of "phase waves", in which the trajectory of a moving particle is identical to the ray of a phase wave along which frequency and the total energy is constant. The length of each orbit is related to a multiple of what is now known as the DeBroglie wavelength of a standing wave, such that each orbit represents a resonant state [12]. The next year Erwin Schrödinger built on the idea of phase waves and proposed that the atom was a wave-system, represented by the well-known Schrödinger equation, and the wave-function represented the probability density associated with the location of an electron [60]. Within a year of Schrödinger's publication of the wave-function his theory became known as wave mechanics, and after contributions from Born, Jordan, and Heisenberg it became known as Quantum Mechanics. Scattering theory (Chapter 3) is derived from it. Despite the birth of quantum mechanics as an explanation for the absence of radiation of electrons in an orbit, George A. Schott continued to work on radiationless models. In 1933 he discovered conditions under which a rigid charged spherical shell could move in a periodic orbit without radiating [23]. In 1937 he also showed how such charged shells could move in similar orbits

in the absence of external forces [24]. In 1948 Bohm and Weinstein extended Schott's theory to other spherically symmetric objects [8]. In 1964 Goedecke demonstrated a radiationless, asymmetric, spinning, extended charge distribution [31]. Many of the authors suggested that these models could be used to explain elementary particles, but it turned out that the existence of nonradiating sources was of greater importance to the solution of the inverse source problem [27]. The inverse source problem is the identification of a source from its radiation pattern. During the seventies, several physicists investigated electromagnetic monochromatic nonradiating sources in the context of the inverse source problem [22, 16]. In 1977 Norman Bleistein and Jack Cohen proved that the existence of monochromatic nonradiating sources implied the nonuniqueness of the solution to the monochromatic inverse source problem [7]. In other words, an invisible object is an object without an image, and therefore it is impossible to distinguish between the absence of an object and the presence of an invisible object. Consequently, there are at least two solutions that would produce the absence of an image, which makes the solution to the inverse problem nonunique. Throughout the remainder of the seventies and early eighties the uniqueness of partially coherent [13, 43, 26] and stochastic sources were also investigated [33, 14].

This led to the study of the mathematical properties of nonradiating sources. The most important result and prescription for the design of a nonradiating sources was proposed by Gamliel, Kim, Nachman, and Wolf [25]. They postulated that the field generated by the the nonradiating source is subject to specific boundary conditions. These are discussed in more detail in Chapter 4. Unrelated to the research involving nonradiating sources, Milton Kerker observed experimentally in the mid-seventies

that certain non-absorbing dielectric spheres did not scatter light. As a result, he proposed that if the scattering cross-section of these non-absorbing spheres was zero, the object was invisible [41]. Alexopoulos and Uzunoglu subsequently studied spheres that exhibited both gain and loss and suggested a less stringent condition for invisibility based on their observations–that the extinction cross-section should be zero for invisibility [1]. Kerker then also experimented on gain-loss spheres and stated that both the extinction and the scattering cross-sections must be zero for true invisibility [42]. Eventually from the Helmholtz equation describing the radiation problem, an analogous equation was written to describe the response of an object or a scattering to an incident field in terms of a scattering potential, an analogue to Schroedinger's quantum potential. Since this equation is impossible to solve exactly due to the presence of the scattered field on both sides of the equation, an approximation for weak scatterers, called the first Born approximation, which assumes that the scattered field is very weak compared to the incident field, became popular [9, Chapter 13]. Anthony Devaney demonstrated within the first Born approximation that a scatterer could be invisible to monochromatic light incident from a finite number of directions and showed that such nonscattering scatterers were also nonunique [15]. Wolf and Habashy later showed that an omnidirectionally invisible nonscattering scatterer could not exist for scalar waves [67].

In 1998 in the field of quantum mechanics, Carl Bender demonstrated that $\mathcal{PT}$ symmetric Hamiltonians applied to the Schrödinger equation could also generate real eigenvalues [3]. In 2000 Pendry showed how negative refractive index materials, first proposed by Victor Veselago in 1968 [66], could be used to construct a perfect lens [54].

This is considered one of the the first meta-material papers applied to optics and sparked a flurry of research in meta-materials, which derive their optical properties from the subwavelength structure of the material instead of the chemical properties of the constituent atoms. In 2006 both Ulf Leonhardt and Sir John Pendry independently discovered an approach to designing an omnidirectionally invisible object using a conformal mapping technique which required both the permittivity and the permeability to be zero [46, 55]. This technique is now known as transformation optics. Pendry also filed the first patent application for an invisibility cloak [53]. This engendered interest in discovering a way to implement a practical invisibility cloak applying transformation optics to the optical, seismic, and acoustic domains. In addition it sparked research into epsilon near zero materials, which might be used to implement such cloaks. As a result the classical approach to invisibility was almost completely forgotten. However these cloaks have proven very difficult to fabricate in the optical domain for the following reasons: (1) Practical implementations with this approach need to incorporate materials with zero permittivity and permeability, which currently do not exist for a broad range of wavelengths. (2) The objects or cloaks are mostly omni-directionally invisible, and, therefore, the hidden object is also completely blind to the outside world. (3) Metamaterials used to implement these solutions have periodic structures which respond to a narrow band of wavelengths and have limited application. Metamaterial structures are not very robust against manufacturing flaws. (4) When this approach has been applied to the optical range, if the metamaterials approach is used, the features are so small that quantum effects appear which are not taken into account by transformation optics. However, the

largest impediment to realizing cloaks with a transformation optics approach is that, in the invisible region, both the electric permittivity and magnetic permeability must be equal to zero, so that the cloak is impedance matched with air and because zero index materials have infinite bandwidth.

In 2015 Gbur combined Gamliel and Nachman's technique with scattering theory to design directionally invisible monochromatic nonscattering scatterers [29]. In Chapter 4, Gbur's framework is employed to design a variety of such directionally invisible objects, some of which are $\mathcal{PT}$-symmetric, and the influence of symmetry on directionality is studied. In Chapter 5, we extend this theory to allow multiple incident plane waves. In Chapter 6, this theory is also extended to the electromagnetic case, and it is shown how it could be related to the permittivity and permeability of a material. We demonstrate here that it is possible to achieve invisibility with nonzero electric permittivity and magnetic permeability values by approaching the problem from the perspective of scattering theory. This implies that there is a much broader solution set for invisible objects beyond what transformation optics and its derivative theories have to offer.

1.3 Introduction to Maxwell's equations

We now provide an introduction to Maxwell's equations in macroscopic media since all of the approaches to invisibility developed here are expressed mathematically through them. Maxwell's equations in macroscopic media describe the behavior of electromagnetic waves in the presence of matter [9, Chapter 2]. The main theoretical approach throughout this thesis has a recurring theme, regardless of whether

we are are dealing with nonradiating sources or nonscattering scatterers: An invisible object responds to an incident field, as if the object were absent. Therefore, let us assume that the total field also satisfies the equations used to describe the absence of an object. By rewriting Maxwell's equations and comparing them to the ideal assumption, we show that it is possible to derive the material properties and relationships between the fields that must be satisfied to ideally achieve invisibility. All the models of invisibility are verified with numerical simulations of Maxwell's equations. These equations in free space in Gaussian units are given by

$$\nabla \cdot \mathbf{E} = 4\pi\rho, \tag{1}$$

$$\nabla \times \mathbf{B} - \frac{1}{c}\frac{\partial}{\partial t}\mathbf{E} = \frac{4\pi}{c}\mathbf{J}, \tag{2}$$

$$\nabla \times \mathbf{E} + \frac{1}{c}\frac{\partial}{\partial t}\mathbf{B} = 0, \tag{3}$$

$$\nabla \cdot \mathbf{B} = 0, \tag{4}$$

where $\mathbf{E}$ is the electric field, ρ is the charge density, $c \approx 2.998 \cdot 10^8 m/s$ is the speed of light in vacuum [19], $\mathbf{B}$ is the magnetic induction, and $\mathbf{J}$ is the current density [38]. Taking the divergence of Eq. (2) and substituting the result into Eq. (1) yields the continuity equation

$$\frac{\partial}{\partial t}\rho + \nabla \cdot \mathbf{J} = 0, \tag{5}$$

which relates the divergence or flux of the current density $\mathbf{J}$ to the change in charge density over time. Since a positive divergence indicates the flux of the current density flows out from a given point, Eq. (5) is only satisfied if the charge density then decreases during the same interval of time, such that charge is conserved. Typically,

ρ and $\mathbf{J}$ are called the sources, which produce the electric field $\mathbf{E}$ and the magnetic induction $\mathbf{B}$. Consequently, if ρ and $\mathbf{J}$ are specified, Maxwell's equations provide a method to evaluate $\mathbf{E}$ and $\mathbf{B}$ in the domain of interest around the sources. However, macroscopic aggregates of matter may be viewed as an equally large aggregate of sources contributing to currents and charge densities, and, therefore, it is almost impossible to solve Maxwell's equations without making simplifying assumptions or approximations. In this case, the macroscopic fields and sources represent a spatially averaged value. The sources may then also be decomposed into *free* and *bound* quantities, as follows,

$$\rho = \rho_f + \rho_b, \tag{6}$$

$$\mathbf{J} = \mathbf{J}_f + \mathbf{J}_b, \tag{7}$$

where the subscripts f and b indicate "free" and "bound", respectively [32]. Free charge generates the $\mathbf{E}$ and $\mathbf{B}$ fields, while bound charge creates electric dipole moments, which are quantified by a macroscopically averaged polarization $\mathbf{P}$, defined as the average dipole moment per unit volume. Similarly, magnetic dipoles induce a macroscopically averaged magnetization $\mathbf{M}$, defined as the average magnetic dipole moment per unit volume. The magnetization and polarization are related to the electromagnetic fields by

$$\mathbf{D} = \mathbf{E} + 4\pi\mathbf{P}, \tag{8}$$

$$\mathbf{B} = \mathbf{H} + 4\pi\mathbf{M}, \tag{9}$$

where $\mathbf{D}$ is the electric displacement and $\mathbf{H}$ is the magnetic field produced by the sources. To clarify, the magnetic induction $\mathbf{B}$ is composed of the magnetic field generated by the free sources and the magnetization associated with the bound magnetic dipoles. Similarly, the electric displacement $\mathbf{D}$ is composed of the electric field generated by the free charge and the polarization, associated with the bound charge. In addition, electrostatics and magnetostatics have two additional relationships, given by

$$\rho_b = -\nabla \cdot \mathbf{P}, \tag{10}$$

$$\mathbf{J}_b = \nabla \times \mathbf{M}, \tag{11}$$

If we take the divergence of Eq. (11), we obtain

$$\nabla \cdot \mathbf{J}_b = \nabla \cdot \nabla \times \mathbf{M} = 0, \tag{12}$$

which indicates that the magnetization, and therefore the bound current density, does not contribute to charge conservation demanded by the continuity equation (Eq. (5). Therefore the polarization must contribute to another current density, $\mathbf{J}_p$, given by

$$\begin{aligned} \nabla \cdot \mathbf{J}_p &= -\frac{\partial}{\partial t}\rho_b \\ &= \frac{\partial}{\partial t}\left(\nabla \cdot \mathbf{P}\right) \\ &= \nabla \cdot \frac{\partial}{\partial t}\mathbf{P} \end{aligned} \tag{13}$$

where it is important to note that the current density due to the polarization is only present when there is a flow of charge through the source. From this perspective, Maxwell's equations may be rewritten in terms of the free charge ρ_f and the free

current density $\mathbf{J}_f$,

$$\nabla\times\mathbf{E} + \frac{1}{c}\frac{\partial}{\partial t}\mathbf{B} = 0, \tag{14}$$

$$\nabla\cdot\mathbf{B} = 0, \tag{15}$$

$$\nabla\times\mathbf{H} - \frac{1}{c}\frac{\partial}{\partial t}\mathbf{D} = \frac{4\pi}{c}\mathbf{J}_f, \tag{16}$$

$$\nabla\cdot\mathbf{D} = 4\pi\rho_f. \tag{17}$$

When Maxwell's equations are written in this form, they may also be separated into homogeneous equations with $\mathbf{E}$ and $\mathbf{B}$ and inhomogeneous equations with $\mathbf{D}$ and $\mathbf{H}$ [9, Chapter 1.1]. The inhomogeneous equations describe the relationship between $\mathbf{H}$, $\mathbf{D}$, $\mathbf{J}_f$, and ρ_f, and consequently evince the influence of matter on the fields. There are other ways of expressing the relationships between the polarization, the magnetization, the fields and their respective material parameters for certain idealized types of materials. For example, the polarization and magnetization of an isotropic, linear medium may be defined by

$$\mathbf{P} = \chi_e\mathbf{E}, \tag{18}$$

$$\mathbf{M} = \chi_m\mathbf{H}, \tag{19}$$

where χ_e and χ_m are the electric susceptibility and the magnetic susceptibility, respectively. If we substitute Eqs. (18) and (19) into Eqs. (8) and (9), we obtain

$$\begin{aligned}\mathbf{D} &= (1+\chi_e)\mathbf{E} \\ &= \varepsilon\mathbf{E}, \end{aligned} \tag{20}$$

$$\begin{aligned}\mathbf{B} &= (1+\chi_m)\mathbf{H} \\ &= \mu\mathbf{H}, \end{aligned} \tag{21}$$

where ε and μ are the effective electric permittivity and magnetic permeability of the macroscopic medium. For anisotropic media the material parameters χ_e, χ_m, ε, and μ are typically second rank tensors.

When we apply Maxwell's equations to invisibility, we assume that there are no sources and that there is no free charge. The modified equations are reduced to

$$\nabla\times\mathbf{E} + \frac{1}{c}\frac{\partial}{\partial t}\mathbf{B} = 0, \tag{22}$$

$$\nabla\cdot\mathbf{B} = 0, \tag{23}$$

$$\nabla\times\mathbf{H} - \frac{1}{c}\frac{\partial}{\partial t}\mathbf{D} = 0, \tag{24}$$

$$\nabla\cdot\mathbf{D} = 0. \tag{25}$$

These are the general Maxwell equations that are used throughout this text.

CHAPTER 2: NULL-FIELD NONRADIATING SOURCES

A simple example of a source that does not radiate outside of its domain was illustrated in a 1910 paper by Ehrenfest [17], in what may be the earliest paper dedicated to nonradiating sources. Paul Ehrenfest approached the problem of how to create such a source by first imagining simple oscillations of symmetric charge distributions. He considered an infinite sheet of electrons with uniform density moving perpendicular to its surface as illustrated in Figure 1. In this case the magnetic flux **H** is automatically zero (or null), since the magnetic field must be simultaneously perpendicular to the propagation direction and to the radial electric field. With this geometry, this is not possible. Consequently, even if the electron plane were oscillating periodically, both the radiated field and radiated power[1], which can be expressed by

[1]In [17], Ehrenfest discusses radiation in terms of the momentum density instead of radiated power.

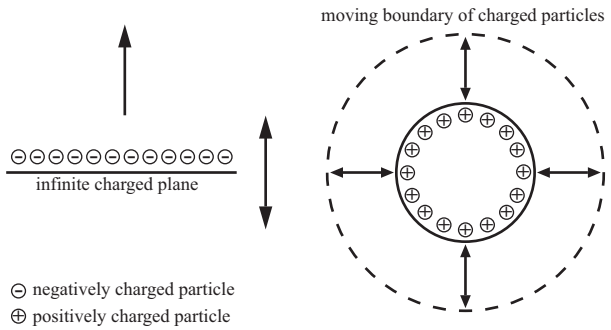

Figure 1: Negatively charged infinite plane moving perpendicular to surface of the plane (left). Positively charged pulsating sphere (right). Neither one of these objects can radiate because the direction of motion is in the direction of the electric field lines, which are normal to the surface.

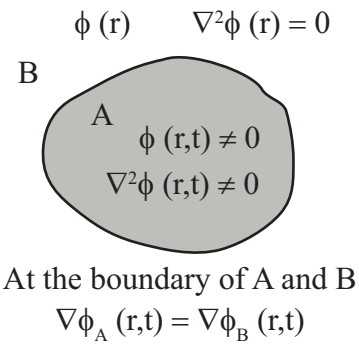

Figure 2: Generalized nonradiating source (domain A) described by Ehrenfest located in domain B. The conditions for the potential $\phi(\mathbf{r}, t)$ are shown.

the Poynting vector, are also zero. However, since the existence of such an infinite charged plane is unrealizable, he suggested, in addition, a positively charged sphere pulsating in the radial direction. Again the magnetic field $\mathbf{H}(\mathbf{r}, t)$, since it can only be perpendicular to the area of the surface charge due to symmetry, should point in the direction of the outward normal. However, since the sphere is pulsating, the charge is also moving in that direction. Therefore this object also cannot radiate. Due to the radial symmetry and the fact that there are no current sources[2] within the sphere, both $\mathbf{H} = 0$ and the $\nabla \cdot \mathbf{H}(\mathbf{r}, t) = 0$.

Building on these two examples, Ehrenfest generalized the conditions to design a source with null-$\mathbf{H}$ field and time-varying charge distribution that does not radiate outside of its domain using the following approach. Suppose the source exists within domain A with a time-varying electric potential $\phi(\mathbf{r}, t)$ and vector potential $\mathbf{A}(\mathbf{r}, t)$, and domain B represents the space outside of domain A (Figure 2). Within domain A, $\phi(\mathbf{r}, t)$ is taken to be time-varying and $\nabla^2\phi(\mathbf{r}, t)$ is nonzero, whereas within B, $\phi(\mathbf{r}, t)$

[2]In [17], the author mentions that there are no "Quellen", i.e. German for sources, and here we translate this term as current sources, since at that time the only type of source in electromagnetic theory discussed before this paper was the current source.

is taken to be a constant over time and satisfies $\nabla^2\phi(\mathbf{r},t)=0$. At the boundary of A and B, $\phi(\mathbf{r},t)$ and $\nabla\phi(\mathbf{r},t)$ are taken to be continuous.

Now the electric field $\mathbf{E}$, the charge density $\rho(\mathbf{r},t)$, and the velocity of the convection current $\mathbf{v}(\mathbf{r},t)$ may all be derived from the potential $\phi(\mathbf{r},t)$ as follows, where

$$\mathbf{E}(\mathbf{r},t) = -\nabla\phi(\mathbf{r},t), \tag{26}$$

$$4\pi\rho(\mathbf{r},t) = -\nabla^2\phi(\mathbf{r},t), \tag{27}$$

$$\mathbf{v}(\mathbf{r},t) = \frac{\frac{\partial}{\partial t}\left[\nabla\phi(\mathbf{r},t)\right]}{\nabla^2\phi(\mathbf{r},t)} \text{ in } A \text{ and } \mathbf{v}=0 \text{ in } B. \tag{28}$$

These equations, together with the conditions that $\mathbf{H}(\mathbf{r},t)=0$ and $\nabla\cdot\mathbf{H}(\mathbf{r},t)=0$, automatically satisfy Maxwell's equations, resulting in a source for which at each point convection and displacement current compensate each other. This was the first type of invisible object that later became classified as a *nonradiating source* – a source that does not radiate outside of its domain.

In general, nonradiating sources do not necessarily have $\mathbf{E}=0$ or $\mathbf{H}=0$; sources that satisfy these conditions we call null-$\mathbf{E}$ or null-$\mathbf{H}$ fields. Decades later, van Bladel explored whether nonradiating sources could be constructed with both electric and magnetic currents [6], and, more recently, Nikolova, Rickard and Yotka hinted that a source could be designated such that either $\mathbf{E}$ or $\mathbf{H}$ could be set to zero [52].

Here, we extend this work and show that it is possible to design sources for which we select which of the fields ($\mathbf{E}$, $\mathbf{H}$, $\mathbf{D}$, or $\mathbf{B}$) is the null-field source within the source domain, and that often multiple fields can be set to zero simultaneously. This is achieved by rewriting Maxwell's equations in terms of the relevant field [35] and can

be verified using a Green's dyadic formalism. Illustrative examples are given, and the implications of the results for invisibility physics are discussed using the known relationship between the electromagnetic radiation and scattering problems.

2.1 Null-field radiationless sources

We begin with the monochromatic macroscopic form of Maxwell's equations in Gaussian units (Chapter 1), and assume that there exist no free currents and charges, i.e.

$$\nabla \cdot \mathbf{D} = 0, \tag{29}$$

$$\nabla \times \mathbf{E} = ik\mathbf{B}, \tag{30}$$

$$\nabla \cdot \mathbf{B} = 0, \tag{31}$$

$$\nabla \times \mathbf{H} = -ik\mathbf{D}, \tag{32}$$

where $k = \frac{2\pi}{\lambda}$ is the wavenumber. We use the definitions of the auxiliary fields $\mathbf{D}$ and $\mathbf{H}$,

$$\mathbf{D} = \mathbf{E} + 4\pi\mathbf{P}, \tag{33}$$

$$\mathbf{B} = \mathbf{H} + 4\pi\mathbf{M}, \tag{34}$$

and substitute these expressions into Maxwell's equations to write the latter entirely in terms of the **E** and **H** fields, as well as the polarization **P** and magnetization **M**,

$$\nabla \cdot \mathbf{E} = -4\pi \nabla \cdot \mathbf{P}, \tag{35}$$

$$\nabla \times \mathbf{E} = ik\mathbf{H} + 4\pi ik\mathbf{M}, \tag{36}$$

$$\nabla \cdot \mathbf{H} = -4\pi \nabla \cdot \mathbf{M}, \tag{37}$$

$$\nabla \times \mathbf{H} = -ik\mathbf{E} - 4\pi ik\mathbf{P}. \tag{38}$$

By use of the curl of Eq. (38) and Eq. (37), we arrive at a monochromatic electromagnetic wave equation with both polarization and magnetization sources,

$$\nabla \times (\nabla \times \mathbf{H}) - k^2\mathbf{H} = 4\pi k^2\mathbf{M} - 4\pi ik\nabla \times \mathbf{P}. \tag{39}$$

The source term on the right of this equation suggests an intriguing possibility: if there are no additional free-propagating fields in the system, there will be no source of magnetic waves, and therefore no magnetic fields at all, if the following condition is satisfied,

$$ik\mathbf{M} + \nabla \times \mathbf{P} = 0. \tag{40}$$

Equation (40) may be considered our condition for a null-**H** source. Because a propagating electromagnetic wave requires both **E** and **H** fields, this also implies that the source must produce no electromagnetic waves outside its domain.

We may also take the curl of Eq. (36) and simplify using Eq. (35); we then arrive at a similar wave equation for the electric field **E**,

$$\nabla \times (\nabla \times \mathbf{E}) - k^2\mathbf{E} = 4\pi k^2\mathbf{P} + 4\pi ik\nabla \times \mathbf{M}. \tag{41}$$

Two observations result from this equation. First, we can see that we will have a null-**E** source if the following condition is satisfied,

$$ik\mathbf{P} - \nabla \times \mathbf{M} = 0. \tag{42}$$

Second, we can see that Eqs. (40) and (42) are different, implying that, in general, a null-**E** source will not be a null-**H** source, and vice-versa.

These results are similar to those reported by Van Bladel and Nikolova and Rickard previously. However, we can go further and express Maxwell's equations entirely in terms of **D** and **B** instead of **E** and **H**, which then leads to a different pair of wave equations,

$$\nabla \times (\nabla \times \mathbf{B}) - k^2\mathbf{B} = -4\pi\nabla \times (ik\mathbf{P} - \nabla \times \mathbf{M}), \tag{43}$$

$$\nabla \times (\nabla \times \mathbf{D}) - k^2\mathbf{D} = 4\pi\nabla \times (ik\mathbf{M} + \nabla \times \mathbf{P}). \tag{44}$$

In analogy with the previous results, we see that we can create null-**B** and null-**D** sources, respectively, if the polarization and magnetization satisfy

$$\nabla \times (ik\mathbf{P} - \nabla \times \mathbf{M}) = 0, \tag{45}$$

$$\nabla \times (ik\mathbf{M} + \nabla \times \mathbf{P}) = 0. \tag{46}$$

On comparison of these new conditions with Eqs. (40) and (42), it is apparent that a null-**E** source is automatically a null-**B** source and a null-**H** source is automatically a null-**D** source, but the converse is not true.

We can confirm the nonradiating nature of sources that satisfy these expressions by directly calculating the fields from the sources using Hertz vectors [9, Section 2.2.2],

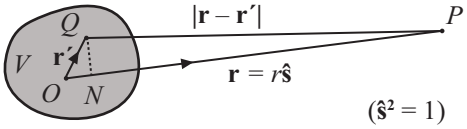

Figure 3: The source is shown with annotated points inside and outside the source to understand the approximation of the Green's function (Eq. (133)). After [9], Figure 13.3.

defined as

$$\vec{\boldsymbol{\pi}}_{\boldsymbol{e}} = \int_V \mathbf{P}(\mathbf{r}')G(|\mathbf{r}-\mathbf{r}'|)\,\mathrm{d}^3r', \tag{47}$$

$$\vec{\boldsymbol{\pi}}_{\boldsymbol{m}} = \int_V \mathbf{M}(\mathbf{r}')G(|\mathbf{r}-\mathbf{r}'|)\,\mathrm{d}^3r', \tag{48}$$

where V is the domain of the source and $G(R) = \exp[ikR]/R$ is the Green's function of the scalar Helmholtz equation. Let Q be any point within the source volume V and P be a point far away from V (Figure 3). If $\mathbf{r}'$ is the position vector of Q, $\mathbf{r} = r\hat{\mathbf{s}}(\hat{\mathbf{s}}^2 = 1)$ is the position vector of P, and N is the foot of the perpendicular from Q to OP, then when r is large enough,

$$|\mathbf{r}-\mathbf{r}'| \sim r - \hat{\mathbf{s}}\cdot\mathbf{r}' \tag{49}$$

and

$$\frac{e^{ik|\mathbf{r}-\mathbf{r}'|}}{|\mathbf{r}-\mathbf{r}'|} \sim \frac{e^{ikr}}{r}e^{-ik\hat{\mathbf{s}}\cdot\mathbf{r}'}. \tag{50}$$

The Fourier transforms of the polarization and magnetization are defined as

$$\tilde{\mathbf{P}}(k\hat{\mathbf{s}}) = \int_V \mathbf{P}(\mathbf{r}')e^{ik\hat{\mathbf{s}}\cdot\mathbf{r}'}\,\mathrm{d}^3r', \tag{51}$$

$$\tilde{\mathbf{M}}(k\hat{\mathbf{s}}) = \int_V \mathbf{M}(\mathbf{r}')e^{ik\hat{\mathbf{s}}\cdot\mathbf{r}'}\,\mathrm{d}^3r'. \tag{52}$$

Employing Eqs. (49) and (50) in Eqs. (47) and (48), respectively, and recognizing

Eqs. (51) and (52) in those substitutions, the Hertz vectors are then in the far field approximately given by

$$\vec{\boldsymbol{\pi}}_{\boldsymbol{e}}(r\hat{\mathbf{s}}) \approx \tilde{\mathbf{P}}(k\hat{\mathbf{s}})\frac{e^{ikr}}{r}, \tag{53}$$

$$\vec{\boldsymbol{\pi}}_{\boldsymbol{m}}(r\hat{\mathbf{s}}) \approx \tilde{\mathbf{M}}(k\hat{\mathbf{s}})\frac{e^{ikr}}{r}, \tag{54}$$

where r is the distance from the origin and $\hat{\mathbf{s}}$ is the unit vector pointing from the origin, which lies inside the source volume. In terms of the Hertz vectors, regardless of the distance from the source, electric field $\mathbf{E}$ and the magnetic field $\mathbf{H}$ satisfy [9]

$$\mathbf{E}(\mathbf{r}) = \nabla \times (\nabla \times \vec{\boldsymbol{\pi}}_{\boldsymbol{e}}) + ik\nabla \times \vec{\boldsymbol{\pi}}_{\boldsymbol{m}} - 4\pi\mathbf{P}, \tag{55}$$

$$\mathbf{H}(\mathbf{r}) = \nabla \times (\nabla \times \vec{\boldsymbol{\pi}}_{\boldsymbol{m}}) - ik\nabla \times \vec{\boldsymbol{\pi}}_{\boldsymbol{e}} - 4\pi\mathbf{M}. \tag{56}$$

The null-$\mathbf{E}$ and null-$\mathbf{H}$ conditions may also be rewritten in terms of the Hertz vectors, which are also known as the polarization potentials, by substituting Eqs. (53) and (54) into the Fourier transform of Eqs. (42) and (40), respectively. Rearranging the terms, the null-$\mathbf{E}$ condition is then given by

$$\vec{\boldsymbol{\pi}}_{\boldsymbol{e}}(r\hat{\mathbf{s}}) = \hat{\mathbf{s}} \times \vec{\boldsymbol{\pi}}_{\boldsymbol{m}}(r\hat{\mathbf{s}}), \tag{57}$$

and the null-$\mathbf{H}$ condition is given by

$$\vec{\boldsymbol{\pi}}_{\boldsymbol{m}}(r\hat{\mathbf{s}}) = -\hat{\mathbf{s}} \times \vec{\boldsymbol{\pi}}_{\boldsymbol{e}}(r\hat{\mathbf{s}}). \tag{58}$$

The behavior of the fields in the far-zone ($kr \gg 1$) can be readily determined by noting that the polarization and magnetization vanish outside of the domain of the source and by exploiting the fact that in the far-zone the Hertz vectors are given by

Eqs. (53) and (54). As a result, we may use the relation $\nabla \rightarrow ik\hat{\mathbf{s}}$ in the same way that in the time domain, one often uses $\frac{\partial}{\partial t} \rightarrow i\omega$ when the temporal Fourier transform is applied to an equation. With these substitutions, we can demonstrate that the **E** and **H** fields, as well as **D** and **B**, are identically zero in the far-zone. We begin by applying the null-**E** condition in terms of the Hertz vectors, Eq. (57), to rewrite Eqs. (55) and (56) as

$$\begin{aligned}
\mathbf{E}(\mathbf{r}) &= ik\hat{\mathbf{s}} \times [ik\hat{\mathbf{s}} \times (\hat{\mathbf{s}} \times \vec{\boldsymbol{\pi}}_{\boldsymbol{m}})] + ik(ik\hat{\mathbf{s}}) \times \vec{\boldsymbol{\pi}}_{\boldsymbol{m}} \\
&= -k^2 \left\{ \hat{\mathbf{s}} \left[\hat{\mathbf{s}} \cdot (\hat{\mathbf{s}} \times \vec{\boldsymbol{\pi}}_{\boldsymbol{m}}) \right] - (\hat{\mathbf{s}} \times \vec{\boldsymbol{\pi}}_{\boldsymbol{m}})(\hat{\mathbf{s}} \cdot \hat{\mathbf{s}}) \right\} - k^2 \hat{\mathbf{s}} \times \vec{\boldsymbol{\pi}}_{\boldsymbol{m}} \\
&= -k^2 \hat{\mathbf{s}} \left[\hat{\mathbf{s}} \cdot (\hat{\mathbf{s}} \times \vec{\boldsymbol{\pi}}_{\boldsymbol{m}}) \right] + k^2 \hat{\mathbf{s}} \times \vec{\boldsymbol{\pi}}_{\boldsymbol{m}} - k^2 \hat{\mathbf{s}} \times \vec{\boldsymbol{\pi}}_{\boldsymbol{m}} \\
&= 0,
\end{aligned} \tag{59}$$

$$\begin{aligned}
\mathbf{H}(\mathbf{r}) &= ik\hat{\mathbf{s}} \times (ik\hat{\mathbf{s}} \times \vec{\boldsymbol{\pi}}_{\boldsymbol{m}}) - ik(ik\hat{\mathbf{s}}) \times (\hat{\mathbf{s}} \times \vec{\boldsymbol{\pi}}_{\boldsymbol{m}}) \\
&= -k^2 \hat{\mathbf{s}} \times (\hat{\mathbf{s}} \times \vec{\boldsymbol{\pi}}_{\boldsymbol{m}}) + k^2 \hat{\mathbf{s}} \times (\hat{\mathbf{s}} \times \vec{\boldsymbol{\pi}}_{\boldsymbol{m}}) \\
&= 0,
\end{aligned} \tag{60}$$

which demonstrates that both the **E** and **H** fields are zero in the far field. **D** and **B** are also zero in the far field since their expressions are contained within the equations above. The same procedure may be performed to demonstrate that null-**H** sources have zero **E** and **H** fields in the far field. We apply the null-**H** condition in terms of

the Hertz vectors (Eq. (58)) to rewrite Eqs. (55) and (56) as

$$\begin{aligned}\mathbf{E}(\mathbf{r}) &= -k^2\hat{\mathbf{s}}\times(\hat{\mathbf{s}}\times\vec{\boldsymbol{\pi}}_{\boldsymbol{e}}) - k^2\hat{\mathbf{s}}\times(-\hat{\mathbf{s}}\times\vec{\boldsymbol{\pi}}_{\boldsymbol{e}}) \\ &= 0,\end{aligned} \tag{61}$$

$$\begin{aligned}\mathbf{H}(\mathbf{r}) &= -k^2\hat{\mathbf{s}}\times[\hat{\mathbf{s}}\times(-\hat{\mathbf{s}}\times\vec{\boldsymbol{\pi}}_{\boldsymbol{e}})] + k^2\hat{\mathbf{s}}\times\vec{\boldsymbol{\pi}}_{\boldsymbol{e}} \\ &= -k^2\left\{\hat{\mathbf{s}}\left[\hat{\mathbf{s}}\cdot(-\hat{\mathbf{s}}\times\vec{\boldsymbol{\pi}}_{\boldsymbol{e}})\right] - (-\hat{\mathbf{s}}\times\vec{\boldsymbol{\pi}}_{\boldsymbol{e}})(\hat{\mathbf{s}}\cdot\hat{\mathbf{s}})\right\} + k^2\hat{\mathbf{s}}\times\vec{\boldsymbol{\pi}}_{\boldsymbol{e}} \\ &= -k^2\hat{\mathbf{s}}\left[\hat{\mathbf{s}}\cdot(-\hat{\mathbf{s}}\times\vec{\boldsymbol{\pi}}_{\boldsymbol{e}})\right] - k^2\hat{\mathbf{s}}\times\vec{\boldsymbol{\pi}}_{\boldsymbol{e}} + k^2\hat{\mathbf{s}}\times\vec{\boldsymbol{\pi}}_{\boldsymbol{e}} \\ &= 0.\end{aligned} \tag{62}$$

The fields *within* null-field sources can also be calculated explicitly using Hertz vectors, though care must be taken in the interchange of derivatives and integrals in the calculation, as has been long known [44]. Since the fields are dependent upon a term using the Green's function which has a singularity within the domain of integration, it is not possible to simply translate a derivative external to the integral inside the integral. To explore the null-**H** field case, first we rewrite the electric field in terms of the polarization and magnetization by substituting Eqs. (47) and (48) into Eqs. (55) and obtain

$$\begin{aligned}\mathbf{E}(\mathbf{r}) = \nabla\times\left[\nabla\times\int_V \mathbf{P}(\mathbf{r}')G(|\mathbf{r}-\mathbf{r}'|)\,\mathrm{d}^3r'\right] - \nabla\times\left\{\int_V[\nabla'\times\mathbf{P}(\mathbf{r}')]\,G(|\mathbf{r}-\mathbf{r}'|)\,\mathrm{d}^3r'\right\} \\ - 4\pi\mathbf{P}(\mathbf{r}),\end{aligned} \tag{63}$$

where ∇' indicates that the operation is performed with respect to $\mathbf{r}'$. To simplify this expression, it is more convenient to write electric field in tensor notation, given

by

$$E_i = \varepsilon_{ijk}\varepsilon_{klm}\partial_j\partial_l \int P_m G \,\mathrm{d}^3r' - \varepsilon_{ijk}\varepsilon_{klm}\partial_j \int (\partial'_l P_m G)\,\mathrm{d}^3r' - 4\pi P_i, \tag{64}$$

where ε_{ijk} is the Levi-Civita tensor. Since the Green's function has a singularity within the region of integration, the integral must be handled with care. The method outlined in [44] enables an integral with a singularity inside and differential operators outside to be rewritten in a more manageable form, as

$$\partial_m\partial_n \int_V JG \,\mathrm{d}^3r' = \int_{V_\epsilon} J\partial'_m\partial'_n G \,\mathrm{d}^3r' - \frac{4\pi}{3} J\delta_{mn}, \tag{65}$$

where V_ϵ is a small volume enclosing the singularity within the source and J is a function with finite support within V. Applying Eq. (65) to Eq. (64), the integral simplifies to

$$\partial_j\partial_l \int_V P_m G \,\mathrm{d}^3r' = \int_{V_\epsilon} P_m\partial'_j\partial'_l G \,\mathrm{d}^3r' - \frac{4\pi}{3} P_m\delta_{jl}, \tag{66}$$

By rewriting Eq. (64) in terms of $\mathbf{D}$, Eq. (33), the integrals are isolated. Then Eq. (66) may be substituted, and to unify the partial derivatives so that all are with respect to r' we also note that with respect to the Green's function $-\partial'_j = \partial_j$ and obtain

$$\begin{aligned} D_i &= E_i + 4\pi P_i \\ &= \varepsilon_{ijk}\varepsilon_{klm}\left\{\int_{V_\epsilon} P_m\partial'_n\partial'_n G \,\mathrm{d}^3r' - \frac{4\pi}{3} P_m\delta_{jl} - \int_V \partial'_l P_m(-\partial'_j) G \,\mathrm{d}^3r'\right\}. \end{aligned} \tag{67}$$

Now we apply integration by parts on the first integral term, resulting in

$$\int_{V_\epsilon} P_m\partial'_j\partial'_l G \,\mathrm{d}^3r' = \int_{V_\epsilon} \partial'_l \left\{P_m\partial'_l G\right\} \,\mathrm{d}^3r' - \int_{V_\epsilon} \partial'_l P_m\partial'_l G \,\mathrm{d}^3r'. \tag{68}$$

Note that the first term on the right of Eq. (68) is one vector component of the divergence theorem. For an arbitrary surface, $\int \partial'_l F \,\mathrm{d}^3r' = \int F n_l \,\mathrm{d}a$, where n_l is the

normal to the surface. The first term can then be rewritten as follows,

$$\int_{V_\epsilon} P_m \partial'_j \partial'_l G \, \mathrm{d}^3 r' = \int_{S_i+S_o} \{P_m \partial'_j G\} n_l \, \mathrm{d}a - \int_{V_\epsilon} \partial'_l P_m \partial'_j G \, \mathrm{d}r', \tag{69}$$

where S_i refers to the inner surface and S_o refers to the outer surface of the sphere. Note that the integral over the outer surface S_o goes to zero, assuming $P_m \to 0$ outside of the sphere. This is a valid assumption since the polarization is directly associated with the material properties of a source and therefore must be zero outside of the volume of the source. Consequently, we focus on the inner surface integral and $\tilde{n}_l$ represents the inward surface normal. For very small surfaces S_i, the polarization $P_m(r') \approx P_m(r)$. Upon evaluation of the derivative of the the Green's function,

$$\begin{aligned} \partial'_j G &= \partial'_j \frac{e^{ikR}}{R} \\ &= \left[\frac{-ik(x_j - x'_j)}{R^2} + \frac{(x_j - x'_j)}{R^3} \right] e^{ikR}, \end{aligned} \tag{70}$$

we see that the first term inside the brackets of Eq. (70) goes to $1/R$ as $R \to 0$, while $e^{ikR} \to 1$ in that limit[3]. Therefore the integral of that term over the surface may be neglected, since the integral of $1/R$ over a vanishingly small surface goes to 0. Labeling the inner surface integral as S_{mjl}, it is then given by

$$\begin{aligned} S_{mjl} &= \int_{S_i} \left\{ P_m \partial'_j G \right\} \tilde{n}_l \, \mathrm{d}a \\ &= -P_m \int_{S_i} \frac{x_j}{r^3} r^2 \tilde{n}_l \, \mathrm{d}\Omega \\ &= P_m \int_{S_i} n_j \tilde{n}_l \, \mathrm{d}\Omega, \end{aligned} \tag{71}$$

where x_j is used instead of $x_j - x'_j$, the normal vector component $n_j = \frac{x_j}{r}$, and

[3]As $R \to 0$, $x_j - x'_j \to R$ since it also becomes smaller. Consequently, the fraction may be approximated by $R/R^2 = 1/R$.

the differential area $\mathrm{d}a = r^2\,\mathrm{d}\Omega$ in terms of the radius and the angles θ and ϕ. If $n_x = \sin\theta\cos\phi$, $n_y = \sin\theta\sin\phi$, and $n_z = \cos\theta$,

$$\int n_j n_l\,\mathrm{d}\Omega = 0 \text{ for } j \neq l, \tag{72}$$

where $\mathrm{d}\omega = \sin\theta\,\mathrm{d}\theta\,\mathrm{d}\phi$. For $j = l$ by symmetry all three components of $\hat{\mathbf{n}}$ are the same, and, for simplicity, we evaluate

$$\begin{aligned}\int n_z^2\,\mathrm{d}\Omega &= 2\pi\int_0^\pi \cos\theta^2\sin\theta\,\mathrm{d}\theta \\ &= 2\pi\left[-\frac{1}{3}\cos^3\theta\right]_0^\pi \\ &= \frac{4\pi}{3},\end{aligned} \tag{73}$$

which upon substitution into Eq. (71) leads to

$$S_{mjl} = 4\pi P_m \delta_{jl} \tag{74}$$

and results in

$$\int_{V_\epsilon} P_m \partial'_j\partial'_l G\,\mathrm{d}^3r' = 4\pi P_m\delta_{jl} - \int_{V_\epsilon}\partial'_l P_m \partial'_j G\,\mathrm{d}r' \tag{75}$$

after substitution in Eq. (69). Now we see that applying the result from Eq. (75) to Eq. (67), we obtain

$$\begin{aligned}D_i &= E_i + 4\pi P_i \\ &= \varepsilon_{ijk}\varepsilon_{klm}\left\{4\pi P_m\delta_{jl} - \frac{4\pi}{3}P_m\delta_{jl} - \int_V \partial'_l P_m(-\partial'_j)G\,\mathrm{d}^3r' - \int_{V_\epsilon}\partial'_l P_m\partial'_j G\,\mathrm{d}r'\right\} \\ &= 0,\end{aligned} \tag{76}$$

and the electric field inside the null-**H** source is

$$E_i = -4\pi P_i. \tag{77}$$

A simpler determination of this result is derived from Eqs. (45) and (46): since a null-**H** source, labeled by $H0$, automatically has $\mathbf{D} = 0$ and a null-**E** source, labeled by $E0$, automatically has $\mathbf{B} = 0$, it follows from Eqs. (33) and (34) that

$$\mathbf{E}_{H0} = -4\pi\mathbf{P}, \tag{78}$$

$$\mathbf{H}_{E0} = -4\pi\mathbf{M}. \tag{79}$$

The full calculation leading to Eq. (77) demonstrates the consistency of our solution with Maxwell's equations.

2.2 Examples of null-field nonradiating sources

To design a null-field source, the polarization and magnetization must be chosen to satisfy one of the four conditions given above, and summarized here again:

$$ik\mathbf{P} - \nabla \times \mathbf{M} = 0, \text{ (Null-}\mathbf{E}\text{ source condition)} \tag{80}$$

$$ik\mathbf{M} + \nabla \times \mathbf{P} = 0, \text{ (Null-}\mathbf{H}\text{ source condition)} \tag{81}$$

$$\nabla \times (ik\mathbf{P} - \nabla \times \mathbf{M}) = 0, \text{ (Null-}\mathbf{B}\text{ source condition)} \tag{82}$$

$$\nabla \times (ik\mathbf{M} + \nabla \times \mathbf{P}) = 0. \text{ (Null-}\mathbf{D}\text{ source condition)} \tag{83}$$

A null-**H** source, for instance, may be designed by choosing functions for **P** and **M** that satisfy Eq. (81). An example of such a source confined to a spherical domain is

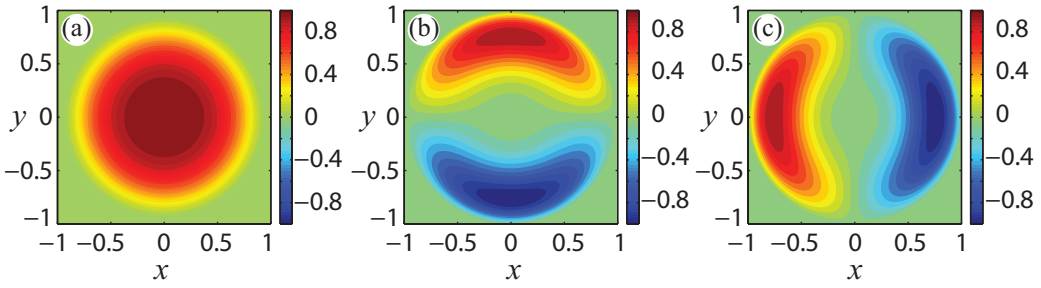

Figure 4: The (a) polarization P_z and magnetization (b) iM_x and (c) iM_y of the null-**H** source given by Eq. (86), with $k = 1$.

given by the choice

$$\mathbf{P}(\mathbf{r}) = \hat{z} f(r), \tag{84}$$

$$f(r) = \begin{cases} \cos^2(\pi r^2/2), & |\mathbf{r}| \leq 1, \\ 0, & \text{otherwise}, \end{cases} \tag{85}$$

$$\mathbf{M}(\mathbf{r}) = -\frac{1}{ik} \nabla \times \mathbf{P}(\mathbf{r}). \tag{86}$$

It is to be noted that the function $f(r)$ has been taken to be continuous; this is not a necessary requirement, but prevents a magnetization singularity from appearing on the outer surface of the sphere due to the curl of Eq. (86). Such singularities can be incorporated, however, and are discussed by Van Bladel [6]. An illustration of this source is given in Fig. 4; the electric field is directly proportional to the polarization.

The previous source, as noted, is also a null-**D** source. With a slight modification, it can be converted into a source with a zero **D** field but a nonzero **H** field. To do so, we introduce a new magnetization $\mathbf{M}'(\mathbf{r}) = \mathbf{M}(\mathbf{r}) + \nabla\phi(r)$, with $\phi(r)$ a function that is continuous and which possesses a continuous first derivative (again to avoid requiring singular sources) and keep the original polarization. Because the curl of the gradient of a function is zero, $\mathbf{M}'(\mathbf{r})$ still satisfies the condition of a null-**D** source

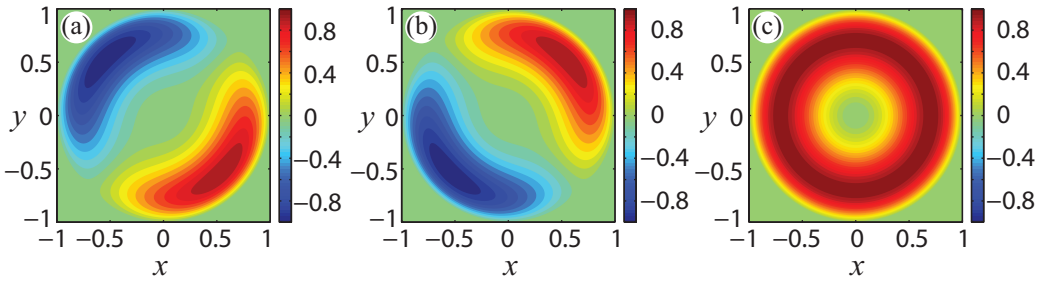

Figure 5: The (a) magnetization iM_x, (b) iM_y and (c) iM_z of the null-**D** source with nonzero **H**, with $k = 1$ and $z = 1$. The quantity P_z is the same as in Fig. 4.

(Eq. (83)) but not the condition of a null-**H** source (Eq. (81)).

A simple example of this is given by choosing

$$\phi(r) = \frac{1}{ik} \begin{cases} \cos^2(\pi r^2/2), & |\mathbf{r}| \leq 1, \\ 0, & \text{otherwise}, \end{cases} \tag{87}$$

and the modified magnetization functions are shown in Fig. 5.

This example suggests other possibilities for null-field sources. If the polarization density is taken to be of the form $\mathbf{P}(\mathbf{r}) = \nabla\phi(r)$, then it will automatically satisfy Eq. (40), the null-**H** condition, without any magnetization at all. Similarly, a source with magnetization $\mathbf{M}(\mathbf{r}) = \nabla\phi(r)$ will satisfy Eq. (42), the null-**E** condition, without any polarization. Such sources produce only longitudinal fields, and cannot, therefore, produce any transverse radiation. They may be considered a generalization of the aforementioned examples considered by Ehrenfest in [17], such as the radially pulsating sphere.

Finally, we may look again at the conditions for null-**E** and null-**H** simultaneously.

These equations, written as

$$ik\mathbf{P} - \nabla \times \mathbf{M} = 0, \tag{88}$$

$$ik\mathbf{M} + \nabla \times \mathbf{P} = 0, \tag{89}$$

respectively, in fact mirror Maxwell's equations, Eqs. (30) and (32), for an electromagnetic wave propagating in a source-free region. If we choose $\mathbf{P}$ and $\mathbf{M}$ to have the same form as the electric and magnetic fields of a free-propagating field, the actual electromagnetic fields will be identically zero in the source.

This cannot be done over a complete source region without introducing singular boundary sources. We can, however, design a source with a null-field region inside and a gradual outer transition region, as the following example shows. For the polarization and magnetization, we use a source of outer radius a and inner radius b, with

$$P_x(\mathbf{r}) = \exp[ikz] \begin{cases} \cos^2[g(r)], & b \le |r| \le a, \\ 1, & |r| < b, \\ 0, & |r| > a, \end{cases} \tag{90}$$

$$M_y(\mathbf{r}) = -\exp[ikz] \begin{cases} \cos^2[g(r)] - \frac{\pi(r-b)^2}{(a-b)^2}\frac{z}{ikr}h(r), & b \le |r| \le a, \\ 1, & |r| < b, \\ 0, & |r| > a, \end{cases} \tag{91}$$

$$M_z(\mathbf{r}) = -\exp[ikz] \begin{cases} \frac{\pi(r-b)}{(a-b)^2}\frac{y}{ikr}h(r), & b \le |r| \le a, \\ 0, & \text{otherwise}, \end{cases} \tag{92}$$

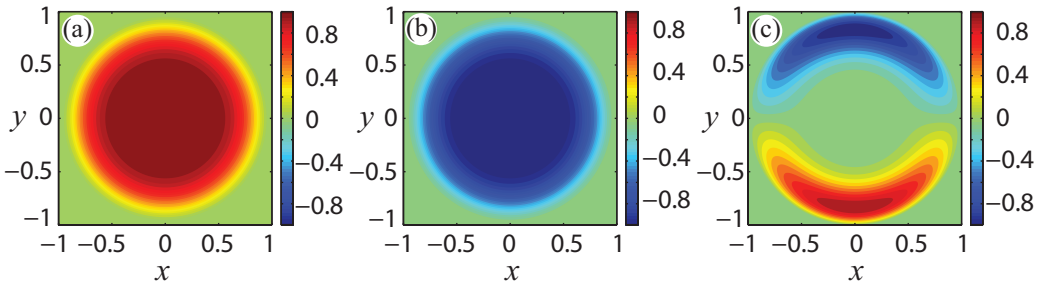

Figure 6: The (a) polarization P_x and magnetization (b) M_y and (c) iM_z of the complete null source, with $k = 1$, $a = 1$, $b = 0.3$ and $z = 0$.

with

$$g(r) = \frac{\pi}{2}\left(\frac{r-b}{a-b}\right)^2, \tag{93}$$

$$h(r) = \sin\left[2g(r)\right]. \tag{94}$$

This source satisfies Eqs. (88) and (89) simultaneously within the sphere $|r| < b$, implying that it has simultaneously zero $\mathbf{E}$ and $\mathbf{H}$ in that region, but only satisfies Eq. (89) in the intermediate region, making it a null-$\mathbf{H}$ source in that region and radiationless overall. The resulting polarization and magnetization are illustrated in Fig. 6.

Since the source satisfies Eq. (89) throughout its domain but only satisfies Eq. (88) in the region $|r| < b$, there is an electric field present in the region $b \leq |r| \leq a$, given by

$$E_x(\mathbf{r}) = 4\pi \exp[ikz] \begin{cases} \cos^2\left[g(r)\right], & b \leq |r| \leq a, \\ 0, & |r| < b, \\ 0, & |r| > a, \end{cases} \tag{95}$$

by substituting Eq. (90) into Eq. (77) for the region $b \leq |r| \leq a$. The other components of the electric and magnetic fields are all zero. The electric field is shown

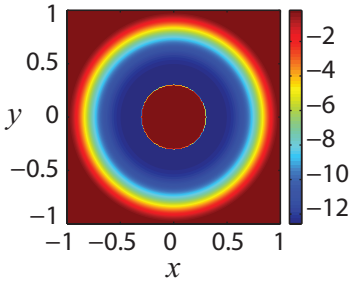

Figure 7: The total electric field $\mathbf{E}(\mathbf{r}) = E_x(\mathbf{r})\hat{\mathbf{x}}$ of the complete null source given by Eq. (95), with $k = 1$, $a = 1$, $b = 0.3$ and $z = 0$.

in Figure 7.

It looks similar to a cloak, which is a type of invisible object with a zero field region inside and a value of negative the incident field's amplitude along the inner boundary.

2.3 Summary

This array of results is of some significance to the theory of invisibility through metamaterials. A primary source of polarization and magnetization is mathematically equivalent to a scattering object with spatially-varying permittivity and permeability excited by an electromagnetic wave; the fields produced by the primary source are equivalent to the scattered fields produced by the interaction. A null-field radiationless source is then equivalent to a scattering object that produces no scattered field–it is invisible–and the interior fields of which take on an exceedingly simple form. A null-**E** source, for instance, is equivalent to a scattering object whose interior electric field is exactly equal to the electric field of the illuminating wave. These results are potentially of use in recent studies of lossless open resonators, which use similar interference effects for light confinement [50, 61].

It does not seem likely that such null-field scattering objects can be produced by

the techniques of transformation optics for the following reason. To design an invisible object using transformation optics or conformal mapping, the material parameters are expanded from a line or a point into a cloaked space through a coordinate-transformation, resulting in an invisible object with a cloaked region (within which the fields are zero). Therefore it would be very difficult to selectively render one or more of the fields zero. In contrast, with this approach we work with the field equations to selectively render one or more of the fields zero, and then we may calculate the material parameters. It is important to note that rendering one of the fields zero, confines the other fields to the domain of the nonradiating source, if so desired. The existence of null-field sources, therefore, indicates that the class of invisible and cloaked objects is broader than previously realized. The techniques applied in this chapter to introduce various types of null-field radiationless sources may be applied later to derive other invisible structures.

CHAPTER 3: SCATTERING THEORY

In this chapter, we introduce the fundamentals of scattering theory, which in general is the mathematical characterization of the response of an object to an incident electromagnetic (EM) field, as a function of its material properties. Scattering theory lays the groundwork for solving two significant challenges: (1) the reconstruction or estimation of the material properties of the scatterer from its response to an incident field, the scattered field; and (2) the manipulation of the object's material properties to achieve a desired scattered field. In the context of invisibility theory, the desired scattered field is zero.

Section 3.1 derives the scalar wave equation, typically used to describe the simpler scattering problems. The general solution of the scalar wave equation leads into the relationship between the *inverse source problem*, the identification of an electromagnetic source from its scattered field, and the *inverse scattering problem*, the identification of the scatterer from its scattered field. But there remains the question of how to quantify light scattering and absorption by the object and extinction of the incident electromagnetic field. The mathematical formalism for this is derived and explained in Section 3.2 and ends the exploration of the scalar wave equation. Next we introduce electromagnetic scattering theory in Section 3.3, beginning with the well-known homogeneous vector wave equation for the electric field $\mathbf{E}(\mathbf{r})$. In Section 3.3.1, this equation is derived and rearranged in an inhomogeneous form so

that it can be applied to scattering problems in the vector case. This is of fundamental importance because the vector framework is needed to accurately model the electromagnetic case, which could eventually be used to design objects for practical applications. In Section 3.3.2, we extend the theory to the vector wave equation for the magnetic field $\mathbf{H}(\mathbf{r})$ and rewrite it terms of scattering theory, which facilitates the design and modeling of purely magnetic objects, which currently do not exist in nature and would have to be designed using artificial structures called metamaterials. In Section 3.3.3, we further extend the theory and derive the inhomogeneous vector wave equations for the electric displacement $\mathbf{D}(\mathbf{r})$ and the magnetic induction $\mathbf{B}(\mathbf{r})$ in terms of scattering theory by exploiting a new connection between the *inverse source problem* and the *inverse scattering problem* in the vector framework. This has several advantages because the scattering behavior is now linked to both the electric and magnetic properties of the scatterer. As a result of these new equations, the electric and magnetic properties can now be independently manipulated to achieve the desired scattering behavior. We conclude this chapter with a summary of the main implications of these results.

3.1 Scalar scattering theory

To show that an object is invisible it is necessary to characterize the object's response to an incident field and demonstrate that the scattered field outside of the object is identically zero. Here, we review the fundamentals of scattering theory as presented in [9, Chapter 2, Chapter 13] and [11]. The interaction between the object and the incident field, including reflection, transmission, and absorption, is

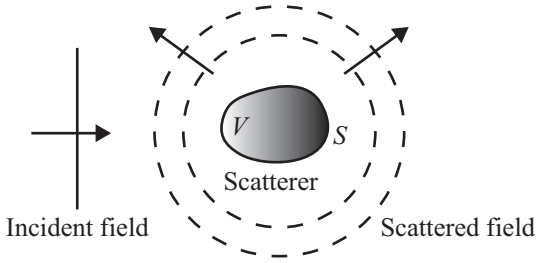

Figure 8: The interaction between a scatterer and the incident field characterized by the scattered field. There are no sources within the scatterer. After [9, Figure 13.1]

called *scattering*. The scatterers discussed here consist of a medium that has a linear response to the incident field and may be characterized by a linear electric permittivity $\varepsilon(\mathbf{r}, \omega)$ and magnetic permeability $\mu(\mathbf{r}, \omega)$, or by the closely related refractive index $n(\mathbf{r}, \omega)$ and impedance ν.

Suppose $\mathbf{E}$ and $\mathbf{H}$ are monochromatic components of the electromagnetic field with a time dependence $e^{-i\omega t}$ incident on a linear, isotropic medium occupying a finite domain V bounded by surface S in which there are no sources (Fig. 8). In electromagnetic theory the most general causal, linear, local, isotropic constitutive relations are

$$\mathbf{D}(\mathbf{r}, t) = \int_0^\infty \varepsilon(\mathbf{r}, \tau)\mathbf{E}(\mathbf{r}, t - \tau)\, \mathrm{d}\tau, \tag{96}$$

$$\mathbf{B}(\mathbf{r}, t) = \int_0^\infty \mu(\mathbf{r}, \tau)\mathbf{H}(\mathbf{r}, t - \tau)\, \mathrm{d}\tau, \tag{97}$$

where $\mathbf{E}$ and $\mathbf{H}$ are the electric and magnetic fields, $\mathbf{D}$ and $\mathbf{B}$ are the electric displacement and the magnetic induction, and ε and μ are the electric permittivity (also known as the dielectric constant) and the magnetic permeability, respectively. Since it is easier to work in the frequency domain, we take the Fourier transforms with respect to t of $\mathbf{D}(\mathbf{r}, t)$ and $\mathbf{B}(\mathbf{r}, t)$, resulting in the following expressions for the electric

displacement and the magnetic induction in terms of frequency ω, given by

$$\mathbf{D}(\mathbf{r},\omega) = \int_0^\infty \left(\int_0^\infty \varepsilon(\mathbf{r},\tau)\mathbf{E}(\mathbf{r},t-\tau)\,\mathrm{d}\tau \right) e^{-i\omega t}\,\mathrm{d}t, \tag{98}$$

$$\mathbf{B}(\mathbf{r},\omega) = \int_0^\infty \left(\int_0^\infty \mu(\mathbf{r},\tau)\mathbf{H}(\mathbf{r},t-\tau)\,\mathrm{d}\tau \right) e^{-i\omega t}\,\mathrm{d}t. \tag{99}$$

By changing the order of integration and applying a variable change to Eq. (98), as follows,

$$\begin{aligned} \mathbf{D}(\mathbf{r},\omega) &= \int_0^\infty \varepsilon(\mathbf{r},\tau) \int_0^\infty \mathbf{E}(\mathbf{r},t-\tau)e^{-i\omega t}\,\mathrm{d}t\,\mathrm{d}\tau \\ &= \int_0^\infty \varepsilon(\mathbf{r},\tau) \int_0^\infty \mathbf{E}(\mathbf{r},u)e^{-i\omega(u+\tau)}\,\mathrm{d}u\,\mathrm{d}\tau \\ &= \int_0^\infty \varepsilon(\mathbf{r},\tau)e^{-i\omega\tau}\,\mathrm{d}\tau \int_0^\infty \mathbf{E}(\mathbf{r},u)e^{-i\omega u}\,\mathrm{d}u, \end{aligned} \tag{100}$$

where $u = t - \tau$, it is shown that the constitutive relations simplify to

$$\tilde{\mathbf{D}}(\mathbf{r},\omega) = \tilde{\varepsilon}(\mathbf{r},\omega)\tilde{\mathbf{E}}(\mathbf{r},\omega), \tag{101}$$

$$\tilde{\mathbf{B}}(\mathbf{r},\omega) = \tilde{\mu}(\mathbf{r},\omega)\tilde{\mathbf{H}}(\mathbf{r},\omega). \tag{102}$$

The Fourier transform of Maxwell's equations (Section 1.3) with no free charges ($\rho = 0$) or currents ($\mathbf{J} = 0$) are given by,

$$\nabla\times\tilde{\mathbf{H}}(\mathbf{r},\omega) - \frac{i\omega}{c}\tilde{\mathbf{D}}(\mathbf{r},\omega) = 0, \tag{103}$$

$$\nabla\times\tilde{\mathbf{E}}(\mathbf{r},\omega) + \frac{i\omega}{c}\tilde{\mathbf{B}}(\mathbf{r},\omega) = 0. \tag{104}$$

If we now substitute Eqs.(101) and (102) into the Maxwell Eqs.(103) and (104), we

obtain

$$\nabla\times\tilde{\mathbf{H}}(\mathbf{r},\omega) - \frac{i\omega\tilde{\varepsilon}(\mathbf{r},\omega)}{c}\tilde{\mathbf{E}}(\mathbf{r},\omega) = 0, \tag{105}$$

$$\nabla\times\tilde{\mathbf{E}}(\mathbf{r},\omega) + \frac{i\omega\tilde{\mu}(\mathbf{r},\omega)}{c}\tilde{\mathbf{H}}(\mathbf{r},\omega) = 0. \tag{106}$$

After dividing by μ and ε, respectively, and taking the curl of Eqs. (105) and (106),

$$\nabla\times\left[\frac{1}{\varepsilon}\nabla\times\mathbf{H}(\mathbf{r},\omega)\right] - \frac{i\omega}{c}\nabla\times\mathbf{E}(\mathbf{r},\omega) = 0, \tag{107}$$

$$\nabla\times\left[\frac{1}{\mu}\nabla\times\mathbf{E}(\mathbf{r},\omega)\right] - \frac{i\omega}{c}\nabla\times\mathbf{H}(\mathbf{r},\omega) = 0, \tag{108}$$

where we drop the tilde and note that dependence on $(\mathbf{r},\omega)$ is sufficient to indicate operation in the frequency domain. Next, we substitute Eq. (106) into the Eq. (107) and Eq. (105) into Eq. (108) and evaluating the expressions we obtain the wave equations

$$\nabla^2\mathbf{E}(\mathbf{r},\omega) + \frac{\varepsilon\mu\omega^2}{c^2}\mathbf{E}(\mathbf{r},\omega) + (\nabla\ln\mu)\times[\nabla\times\mathbf{E}(\mathbf{r},\omega)] + \nabla[\mathbf{E}(\mathbf{r},\omega)\cdot\nabla\ln\varepsilon] = 0, \tag{109}$$

$$\nabla^2\mathbf{H}(\mathbf{r},\omega) + \frac{\varepsilon\mu\omega^2}{c^2}\mathbf{H}(\mathbf{r},\omega) + (\nabla\ln\varepsilon)\times[\nabla\times\mathbf{H}(\mathbf{r},\omega)] + \nabla[\mathbf{H}(\mathbf{r},\omega)\cdot\nabla\ln\mu] = 0. \tag{110}$$

These equations are very difficult to solve, because of the expressions involving $\nabla\ln\varepsilon$ and $\nabla\ln\mu$, and because the last term of each couples the Cartesian components of the respective field. We may eliminate the last two terms of Eqs. (109) and (110) by assuming that the permittivity ε and the permeability μ vary so slowly that each is effectively constant over a wavelength $\lambda = 2\pi/k = 2\pi c/\omega$ [9, Chapter 13.1]. Writing ω and c in terms of the wave number $k = \omega/c$ and the material properties in terms

of the refractive index of the medium $n(\mathbf{r},\omega)$, where $n^2(\mathbf{r},\omega) = \varepsilon(\mathbf{r},\omega)\mu(\mathbf{r},\omega)$ the equations above are simplified to

$$\nabla^2\mathbf{E}(\mathbf{r},\omega) + k^2n^2(\mathbf{r},\omega)\mathbf{E}(\mathbf{r},\omega) = 0, \tag{111}$$

$$\nabla^2\mathbf{H}(\mathbf{r},\omega) + k^2n^2(\mathbf{r},\omega)\mathbf{H}(\mathbf{r},\omega) = 0. \tag{112}$$

In this form the equations are more manageable, and it is still possible to understand the behavior of the scattered field if, for example, only one Cartesian component $U(\mathbf{r},\omega)$ of the electric field $\mathbf{E}(\mathbf{r},\omega)$ is studied. In terms of the single component $U(\mathbf{r},\omega)$, Eq. (111) becomes the homogeneous scalar wave equation with inhomogeneous wave number

$$\nabla^2U(\mathbf{r},\omega) + k^2n^2(\mathbf{r},\omega)U(\mathbf{r},\omega) = 0. \tag{113}$$

To establish the relationship between the scattered field and the scatterer, it is convenient to write Eq. (113) in terms of a scattering potential $F(\mathbf{r},\omega)$, and we obtain the inhomogeneous wave equation or reduced wave equation given by

$$\nabla^2U(\mathbf{r},\omega) + k^2U(\mathbf{r},\omega) = -4\pi F(\mathbf{r},\omega)U(\mathbf{r},\omega), \tag{114}$$

where the scattering potential $F(\mathbf{r},\omega)$ is given by

$$F(\mathbf{r},\omega) = \frac{k^2}{4\pi}\left[n^2(\mathbf{r},\omega) - 1\right]. \tag{115}$$

Because, in the derivation of the scalar wave equation, $U(\mathbf{r},\omega)$ is one Cartesian component of the electric field, the refractive index is typically defined as $n^2 = \varepsilon(\mathbf{r})$, and in this framework the material is assumed to be nonmagnetic, i.e. the magnetic permeability $\mu(\mathbf{r}) = 1$. Alternatively, we may also take $U(\mathbf{r},\omega)$ to be a component

of the magnetic field and then derive the scattering potential from Eq. (112), and we would arrive at a similar definition of $F(\mathbf{r}, \omega)$. However, in such a case we define the refractive index in terms of the magnetic permeability,

$$n^2(\mathbf{r}) = \mu(\mathbf{r}), \tag{116}$$

and $\varepsilon(\mathbf{r}) = 1$. Defining the scattering potential in terms of its magnetic permeability, derived from the scalar magnetic wave equation, has interesting implications which will be discussed in section 3.3.2 and in Chapter 6.

Framing the problem in this form facilitates drawing parallels between optical and quantum mechanical scattering, since the quantum potential in the time-independent, non-relativistic Schrödinger equation plays the same role as the scattering potential $F(\mathbf{r}, \omega)$ in Eq. (114). We will apply quantum mechanical ideas to scattering theory to derive novel results in Chapters 4 and 5. Rearranging the scalar scattering problem in the form of an inhomogeneous Helmholtz equation (Eq. (114)) also elucidates its relationship to the *inverse source problem*: the determination of a source from its radiation pattern. Comparing Eq. (114) to

$$\nabla^2 u(\mathbf{r}, \omega) + k^2 u(\mathbf{r}, \omega) = -4\pi q(\mathbf{r}, \omega), \tag{117}$$

where $u(\mathbf{r}, \omega)$ is a scalar monochromatic field, $k = \omega/c$, and the source $q(\mathbf{r}, \omega)$ is restricted to its domain D, we see that the equations are identical if we identify

$$F(\mathbf{r}, \omega) U(\mathbf{r}, \omega) = q(\mathbf{r}, \omega) \tag{118}$$

and

$$U(\mathbf{r},\omega) = u(\mathbf{r},\omega). \tag{119}$$

The solution to Eq. (117) in terms of the Green's function for the Helmholtz equation,

$$u(\mathbf{r}) = \int_D q(\mathbf{r}')\frac{e^{ik|\mathbf{r}-\mathbf{r}'|}}{|\mathbf{r}-\mathbf{r}'|}\,\mathrm{d}^3r', \tag{120}$$

is, consequently, applicable to the scattering problem, as will now be formally derived.

An elegant way of describing the scattering process is to write the total field in two parts: the field incident upon the scatterer and the response of the scatterer embodied by the scattered field. If no object is present, the refractive index $n(\mathbf{r},\omega) = 1$ (equivalent to free space) and the scattering potential is zero, and we are left with only the incident field because the scattered field, the response to the scattering potential, must also be zero. Therefore, the total field $U(\mathbf{r},\omega)$ may be defined by

$$U(\mathbf{r},\omega) = U^{(i)}(\mathbf{r},\omega) + U^{(s)}(\mathbf{r},\omega), \tag{121}$$

where $U^{(i)}(\mathbf{r},\omega)$ is the incident field and $U^{(s)}(\mathbf{r},\omega)$ is the scattered field. The incident field is defined as satisfying the homogeneous Helmholtz equation

$$\left(\nabla^2 + k^2\right)U^{(i)}(\mathbf{r},\omega) = 0. \tag{122}$$

Suppose the incident field is a plane wave[4], given by

$$U^{(i)}(\mathbf{r},\omega) = U_0 e^{ik\hat{\mathbf{s}}_0\cdot\mathbf{r}}, \tag{123}$$

where U_0 is the complex amplitude and $\hat{\mathbf{s}}_0$ is the propagation direction. For now, we

[4]A plane is often used to approximate a beam or a distant source.

will assume that $U_0 = 1$. Upon substitution of Eqs. (121) and (122) into Eq. (115), we obtain

$$\big(\nabla^2 + k^2\big)U^{(s)}(\mathbf{r},\omega) = -4\pi F(\mathbf{r},\omega)U(\mathbf{r},\omega). \tag{124}$$

Since it is difficult to calculate the scattered field from the differential form of this equation, it is converted to integral form using the procedure outlined in [9, Chapter 13.1]. Let G denote the free-space Green's function for the Helmholtz operator, defined as a solution to

$$\big(\nabla^2 + k^2\big)G(\mathbf{r}-\mathbf{r}') = -4\pi\delta^{(3)}(\mathbf{r}-\mathbf{r}'), \tag{125}$$

where $\delta^{(3)}(\mathbf{r}-\mathbf{r}')$ is the three-dimensional Dirac delta function. Multiplying Eq. (124) by $G(\mathbf{r}-\mathbf{r}')$, Eq. (125) by $U^{(s)}(\mathbf{r},\omega)$, and subtracting the resulting equations from each other, we obtain

$$\begin{aligned} U^{(s)}(\mathbf{r},\omega)\nabla^2 G(\mathbf{r}-\mathbf{r}') - G(\mathbf{r}-\mathbf{r}')\nabla^2 U^{(s)}(\mathbf{r},\omega) = \\ 4\pi F(\mathbf{r},\omega)U(\mathbf{r},\omega)G(\mathbf{r}-\mathbf{r}') - 4\pi U^{(s)}(\mathbf{r},\omega)\delta^{(3)}(\mathbf{r}-\mathbf{r}'). \end{aligned} \tag{126}$$

Now we assume the Green's function is symmetric, i.e. that $G(\mathbf{r}-\mathbf{r}') = G(\mathbf{r}'-\mathbf{r})$, and interchange $\mathbf{r}$ and $\mathbf{r}'$, which converts $\nabla \to \nabla'$. Then it is possible to integrate both sides of Eq. (126) with respect to $\mathbf{r}'$ throughout volume V_R, bounded by a large sphere of surface S_R and radius R, centered on the origin O and containing the scatterer in its interior (Fig. 9), producing the following expression

$$\begin{aligned} &\int_{V_R}\Big[U^{(s)}(\mathbf{r}',\omega)\nabla^{2'}G(\mathbf{r}-\mathbf{r}') - G(\mathbf{r}-\mathbf{r}')\nabla^{2'}U^{(s)}(\mathbf{r}',\omega)\Big]\,\mathrm{d}^3r' = \\ &4\pi\int_V F(\mathbf{r}',\omega)U(\mathbf{r}',\omega)G(\mathbf{r}-\mathbf{r}')\,\mathrm{d}^3r' - 4\pi\int_{V_R} U^{(s)}(\mathbf{r}',\omega)\delta^{(3)}(\mathbf{r}-\mathbf{r}')\,\mathrm{d}^3r', \end{aligned} \tag{127}$$

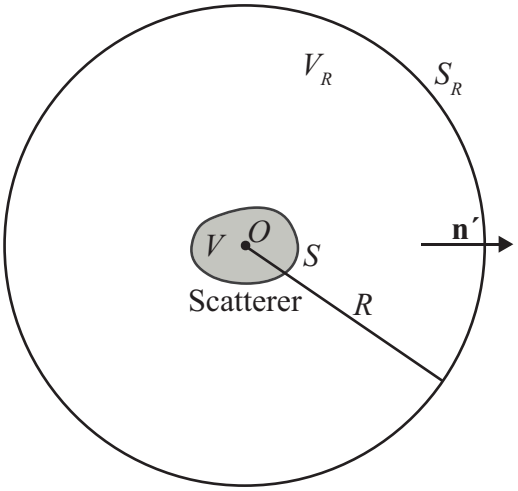

Figure 9: The scatterer is bounded by volume V and closed surface S and contains the origin O of the very large sphere S_R bounded by volume V_R and radius R. The outward normal is denoted by n'. After [9, Figure 13.2]

where we recognize that the last integral is simply $U^{(s)}(\mathbf{r}, \omega)$. The first integral is taken only over V because the scattering potential F is only nonzero within it. After reorganizing the terms and applying Green's second identity [9, Chapter 13.1] to convert the volume integral with respect to V_R to a surface integral, we obtain the following expression

$$\begin{aligned} U^{(s)}(\mathbf{r}, \omega) = &\int_V F(\mathbf{r}', \omega) U(\mathbf{r}', \omega) G(\mathbf{r} - \mathbf{r}') \, \mathrm{d}^3 r' \\ &- \frac{1}{4\pi} \int_{S_R} \left[U^{(s)}(\mathbf{r}', \omega) \frac{\partial G(\mathbf{r} - \mathbf{r}')}{\partial n'} - G(\mathbf{r} - \mathbf{r}') \frac{\partial U^{(s)}(\mathbf{r}', \omega)}{\partial n'} \right] \mathrm{d}S_R, \end{aligned} \tag{128}$$

where $\partial / \partial n'$ denotes differentiation along the outward normal n' to S_R. To ensure that the scattered field $U^{(s)}(\mathbf{r}, \omega)$ will behave like an outgoing spherical wave sufficiently far away from the scatterer, we select the the following symmetric Green's function

$$G(\mathbf{r} - \mathbf{r}') = \frac{e^{ik|\mathbf{r} - \mathbf{r}'|}}{|\mathbf{r} - \mathbf{r}'|}, \tag{129}$$

also known as the outgoing free-space Green's function of the Helmholtz operator, to

be the solution to Eq. (125). Under this condition, as $R \to \infty$, the surface integral vanishes [2], and the scattered field is given by

$$U^{(s)}(\mathbf{r},\omega) = \int_V F(\mathbf{r}',\omega)U(\mathbf{r}',\omega)\frac{e^{ik|\mathbf{r}-\mathbf{r}'|}}{|\mathbf{r}-\mathbf{r}'|}\,\mathrm{d}^3r', \tag{130}$$

which is very similar to Eq. (120) if Eq. (118) is substituted. Recall that the total field is the sum of the scattered and the incident fields (Eq. (121)), and assuming the incident field is a plane wave (Eq. (123)) with a real unit amplitude, the total field is

$$U(\mathbf{r},\omega) = e^{ik\hat{\mathbf{s}}_0\cdot\mathbf{r}} + \int_V F(\mathbf{r}',\omega)U(\mathbf{r}',\omega)\frac{e^{ik|\mathbf{r}-\mathbf{r}'|}}{|\mathbf{r}-\mathbf{r}'|}\,\mathrm{d}^3r', \tag{131}$$

and is called the *integral equation of potential scattering*. It is the basic equation used to determine the total field U, which appears on both sides of the equation and is, consequently, difficult to solve. Therefore, Eq. (131) is typically discretized for numerical computation of both the scattered and total fields, as shown in Chapter 4, section 4.3. It is important to note that Eq. (131) is used in the following manner: within the scattering volume V it is an integral equation for the total field $U(\mathbf{r},\omega)$, since $F(\mathbf{r},\omega)$ is only nonzero within V. Once the interior solution throughout V is known, the solution at points exterior to V may be calculated by substituting the interior solution into Eq. (131) [9, Chapter 13.1.1].

In contrast to Eq. (124), any solution to Eq. (131) will have the correct outgoing behavior far away from the scatterer as a result of the choice of the Green's function in Eq. (129), and this can be shown as follows.

Let Q be any point within the scattering volume V and P be a point far away from V. If $\mathbf{r}'$ is the position vector of Q, $\mathbf{r} = r\hat{\mathbf{s}}$ ($\hat{\mathbf{s}}^2 = 1$) is the position vector of P, and

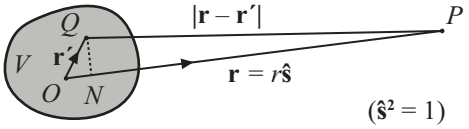

Figure 10: The scatterer is shown with annotated points inside and outside the scatterer to understand the approximations in Eqs. (132) − (136). After [9], Figure 13.3.

N is the foot of the perpendicular from Q to OP, then when r is large enough,

$$|\mathbf{r} - \mathbf{r}'| \sim r - \hat{\mathbf{s}} \cdot \mathbf{r}', \tag{132}$$

and

$$\frac{e^{ik|\mathbf{r}-\mathbf{r}'|}}{|\mathbf{r} - \mathbf{r}'|} \sim \frac{e^{ikr}}{r} e^{-ik\hat{\mathbf{s}}\cdot\mathbf{r}'}. \tag{133}$$

On substitution of Eq. (133) in Eq. (131), it reduces to

$$U(r\hat{\mathbf{s}}, \omega) \sim e^{ik\hat{\mathbf{s}}_0\cdot\mathbf{r}} + U^{(s)}(r\hat{\mathbf{s}}, \omega), \tag{134}$$

where $\hat{\mathbf{s}}_0$ is the direction of incidence and

$$U^{(s)}(r\hat{\mathbf{s}}, \omega) = f(\hat{\mathbf{s}}, \hat{\mathbf{s}}_0; \omega)\frac{e^{ikr}}{r}, \tag{135}$$

and

$$f(\hat{\mathbf{s}}, \hat{\mathbf{s}}_0; \omega) = \int_V F(\mathbf{r}', \omega) U(\mathbf{r}', \omega) e^{ik\hat{\mathbf{s}}\cdot\mathbf{r}'} \, \mathrm{d}^3 r', \tag{136}$$

where $f(\hat{\mathbf{s}}, \hat{\mathbf{s}}_0; \omega)$ is called the *scattering amplitude*. From Eq. (135), it can be seen that as $r \to \infty$ the scattered field does behave as an outgoing spherical wave. The scattering amplitude defined by Eq. (136) plays an important role in scattering theory and is a central parameter in the optical cross-section theorem.

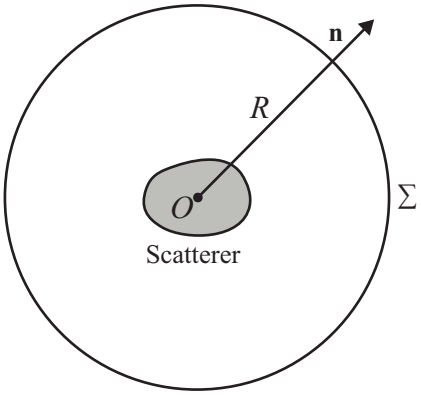

Figure 11: Illustration of scatterer, outward normal vector, and integration surface Σ. After [9, Figure 13.13]

3.2 The optical cross-section theorem

Another way of characterizing the processes associated with scattering is by quantifying the rate at which energy is scattered and absorbed by the object in response to the incident field. The optical cross-section theorem relates these properties to the scattering amplitude, and reveals a relationship between the forward (in the direction of incidence) scattering amplitude and the rate at which energy is removed from the incident field. In electromagnetic theory, energy propagation is represented by the Poynting vector, but in scalar wave theory it is the *energy flux vector* that represents energy propagation [9, Chapter 13.3] with complex representation $U(\mathbf{r})$, which we will now define.

The average value of the energy flux vector over a period that is long compared to the wavelength is given by the expression

$$\langle \mathbf{F}(\mathbf{r}) \rangle = -i\beta[U^\star \nabla U - U \nabla U^\star], \tag{137}$$

where β is a positive constant. We assume a plane monochromatic wave of unit

amplitude (Eq. (123)) is incident on the scatterer in the direction $\hat{\mathbf{s}}_0$ and that the total field is composed of the incident and scattered field (Eq. (121)). Substituting Eq. (121) into Eq. (137) reveals that the total energy flux may be separated into contributions from the incident field $\langle \mathbf{F}^{(i)}(\mathbf{r}) \rangle$, the scattered field $\langle \mathbf{F}^{(s)}(\mathbf{r}) \rangle$, and their cross-terms $\langle \mathbf{F}^{(c)}(\mathbf{r}) \rangle$, and is given by

$$\langle \mathbf{F}(\mathbf{r}) \rangle = \langle \mathbf{F}^{(i)}(\mathbf{r}) \rangle + \langle \mathbf{F}^{(s)}(\mathbf{r}) \rangle + \langle \mathbf{F}^{(c)}(\mathbf{r}) \rangle, \tag{138}$$

where

$$\langle \mathbf{F}^{(i)}(\mathbf{r}) \rangle = -i\beta [U^{(i)\star} \nabla U^{(i)} - U^{(i)} \nabla U^{(i)\star}], \tag{139}$$

$$\langle \mathbf{F}^{(s)}(\mathbf{r}) \rangle = -i\beta [U^{(s)\star} \nabla U^{(s)} - U^{(s)} \nabla U^{(s)\star}], \tag{140}$$

$$\langle \mathbf{F}^{(c)}(\mathbf{r}) \rangle = -i\beta [U^{(i)\star} \nabla U^{(s)} - U^{(s)} \nabla U^{(i)\star} - U^{(i)} \nabla U^{(s)\star} + U^{(s)\star} \nabla U^{(i)}]. \tag{141}$$

Let us now consider the outward flow of energy through a surface of a large sphere Σ of radius R, centered at some point O in the region occupied by the scatterer (Fig. 11). It is given by the expression

$$\mathcal{W} = \iint_{\Sigma} \langle \mathbf{F}(\mathbf{r}) \rangle \cdot \, \mathrm{d}\vec{\mathbf{S}}, \tag{142}$$

where in three-dimensional space $\mathrm{d}\vec{\mathbf{S}} = \hat{\mathbf{n}} \, \mathrm{d}\Sigma$, and $\hat{\mathbf{n}}$ is the outward unit normal to the surface Σ. In two dimensions, instead of integrating over the surface area, we integrate over the circumference of the sphere L, and $\mathrm{d}\vec{\mathbf{S}} = \hat{\mathbf{n}} \, \mathrm{d}l$, where $\hat{\mathbf{n}}$ is the outward unit normal to L. Therefore Eq. (142) reduces to

$$\mathcal{W} = \int_{L} \langle \mathbf{F}(\mathbf{r}) \rangle \cdot \hat{\mathbf{n}} \, \mathrm{d}l. \tag{143}$$

If the scatterer is a dielectric (i.e. a nonabsorbing medium), this integral will be zero because energy will neither be created nor destroyed by scattering. However, if the scatterer absorbs energy (for example, it is a conductor), the law of conservation of energy demands that the net outward energy flux through the surface Σ is equal to the rate $\mathcal{W}^{(a)}$ at which absorption takes place

$$\mathcal{W} = -\mathcal{W}^{(a)} = \mathcal{W}^{(s)} + \mathcal{W}^{(i)} + \mathcal{W}^{(c)}. \tag{144}$$

By definition of the incident field, evaluation of the integral defining $\mathcal{W}^{(i)}$ reveals that $\mathcal{W}^{(i)} = 0$. By substituting Eq. (138) into Eq. (142) and using Eq. (144) we obtain

$$\begin{aligned} -\mathcal{W}^{(c)} &= \mathcal{W}^{(s)} + \mathcal{W}^{(a)} \\ &= i\beta \int (U^{(i)\star}\nabla U^{(s)} - U^{(s)}\nabla U^{(i)\star} - U^{(i)}\nabla U^{(s)\star} + U^{(s)\star}\nabla U^{(i)}) \cdot \mathrm{d}\vec{\mathbf{S}}. \end{aligned} \tag{145}$$

In the far field, the scattered field $U^{(s)}(\mathbf{r}, \omega)$ takes the form of an outgoing Green's function $G(r)$ and is a function of the scattering amplitude $f(\hat{\mathbf{s}}, \hat{\mathbf{s}}_0; \omega)$ (Eq. (135)), given by

$$U^{(s)}(r\hat{\mathbf{s}}, \omega) = f(\hat{\mathbf{s}}, \hat{\mathbf{s}}_0; \omega) G(r), \tag{146}$$

where the $G(r)$ may be the three-dimensional Green's function,

$$G_{3D}(r) = \frac{e^{ikr}}{r}, \tag{147}$$

and the scattering amplitude is given by

$$f(\hat{\mathbf{s}}, \hat{\mathbf{s}}_0; \omega) = \int_V F(\mathbf{r}', \omega) U(\mathbf{r}', \omega) e^{ik\hat{\mathbf{s}}\cdot\mathbf{r}'} \, \mathrm{d}^3 r'. \tag{148}$$

Again, we require the Green's function to be a solution of the Helmholtz operator

(Eq. (125)). Since the scattering simulations are performed in two-dimensional space, we also present the corresponding equations used in Chapters 4, 5, and 6. The two dimensional Green's function[5], evaluated such that the scattered field approximates an outgoing cylindrical wave far away from the scatterer [30, Pages 678–679], is

$$G_{2D}(r) = i\pi H_0^{(1)}(kr). \tag{149}$$

The Hankel function $H_0^1(kr)$ is composed of the Bessel J_0 and Neumann N_0 functions, and for large r the behavior of the zeroeth order Bessel and Neumann functions can be calculated using the stationary phase method [30, pages 566–567]. Consequently the Hankel function may be rewritten as follows:

$$\begin{aligned} H_0^{(1)}(kr) &= J_0(kr) + iN_0(x), \\ J_0(kr) &\approx \sqrt{\frac{2}{\pi kr}}[\cos(kr - \pi/4)], \\ N_0(kr) &\approx \sqrt{\frac{2}{\pi kr}}[\sin(kr - \pi/4)], \\ H_0^{(1)}(kr) &\approx \sqrt{\frac{2}{\pi kr}} e^{i(kr-\pi/4)}. \end{aligned} \tag{150}$$

Combining Eqs. (135), (149), and (150) gives us the following definition for the scattered field

$$\begin{aligned} U^{(s)}(r\hat{\mathbf{s}}, \omega) &= f(\hat{\mathbf{s}}, \hat{\mathbf{s}}_0; \omega) i\pi \sqrt{\frac{2}{\pi kr}} e^{i(kr-\pi/4)} \\ &= f(\hat{\mathbf{s}}, \hat{\mathbf{s}}_0; \omega) i \sqrt{\frac{2\pi}{kr}} e^{i(kr-\pi/4)} \end{aligned} \tag{151}$$

Next, we calculate the components of $U^{(i)\star}\nabla U^{(s)} - U^{(s)}\nabla U^{(i)\star}$ from Eq. (145). $U^{(i)\star}$

[5]In the two-dimensional case, $G_{2D}(r) = A_+ H_0^{(1)}(kr)$ so that the scattered field approximates an outgoing cylindrical wave far away from the scatterer. The constant may be evaluated by integrating the Helmholtz equation for two dimensions around a small circle, as shown in [30, Pages 678–679].

is given by

$$U^{(i)\star} = e^{-ik\hat{\mathbf{s}}_0\cdot\mathbf{r}} = e^{-ikr\hat{\mathbf{s}}_0\cdot\hat{\mathbf{s}}}. \tag{152}$$

The quantity $\nabla U^{(i)\star}$ is

$$\nabla U^{(i)\star} = \nabla e^{-ikr\hat{\mathbf{s}}_0\cdot\hat{\mathbf{s}}} = -ik\hat{\mathbf{s}}e^{-ikr\hat{\mathbf{s}}_0\cdot\hat{\mathbf{s}}}. \tag{153}$$

In the far field the following approximation holds, as follows

$$\nabla\frac{1}{\sqrt{kr}}e^{ikr\hat{\mathbf{s}}\cdot\hat{\mathbf{s}}} \approx ik\hat{\mathbf{s}}\frac{1}{\sqrt{kr}}e^{ikr\hat{\mathbf{s}}\cdot\hat{\mathbf{s}}}. \tag{154}$$

Using Eq. (151), the gradient of the scattered field is given by

$$\begin{aligned}\nabla U^{(s)} &= \nabla\left(f(\hat{\mathbf{s}},\hat{\mathbf{s}}_0;\omega)i\sqrt{\frac{2\pi}{kr}}e^{i(kr\hat{\mathbf{s}}\cdot\hat{\mathbf{s}}-\pi/4)}\right)\\ &= f(\hat{\mathbf{s}},\hat{\mathbf{s}}_0;\omega)\cdot\nabla\left[i\sqrt{\frac{2\pi}{kr}}e^{i(kr\hat{\mathbf{s}}\cdot\hat{\mathbf{s}}-\pi/4)}\right]\\ &= -f(\hat{\mathbf{s}},\hat{\mathbf{s}}_0;\omega)\cdot k\hat{\mathbf{s}}\sqrt{\frac{2\pi}{kr}}e^{i(kr\hat{\mathbf{s}}\cdot\hat{\mathbf{s}}-\pi/4)}.\end{aligned} \tag{155}$$

Combining the last three results, the first term of the integral given by Eq. (145) is

$$U^{(i)\star}\nabla U^{(s)} = -f(\hat{\mathbf{s}},\hat{\mathbf{s}}_0;\omega)e^{-ikr\hat{\mathbf{s}}_0\cdot\hat{\mathbf{s}}}\cdot k\hat{\mathbf{s}}\sqrt{\frac{2\pi}{kr}}e^{i(kr\hat{\mathbf{s}}\cdot\hat{\mathbf{s}}-\pi/4)}. \tag{156}$$

The second term of the integral is given by

$$\begin{aligned}U^{(s)}\nabla U^{(i)\star} &= f(\hat{\mathbf{s}},\hat{\mathbf{s}}_0;\omega)i\sqrt{\frac{2\pi}{kr}}e^{i(kr\hat{\mathbf{s}}\cdot\hat{\mathbf{s}}-\pi/4)}\cdot(-ik)\hat{\mathbf{s}}_0e^{-ikr\hat{\mathbf{s}}_0\cdot\hat{\mathbf{s}}}\\ &= f(\hat{\mathbf{s}},\hat{\mathbf{s}}_0;\omega)\sqrt{\frac{2\pi}{kr}}k\hat{\mathbf{s}}_0e^{-ikr\hat{\mathbf{s}}_0\cdot\hat{\mathbf{s}}}.\end{aligned} \tag{157}$$

The integrand may then be simplified to

$$\begin{aligned}
&U^{(i)\star}\nabla U^{(s)} - U^{(s)}\nabla U^{(i)\star} \\
&\qquad = -f(\hat{\mathbf{s}},\hat{\mathbf{s}}_0;\omega)\left(e^{-ikr\hat{\mathbf{s}}_0\cdot\hat{\mathbf{s}}}k\hat{\mathbf{s}}\sqrt{\frac{2\pi}{kr}}e^{i(kr\hat{\mathbf{s}}\cdot\hat{\mathbf{s}}-\pi/4)} + \sqrt{\frac{2\pi}{kr}}e^{i(kr\hat{\mathbf{s}}\cdot\hat{\mathbf{s}}-\pi/4)}k\hat{\mathbf{s}}_0 e^{-ikr\hat{\mathbf{s}}_0\cdot\hat{\mathbf{s}}}\right) \\
&\qquad = -f(\hat{\mathbf{s}},\hat{\mathbf{s}}_0;\omega)\sqrt{\frac{2\pi}{kr}}e^{i(kr\hat{\mathbf{s}}\cdot\hat{\mathbf{s}}-\pi/4)}e^{-ikr\hat{\mathbf{s}}_0\cdot\hat{\mathbf{s}}}\cdot k(\hat{\mathbf{s}}+\hat{\mathbf{s}}_0) \\
&\qquad = -f(\hat{\mathbf{s}},\hat{\mathbf{s}}_0;\omega)\sqrt{\frac{2\pi}{kr}}e^{-i\pi/4}\cdot k(\hat{\mathbf{s}}+\hat{\mathbf{s}}_0)e^{-ikr\hat{\mathbf{s}}\cdot(\hat{\mathbf{s}}_0-\hat{\mathbf{s}})}
\end{aligned} \tag{158}$$

Now we calculate the energy flux as in Eq. (145) by integrating Eq. (158) multiplied by $\hat{\mathbf{n}}\,\mathrm{d}l = \hat{\mathbf{s}}r\,\mathrm{d}\phi$ (two-dimensional case), take $\hat{\mathbf{s}}_0\cdot\mathbf{r} = r\cos\phi$ and take ϕ to be the angle between $\hat{\mathbf{s}}$ and $\hat{\mathbf{s}}_0$ where $\mathbf{r} = r\hat{\mathbf{s}}$.

$$\begin{aligned}
&\int \left[U^{(i)\star}\nabla U^{(s)} - U^{(s)}\nabla U^{(i)\star}\right]\cdot\hat{\mathbf{s}}\,\mathrm{d}l \\
&\qquad = -e^{-i\pi/4}k\sqrt{\frac{2\pi}{kr}}\int_{-\pi}^{\pi} f(\hat{\mathbf{s}},\hat{\mathbf{s}}_0;\omega)\cdot(\hat{\mathbf{s}}+\hat{\mathbf{s}}_0)e^{-ikr\hat{\mathbf{s}}\cdot(\hat{\mathbf{s}}_0-\hat{\mathbf{s}})}\cdot\hat{\mathbf{s}}r\,\mathrm{d}\phi \\
&\qquad = -e^{-i\pi/4}kr\sqrt{\frac{2\pi}{kr}}\underbrace{\int_{-\pi}^{\pi} f(\hat{\mathbf{s}},\hat{\mathbf{s}}_0;\omega)\cdot(1+\cos\phi)e^{-ikr(\cos\phi-1)}\,\mathrm{d}\phi}_{\text{stationary phase!}}
\end{aligned} \tag{159}$$

This integral can be simplified via the *method of stationary phase* which is valid in the far field [30, Page 566].

$$\begin{aligned}
F(k) &= \int_a^b f(x)e^{ikg(x)}\,\mathrm{d}x \\
&\approx f(x_0)e^{ikg(x_0)}e^{i\pi/4}\sqrt{\frac{2\pi}{g''(x_0)k}},
\end{aligned} \tag{160}$$

where

$$
\begin{aligned}
x_0 &\leftrightarrow \phi = 0, \hat{\mathbf{s}} = \hat{\mathbf{s}}_0, \\
f(x) &\leftrightarrow -[1+\cos\phi] f(\hat{\mathbf{s}}, \hat{\mathbf{s}}_0), \\
g(x) &\leftrightarrow -[\cos\phi - 1], \\
g''(x) &\leftrightarrow \cos\phi, \\
k &\leftrightarrow kr. \\
F(k) &\approx f(x_0) e^{ikg(x_0)} e^{i\pi/4} \sqrt{\frac{2\pi}{g''(x_0)k}}.
\end{aligned} \tag{161}
$$

If we apply Eq. (161) to the energy flux integral, given by Eq. (158), we obtain

$$
\begin{aligned}
&\int \left[U^{(i)\star} \nabla U^{(s)} - U^{(s)} \nabla U^{(i)\star}\right] \cdot \hat{\mathbf{s}} \, \mathrm{d}l \\
&= -e^{-i\pi/4} kr \sqrt{\frac{2\pi}{kr}} \int_{-\pi}^{\pi} f(\hat{\mathbf{s}}, \hat{\mathbf{s}}_0; \omega) \cdot (1+\cos\phi) e^{-ikr(\cos\phi - 1)} \, \mathrm{d}\phi \\
&= -e^{-i\pi/4} kr \sqrt{\frac{2\pi}{kr}} 2 f(\hat{\mathbf{s}}_0, \hat{\mathbf{s}}_0; \omega) e^{i\pi/4} \sqrt{\frac{2\pi}{kr}} \\
&= -4\pi f(\hat{\mathbf{s}}_0, \hat{\mathbf{s}}_0; \omega).
\end{aligned} \tag{162}
$$

Now, we are in a position to apply the relationship in Eq. (162) to Eq. (145) and obtain the rate of dissipated energy, given by

$$
\begin{aligned}
\mathcal{W}^{(s)} + \mathcal{W}^{(a)} &= i\beta \int (U^{(i)\star} \nabla U^{(s)} - U^{(s)} \nabla U^{(i)\star} - U^{(i)} \nabla U^{(s)\star} + U^{(s)\star} \nabla U^{(i)}) \cdot \hat{\mathbf{n}} \, \mathrm{d}l \\
&= -i\beta \left[4\pi f(\hat{\mathbf{s}}_0, \hat{\mathbf{s}}_0; \omega) - 4\pi f^{\star}(\hat{\mathbf{s}}_0, \hat{\mathbf{s}}_0; \omega)\right] \\
&= 8\pi\beta \mathrm{Im}\{f(\hat{\mathbf{s}}_0, \hat{\mathbf{s}}_0; \omega)\},
\end{aligned} \tag{163}
$$

where Im refers to the imaginary part of the expression. Eq. (163) indicates that the rate of energy removed from the incident field by scattering and absorption is

proportional to the imaginary part of the forward scattering amplitude $f(\hat{\mathbf{s}}_0, \hat{\mathbf{s}}_0; \omega)$, the scattering amplitude $f(\hat{\mathbf{s}}, \hat{\mathbf{s}}_0; \omega)$ evaluated at $\hat{\mathbf{s}} = \hat{\mathbf{s}}_0$. The ratio $Q^{(ext)}$ between the rate of dissipated energy (Eq. (145)) and the rate at which energy is incident on a unit cross-sectional area of the scatterer perpendicular to the direction of propagation $\hat{\mathbf{s}}_0$, $|\langle \mathbf{F}^{(i)}(\mathbf{r}) \rangle|$ (magnitude of Eq. (139)),

$$|\langle \mathbf{F}^{(i)}(\mathbf{r}) \rangle| = 2\beta k \hat{\mathbf{s}}_0, \tag{164}$$

is called the extinction cross-section. It is given by

$$Q^{(ext)} = \frac{4\pi}{k} \mathrm{Im}\{f(\hat{\mathbf{s}}_0, \hat{\mathbf{s}}_0; \omega)\}. \tag{165}$$

Eq. (165) is the mathematical expression for the optical cross-section theorem, also known as the optical theorem. It was first derived in English for an arbitrary obstacle by van de Hulst [34] in classical optics, but this relationship was expressed earlier by Bricard in his study of a spherical water drop [10] and was derived from an analogous theorem describing atomic collisions [20]. The absorption and scattering cross-sections, $Q^{(abs)}$ and $Q^{(sca)}$, are defined similarly by

$$Q^{(sca)} = \frac{\mathcal{W}^{(s)}}{|\langle \mathbf{F}^{(i)}(\mathbf{r}) \rangle|} \qquad\qquad Q^{(abs)} = \frac{\mathcal{W}^{(a)}}{|\langle \mathbf{F}^{(i)}(\mathbf{r}) \rangle|}, \tag{166}$$

where $\mathcal{W}^{(s)}$ is the energy flow associated with the scattered field and $\mathcal{W}^{(a)}$ is the energy flow associated with absorption. To express the scattering cross-section in terms of the scattering amplitude, recall that the flow of scattered energy $\mathcal{W}^{(s)}$ is defined by Eq. (142) using the definition for the scattered flux $\langle \mathbf{F}^{(s)}(\mathbf{r}) \rangle$ given by Eq. (140). For a point in the far zone at distance R from the scatterer, the scattered flux $\langle \mathbf{F}^{(s)}(\mathbf{r}) \rangle$

in direction $\hat{\mathbf{s}}$ may be rewritten in terms of the scattering amplitude by substituting Eq. (146) into Eq. (140) resulting in

$$\langle \mathbf{F}^{(s)}(\mathbf{r}) \rangle \approx \frac{2\beta k}{R^2} |f(\hat{\mathbf{s}}, \hat{\mathbf{s}}_0; \omega)|^2 \hat{\mathbf{s}}, \qquad \text{as } R \to \infty \text{ with } \hat{\mathbf{s}} \text{ fixed.} \tag{167}$$

The rate at which the scattered energy crosses the scatterer using $\hat{\mathbf{n}} = \hat{\mathbf{s}}$ in Eqs. (140), and (143) is given by

$$\mathcal{W}^{(s)} = 2\beta k \iint_{\Sigma} \langle \mathbf{F}^{(s)}(\mathbf{r}) \rangle \cdot \hat{\mathbf{s}} \, \mathrm{d}\Sigma = 2\beta k \int_{4\pi} |f(\hat{\mathbf{s}}, \hat{\mathbf{s}}_0; \omega)|^2 \, \mathrm{d}\Omega, \tag{168}$$

where $\mathrm{d}\Omega = \mathrm{d}\Sigma / R^2$ is the element of solid angle subtended at the origin O by the element $\mathrm{d}\Sigma$ and the integration extends over the whole 4π solid angle of directions $\hat{\mathbf{s}}$. After applying this result in Eq. (166) with Eq. (139), the scattering cross-section for the three dimensional case is given by

$$Q^{(sca)} = \int_{4\pi} |f(\hat{\mathbf{s}}, \hat{\mathbf{s}}_0; \omega)|^2 \, \mathrm{d}\Omega. \tag{169}$$

For two-dimensional calculations, Eq. (169) becomes

$$Q^{(sca)} = \int_{L} |f(\hat{\mathbf{s}}, \hat{\mathbf{s}}_0; \omega)|^2 \, \mathrm{d}l, \tag{170}$$

where L is a bounded line enclosing the scatterer. The conditions for invisibility are that, when the incident field is propagating in the invisibility direction, both the extinction cross-section $Q^{(ext)}$ and the scattering cross-section $Q^{(sca)}$ are equal to zero. To calculate the scattering cross-section, we use the definition of the scattering amplitude given by Eq. (151) in Eq. (170) and obtain

$$Q^{(sca)} = -i\sqrt{\frac{kr}{2\pi}} e^{-i\left(kr - \frac{\pi}{4}\right)} \int_{L} |U^{(s)}(\mathbf{r})|^2 \, \mathrm{d}l, , \tag{171}$$

where the scattering cross-section is now defined in terms of the scattered field. We make use of this relationship to numerically calculate the scattering cross-section for a variety of invisible objects.

3.3 Electromagnetic scattering theory

3.3.1 The Electric field vector wave equation

Previously, we considered the scalar wave equation. Now, we present scattering theory in terms of the vector wave equation. We begin with the monochromatic forms of Faraday's Law and the Maxwell-Ampère Law (Chapter 2, Section 2.1),

$$\nabla \times \mathbf{E}(\mathbf{r}) = ik\mathbf{B}(\mathbf{r}), \tag{172}$$

$$\nabla \times \mathbf{B}(\mathbf{r}) = -ik\overleftrightarrow{\boldsymbol{\varepsilon}}(\mathbf{r}) \cdot \mathbf{E}(\mathbf{r}), \tag{173}$$

where $\overleftrightarrow{\boldsymbol{\varepsilon}}$ is the electric permittivity tensor, the scatterer consists of a nonmagnetic material, $\overleftrightarrow{\boldsymbol{\mu}} = \overleftrightarrow{\mathbf{I}}$ ($\overleftrightarrow{\mathbf{I}}$ is the identity matrix) and we have substituted Eq. (101) for $\mathbf{D}(\mathbf{r})$. If we take the curl of Eq. (172) and substitute Eq. (173) into the result, we obtain

$$\nabla \times [\nabla \times \mathbf{E}(\mathbf{r})] = k^2 \overleftrightarrow{\boldsymbol{\varepsilon}}(\mathbf{r}) \cdot \mathbf{E}(\mathbf{r}). \tag{174}$$

Rearranging the terms, we obtain the familiar homogeneous electric field vector wave equation with inhomogeneous wave number,

$$\nabla \times [\nabla \times \mathbf{E}(\mathbf{r})] - k^2 \overleftrightarrow{\boldsymbol{\varepsilon}}(\mathbf{r}) \cdot \mathbf{E}(\mathbf{r}) = 0. \tag{175}$$

To restate this equation in terms of a scattering potential dyadic, we write the total field in terms of its components, $\mathbf{E}(\mathbf{r}) = \mathbf{E}^{(i)}(\mathbf{r}) + \mathbf{E}^{(s)}(\mathbf{r})$, on the left side of the

equation and subtract $k^2\mathbf{E}$ from both sides, resulting in the expression

$$\nabla \times \left\{\nabla \times \left[\mathbf{E}^{(i)}(\mathbf{r}) + \mathbf{E}^{(s)}(\mathbf{r})\right]\right\} - k^2 \left[\mathbf{E}^{(i)}(\mathbf{r}) + \mathbf{E}^{(s)}(\mathbf{r})\right] = k^2 \left[\overleftrightarrow{\boldsymbol{\varepsilon}}(\mathbf{r}) - \overleftrightarrow{\mathbf{I}}\right] \cdot \mathbf{E}(\mathbf{r}). \quad (176)$$

Realizing that, by definition, $\nabla \times \left[\nabla \times \mathbf{E}^{(i)}(\mathbf{r})\right] - k^2\mathbf{E}^{(i)}(\mathbf{r}) = 0$, and rearranging the terms, an inhomogeneous wave equation is produced with

$$\nabla \times \left[\nabla \times \mathbf{E}^{(s)}(\mathbf{r})\right] - k^2\mathbf{E}^{(s)}(\mathbf{r}) = 4\pi \overleftrightarrow{\mathbf{F}}_E(\mathbf{r}) \cdot \mathbf{E}(\mathbf{r}), \quad (177)$$

where $\overleftrightarrow{\mathbf{F}}(\mathbf{r})$ is the scattering dyadic, defined as

$$\overleftrightarrow{\mathbf{F}}_E(\mathbf{r}) = \frac{k^2}{4\pi} \left[\overleftrightarrow{\boldsymbol{\varepsilon}}(\mathbf{r}) - \overleftrightarrow{\mathbf{I}}\right]. \quad (178)$$

This equation is analogous to the scalar scattering potential, where we examine the behavior of one component of the electric field, usually the transverse-electric (TE) component, $\overleftrightarrow{\boldsymbol{\varepsilon}}(\mathbf{r})$ is simplified to $\varepsilon(\mathbf{r})$ and $\overleftrightarrow{\mathbf{I}}$ becomes 1.

We may also consider the case when both the permittivity and the permeability are spatially varying tensors, $\overleftrightarrow{\boldsymbol{\varepsilon}}(\mathbf{r})$ and $\overleftrightarrow{\boldsymbol{\mu}}(\mathbf{r})$. We begin with Faraday's and the Maxwell-Ampère Laws in terms of the magnetic field $\mathbf{H}(\mathbf{r})$,

$$\nabla \times \mathbf{E}(\mathbf{r}) = ik\overleftrightarrow{\boldsymbol{\mu}}(\mathbf{r}) \cdot \mathbf{H}(\mathbf{r}), \quad (179)$$

$$\nabla \times \mathbf{H}(\mathbf{r}) = -ik\overleftrightarrow{\boldsymbol{\varepsilon}}(\mathbf{r}) \cdot \mathbf{E}(\mathbf{r}). \quad (180)$$

Taking the curl of Eq. (179) and substituting Eq. (180), we obtain

$$\nabla \times [\nabla \times \mathbf{E}(\mathbf{r})] - ik\nabla \times \overleftrightarrow{\boldsymbol{\mu}} \cdot \mathbf{H}(\mathbf{r}) - k^2 \overleftrightarrow{\boldsymbol{\mu}}(\mathbf{r}) \cdot \overleftrightarrow{\boldsymbol{\varepsilon}}(\mathbf{r}) \cdot \mathbf{E}(\mathbf{r}) = 0. \quad (181)$$

Next, we rewrite Eq. (179) in terms of $\mathbf{E}(\mathbf{r})$ to eliminate the remaining $\mathbf{H}(\mathbf{r})$ from

Eq. (181),

$$\nabla \times [\nabla \times \mathbf{E}(\mathbf{r})] - \left[\nabla \times \overleftrightarrow{\boldsymbol{\mu}}(\mathbf{r})\right] \cdot \overleftrightarrow{\boldsymbol{\mu}}^{-1}(\mathbf{r}) \cdot \nabla \times \mathbf{E}(\mathbf{r}) - k^2 \overleftrightarrow{\boldsymbol{\mu}}(\mathbf{r}) \cdot \overleftrightarrow{\boldsymbol{\varepsilon}}(\mathbf{r}) \cdot \mathbf{E}(\mathbf{r}) = 0, \quad (182)$$

Rearranging the terms in Eq. (182) and subtracting $-k^2\mathbf{E}$ from both sides, we may rewrite it as

$$\nabla \times [\nabla \times \mathbf{E}(\mathbf{r})] - k^2\mathbf{E}(\mathbf{r}) = -k^2\mathbf{E}(\mathbf{r}) + [\nabla \times \overleftrightarrow{\boldsymbol{\mu}}(\mathbf{r})] \cdot \overleftrightarrow{\boldsymbol{\mu}}^{-1}(\mathbf{r}) \cdot \nabla \times \mathbf{E}(\mathbf{r}) + k^2 \overleftrightarrow{\boldsymbol{\mu}}(\mathbf{r}) \cdot \overleftrightarrow{\boldsymbol{\varepsilon}}(\mathbf{r}) \cdot \mathbf{E}(\mathbf{r}), \quad (183)$$

where the left side of the equation is now written with a homogeneous wave number k. Finally, realizing that $\nabla \times \left[\nabla \times \mathbf{E}^{(i)}(\mathbf{r})\right] - k^2\mathbf{E}^{(i)}(\mathbf{r}) = 0$, we may rewrite this equation in its inhomogeneous form in terms of a more complete scattering potential tensor operator $\overleftrightarrow{\mathbf{F}}(\mathbf{r})$, given by

$$\nabla \times \left[\nabla \times \mathbf{E}^{(s)}(\mathbf{r})\right] - k^2\mathbf{E}^{(s)}(\mathbf{r}) = 4\pi \overleftrightarrow{\mathbf{F}}_E(\mathbf{r}) \cdot \mathbf{E}(\mathbf{r}), \quad (184)$$

where the tensor operator $\overleftrightarrow{\mathbf{F}}_E(\mathbf{r})$ is given by

$$\overleftrightarrow{\mathbf{F}}_E(\mathbf{r}) = \frac{k^2}{4\pi} \left\{ \overleftrightarrow{\boldsymbol{\mu}}(\mathbf{r}) \cdot \overleftrightarrow{\boldsymbol{\varepsilon}}(\mathbf{r}) - \overleftrightarrow{\mathbf{I}} + \frac{1}{k^2} \left[\nabla \times \overleftrightarrow{\boldsymbol{\mu}}(\mathbf{r})\right] \cdot \overleftrightarrow{\boldsymbol{\mu}}^{-1}(\mathbf{r}) \cdot \nabla \times \right\}. \quad (185)$$

Eqs. (184) and (185) allows greater flexibility in designing scatterers with specific properties as will be shown in the remainder of this text. This scattering potential operator is simplified to the earlier expression for the scattering potential (Eq. (178)), if the permeability tensor is defined as $\overleftrightarrow{\boldsymbol{\mu}}(\mathbf{r}) = \boldsymbol{\mu}(\mathbf{r})\overleftrightarrow{\mathbf{I}}$. If the permeability is defined as a scalar function of $\mathbf{r}$, the scattering potential reduces to

$$\overleftrightarrow{\mathbf{F}}_E(\mathbf{r}) = \frac{k^2}{4\pi} \left[\boldsymbol{\mu}(\mathbf{r}) \cdot \overleftrightarrow{\boldsymbol{\varepsilon}}(\mathbf{r}) - \overleftrightarrow{\mathbf{I}}\right], \quad (186)$$

since $\boldsymbol{\mu}^{-1}(\mathbf{r}) = \nabla \ln \boldsymbol{\mu}(\mathbf{r}) \cdot [\nabla \boldsymbol{\mu}(\mathbf{r})]^{-1}$ and $\nabla \ln \boldsymbol{\mu}(\mathbf{r}) \approx 0$ if the permeability $\boldsymbol{\mu}(\mathbf{r})$ varies slowly compared to wavelength. It is also easy to write an analogous scalar expression, which to date has not been written, assuming that both the permittivity and the permeability are scalar, given by

$$\overleftrightarrow{\mathbf{F}}_E(\mathbf{r}) = \frac{k^2}{4\pi} \left[\boldsymbol{\mu}(\mathbf{r})\boldsymbol{\varepsilon}(\mathbf{r}) - 1\right] \overleftrightarrow{\mathbf{I}}. \tag{187}$$

The scalar scattering potential is analogous to the previous equation,

$$F(\mathbf{r}) = \frac{k^2}{4\pi} \left[\boldsymbol{\mu}(\mathbf{r})\boldsymbol{\varepsilon}(\mathbf{r}) - 1\right], \tag{188}$$

where $F(\mathbf{r})$ is now the scalar scattering potential in terms of spatially varying $\boldsymbol{\varepsilon}(\mathbf{r})$ and $\boldsymbol{\mu}(\mathbf{r})$.

3.3.2 The Magnetic field vector wave equation

In the previous section, we first considered the electric field vector wave equation with nonmagnetic materials with $\overleftrightarrow{\boldsymbol{\mu}} = \overleftrightarrow{\mathbf{I}}$ and then with both a permittivity and a permeability tensor. Here, we derive the vector wave equation for the magnetic field which allows us to consider magnetic materials which have a free space permittivity, so that $\overleftrightarrow{\boldsymbol{\varepsilon}}(\mathbf{r}) = \overleftrightarrow{\mathbf{I}}$ in Gaussian units. The advantage of this approach is that we avoid the more difficult task of working with the magnetic permeability tensor using the electric field wave equation. Once the behavior of the magnetic field is established, the calculation of electric field follows in a straightforward manner by application of Ampère's Law. We begin again with the monochromatic forms of Faraday's law and

the Maxwell-Ampère law in terms of the magnetic field $\mathbf{H}$, given by

$$\nabla \times \mathbf{E}(\mathbf{r}) = ik\overleftrightarrow{\boldsymbol{\mu}}(\mathbf{r}) \cdot \mathbf{H}(\mathbf{r}), \tag{189}$$

$$\nabla \times \mathbf{H}(\mathbf{r}) = -ik\mathbf{E}(\mathbf{r}). \tag{190}$$

This time, we take the curl of the Maxwell-Ampère Law given by Eq. (190) and substitute Faraday's Law given by Eq. (189) and obtain

$$\nabla \times [\nabla \times \mathbf{H}(\mathbf{r})] = k^2\overleftrightarrow{\boldsymbol{\mu}}(\mathbf{r}) \cdot \mathbf{H}(\mathbf{r}), \tag{191}$$

and rearranging the components, we obtain the homogeneous magnetic field vector wave equation

$$\nabla \times [\nabla \times \mathbf{H}(\mathbf{r})] - k^2\overleftrightarrow{\boldsymbol{\mu}}(\mathbf{r}) \cdot \mathbf{H} = 0. \tag{192}$$

Now, to convert this equation to an inhomogeneous form, we substitute $\mathbf{H}(\mathbf{r}) = \mathbf{H}^{(i)}(\mathbf{r}) + \mathbf{H}^{(s)}(\mathbf{r})$ on the right side of the equation and subtract $k^2\mathbf{H}(\mathbf{r})$ from both sides, and obtain

$$\nabla \times \left\{\nabla \times \left[\mathbf{H}^{(i)}(\mathbf{r}) + \mathbf{H}^{(s)}(\mathbf{r})\right]\right\} - k^2\left[\mathbf{H}^{(i)}(\mathbf{r}) + \mathbf{H}^{(s)}(\mathbf{r})\right] = k^2\left[\overleftrightarrow{\boldsymbol{\mu}}(\mathbf{r}) - \overleftrightarrow{\mathbf{I}}\right] \cdot \mathbf{H}(\mathbf{r}). \tag{193}$$

Realizing that $\nabla \times \left[\nabla \times \mathbf{H}^{(i)}(\mathbf{r})\right] - k^2\mathbf{H}^{(i)}(\mathbf{r}) = 0$, and rearranging the components, the inhomogeneous magnetic field wave equation may be written as

$$\nabla \times \left[\nabla \times \mathbf{H}^{(s)}(\mathbf{r})\right] - k^2\mathbf{H}^{(s)}(\mathbf{r}) = 4\pi\overleftrightarrow{\mathbf{F}}_H(\mathbf{r}) \cdot \mathbf{H}(\mathbf{r}), \tag{194}$$

where $\overleftrightarrow{\mathbf{F}}_H(\mathbf{r})$ is the scattering dyadic, defined as

$$\overleftrightarrow{\mathbf{F}}_H(\mathbf{r}) = \frac{k^2}{4\pi}\left[\overleftrightarrow{\boldsymbol{\mu}}(\mathbf{r}) - \overleftrightarrow{\mathbf{I}}\right]. \tag{195}$$

This equation is also analogous to the scalar one, where only one component of the magnetic field is represented and $\overleftrightarrow{\boldsymbol{\mu}}$ is simplified to a spatially varying $\mu(\mathbf{r})$ and $\overleftrightarrow{\mathbf{I}}$ is reduced to 1. However, materials with $\boldsymbol{\varepsilon} = 1$ currently do not exist in nature but might be designed using metamaterials.

We may also consider solving the vector magnetic field wave equation assuming that both the permeability and the permittivity are described by spatially varying tensors, $\overleftrightarrow{\boldsymbol{\mu}}(\mathbf{r})$ and $\overleftrightarrow{\boldsymbol{\varepsilon}}(\mathbf{r})$. We begin with Faraday's and Ampère's Laws written in terms of $\mathbf{E}$, $\mathbf{H}$, $\overleftrightarrow{\boldsymbol{\varepsilon}}$, and $\overleftrightarrow{\boldsymbol{\mu}}$ as in Section 3.3.1, Eqs. (179) and (180), given by

$$\nabla\times\mathbf{E}(\mathbf{r}) = ik\overleftrightarrow{\boldsymbol{\mu}}(\mathbf{r})\cdot\mathbf{H}(\mathbf{r}), \tag{196}$$

$$\nabla\times\mathbf{H}(\mathbf{r}) = -ik\overleftrightarrow{\boldsymbol{\varepsilon}}(\mathbf{r})\cdot\mathbf{E}(\mathbf{r}). \tag{197}$$

This time, we take the curl of Eq. (197) and substitute Eq. (196), producing the expression

$$\nabla\times[\nabla\times\mathbf{H}(\mathbf{r})] - ik\nabla\times\overleftrightarrow{\boldsymbol{\varepsilon}}(\mathbf{r})\cdot\mathbf{E}(\mathbf{r}) - k^2\overleftrightarrow{\boldsymbol{\varepsilon}}(\mathbf{r})\cdot\overleftrightarrow{\boldsymbol{\mu}}(\mathbf{r})\cdot\mathbf{H}(\mathbf{r}) = 0. \tag{198}$$

To eliminate the term containing the electric field, we rearrange Eq. (197) and substitute it into Eq. (198) and obtain

$$\nabla\times[\nabla\times\mathbf{H}(\mathbf{r})] - \nabla\times\overleftrightarrow{\boldsymbol{\varepsilon}}(\mathbf{r})\cdot\overleftrightarrow{\boldsymbol{\varepsilon}}^{-1}(\mathbf{r})\cdot\nabla\times\mathbf{H}(\mathbf{r}) - k^2\overleftrightarrow{\boldsymbol{\varepsilon}}(\mathbf{r})\cdot\overleftrightarrow{\boldsymbol{\mu}}(\mathbf{r})\cdot\mathbf{H}(\mathbf{r}) = 0. \tag{199}$$

At this point, we subtract $k^2\mathbf{H}(\mathbf{r})$ from both sides and rearrange the terms so that the left side takes the form of a wave equation with homogeneous wave number,

$$\nabla\times[\nabla\times\mathbf{H}(\mathbf{r})] - k^2\mathbf{H}(\mathbf{r}) = k^2\overleftrightarrow{\boldsymbol{\varepsilon}}(\mathbf{r})\cdot\overleftrightarrow{\boldsymbol{\mu}}(\mathbf{r})\cdot\mathbf{H}(\mathbf{r}) - k^2\mathbf{H}(\mathbf{r}) + \nabla\times\overleftrightarrow{\boldsymbol{\varepsilon}}(\mathbf{r})\cdot\overleftrightarrow{\boldsymbol{\varepsilon}}^{-1}(\mathbf{r})\cdot\nabla\times\mathbf{H}(\mathbf{r}). \tag{200}$$

Now Eq. (200) may be written in terms of a scattering potential tensor operator, given by

$$\nabla \times [\nabla \times \mathbf{H}(\mathbf{r})] - k^2 \mathbf{H}(\mathbf{r}) = 4\pi \overleftrightarrow{\mathbf{F}}_H(\mathbf{r}) \cdot \mathbf{H}(\mathbf{r}), \tag{201}$$

where the scattering potential tensor operator is defined by

$$\overleftrightarrow{\mathbf{F}}_H(\mathbf{r}) = \frac{k^2}{4\pi} \left\{ \overleftrightarrow{\boldsymbol{\varepsilon}}(\mathbf{r}) \cdot \overleftrightarrow{\boldsymbol{\mu}}(\mathbf{r}) - \overleftrightarrow{\mathbf{I}} + \frac{1}{k^2} \nabla \times \overleftrightarrow{\boldsymbol{\varepsilon}}(\mathbf{r}) \cdot \overleftrightarrow{\boldsymbol{\varepsilon}}^{-1}(\mathbf{r}) \cdot \nabla \times \right\}. \tag{202}$$

If the permittivity is a scalar function of position $\boldsymbol{\varepsilon}(\mathbf{r})$, then the term $\boldsymbol{\varepsilon}^{-1}(\mathbf{r}) = \nabla \ln \boldsymbol{\varepsilon}(\mathbf{r}) \cdot [\nabla \boldsymbol{\varepsilon}(\mathbf{r})]^{-1}$. Furthermore, if the permittivity varies slowly compared to the wavelength, then $\nabla \ln \boldsymbol{\varepsilon}(\mathbf{r}) \approx 0$ and Eq. (202) may be simplified substantially to

$$\overleftrightarrow{\mathbf{F}}_H(\mathbf{r}) = \frac{k^2}{4\pi} \left[\boldsymbol{\varepsilon}(\mathbf{r}) \cdot \overleftrightarrow{\boldsymbol{\mu}}(\mathbf{r}) - \overleftrightarrow{\mathbf{I}} \right], \tag{203}$$

so that it is no longer a tensor operator. If both the permittivity and the permeability are scalar functions of $\mathbf{r}$, then Eq. (203) further simplifies to the scalar scattering potential, given by

$$\overleftrightarrow{\mathbf{F}}_H(\mathbf{r}) = \frac{k^2}{4\pi} \left[\boldsymbol{\varepsilon}(\mathbf{r}) \boldsymbol{\mu}(\mathbf{r}) - 1 \right] \overleftrightarrow{\mathbf{I}}, \tag{204}$$

$$F(\mathbf{r}) = \frac{k^2}{4\pi} \left[\boldsymbol{\varepsilon}(\mathbf{r}) \boldsymbol{\mu}(\mathbf{r}) - 1 \right], \tag{205}$$

which is identical to Eq. (188). This makes perfect sense because the scalar equation implies that one component of either electric field or the magnetic field is generalized as the field $U(\mathbf{r})$ and represents the whole system. By deriving the scattering potential in this way, we are able to find the scalar scattering potential in terms of both the permittivity and the permeability, which permits a more general analysis of a material in both the scalar and the vector case.

3.3.3 Other field vector wave equations

Only Maxwell's electric field equation has ever been written in terms of the scattering potential dyadic [9, 29], which is defined as a function of the electric permittivity tensor $\overleftrightarrow{\boldsymbol{\varepsilon}}$, assuming free-space permeability. This enables the design of a material's scattering properties as a function of the electric permittivity. Earlier in this chapter, it was shown how the magnetic field equation could also be written in terms of a scattering potential dyadic defined as a function of the permeability tensor $\overleftrightarrow{\boldsymbol{\mu}}$ assuming free-space permittivity. It was also shown how to derive either scattering potential tensor operator for either the electric or the magnetic field wave equation assuming both the permittivities and the permeabilities are tensors. This permits the design of an object's scattering properties with the freedom to manipulate the permittivity and permeability independently to control either the electric or magnetic field. In Chapter 2, the advantages of deriving the wave equations in terms of $\mathbf{B}$ and $\mathbf{D}$ were demonstrated, but such equations currently do not exist for these fields to describe nonscattering scatterers. Here, we present for the first time the inhomogeneous vector wave equations with homogeneous wavenumber k for $\mathbf{B}$ and $\mathbf{D}$ in terms of scattering potential dyadics, which are functions of both $\overleftrightarrow{\boldsymbol{\varepsilon}}$ and $\overleftrightarrow{\boldsymbol{\mu}}$. These allow greater flexibility in the design of a scatterer and also open new avenues of research in invisibility theory, as will be shown in Chapter 6.

We begin by noticing an interesting relationship between Maxwell's equations derived in terms of the polarization $\mathbf{P}$ and magnetization $\mathbf{M}$ in Chapter 2, repeated

again here,

$$\nabla \times (\nabla \times \mathbf{E}) - k^2\mathbf{E} = 4\pi ik\left(-ik\mathbf{P} + \nabla \times \mathbf{M}\right), \tag{206}$$

$$\nabla \times (\nabla \times \mathbf{H}) - k^2\mathbf{H} = 4\pi(-ik)(ik\mathbf{M} + \nabla \times \mathbf{P}), \tag{207}$$

$$\nabla \times (\nabla \times \mathbf{B}) - k^2\mathbf{B} = 4\pi\nabla \times (-ik\mathbf{P} + \nabla \times \mathbf{M}), \tag{208}$$

$$\nabla \times (\nabla \times \mathbf{D}) - k^2\mathbf{D} = 4\pi\nabla \times (ik\mathbf{M} + \nabla \times \mathbf{P}). \tag{209}$$

Upon closer examination, we recognize that Eq. (208) is equal to $1/(ik)\nabla\times$ of Eq. (206) and that Eq. (209) is equal to $1/(-ik)\nabla\times$ of Eq. (207). We now write an analogous vector equation for the scalar inverse source problem described in Eq. (117), given by

$$\nabla \times [\nabla \times \mathbf{U}(\mathbf{r})] - k^2\mathbf{U}(\mathbf{r}) = 4\pi\mathbf{Q}_U(\mathbf{r}), \tag{210}$$

where $\mathbf{U}$ may be any of the electromagnetic vector fields and $\mathbf{Q}_U$ is the source field vector associated with field $\mathbf{U}$. We may write a similar general equation for the scattering problem, given by

$$\nabla \times \left[\nabla \times \mathbf{U}^{(s)}(\mathbf{r})\right] - k^2\mathbf{U}^{(s)}(\mathbf{r}) = 4\pi\overleftrightarrow{\mathbf{F}}_U(\mathbf{r}) \cdot \mathbf{U}(\mathbf{r}), \tag{211}$$

where $\mathbf{U}(\mathbf{r}) = \mathbf{U}^{(i)} + \mathbf{U}^{(s)}$ is the total vector field of any of the electromagnetic fields, $\mathbf{F}_U(\mathbf{r})$ is the scattering potential tensor operator corresponding to the electromagnetic field $\mathbf{U}(\mathbf{r})$, $\mathbf{U}^{(s)}$ is the scattered field, and the incident field $\mathbf{U}^{(i)}$ satisfies the homogeneous Helmholtz equation

$$\nabla \times \left[\nabla \times \mathbf{U}^{(i)}(\mathbf{r})\right] - k^2\mathbf{U}^{(i)}(\mathbf{r}) = 0. \tag{212}$$

Adding Eq. (212) to Eq. (211), we obtain

$$\nabla \times [\nabla \times \mathbf{U}(\mathbf{r})] - k^2 \mathbf{U}(\mathbf{r}) = 4\pi \overleftrightarrow{\mathbf{F}}_U(\mathbf{r}) \cdot \mathbf{U}(\mathbf{r}), \tag{213}$$

and notice that Eq. (213) and Eq. (210) are mathematically equivalent if

$$\overleftrightarrow{\mathbf{F}}_U(\mathbf{r}) \cdot \mathbf{U}(\mathbf{r}) = \mathbf{Q}_U(\mathbf{r}). \tag{214}$$

Rewriting the Eqs. (206), (207), (208), and (209) in terms of source terms,

$$\nabla \times [\nabla \times \mathbf{E}(\mathbf{r})] - k^2 \mathbf{E}(\mathbf{r}) = 4\pi \mathbf{Q}_E(\mathbf{r}), \tag{215}$$

$$\nabla \times [\nabla \times \mathbf{H}(\mathbf{r})] - k^2 \mathbf{H}(\mathbf{r}) = 4\pi \mathbf{Q}_H(\mathbf{r}), \tag{216}$$

$$\nabla \times [\nabla \times \mathbf{B}(\mathbf{r})] - k^2 \mathbf{B}(\mathbf{r}) = 4\pi \mathbf{Q}_B(\mathbf{r}), \tag{217}$$

$$\nabla \times [\nabla \times \mathbf{D}(\mathbf{r})] - k^2 \mathbf{D}(\mathbf{r}) = 4\pi \mathbf{Q}_D(\mathbf{r}), \tag{218}$$

where the source terms

$$\mathbf{Q}_E(\mathbf{r}) = ik \left[-ik\mathbf{P}(\mathbf{r}) + \nabla \times \mathbf{M}(\mathbf{r})\right], \tag{219}$$

$$\mathbf{Q}_H(\mathbf{r}) = -ik \left[ik\mathbf{M}(\mathbf{r}) + \nabla \times \mathbf{P}(\mathbf{r})\right], \tag{220}$$

$$\mathbf{Q}_B(\mathbf{r}) = \nabla \times \left[-ik\mathbf{P}(\mathbf{r}) + \nabla \times \mathbf{M}(\mathbf{r})\right], \tag{221}$$

$$\mathbf{Q}_D(\mathbf{r}) = \nabla \times \left[ik\mathbf{M}(\mathbf{r}) + \nabla \times \mathbf{P}(\mathbf{r})\right], \tag{222}$$

and we notice that

$$\mathbf{Q}_B(\mathbf{r}) = \frac{1}{ik} \nabla \times \mathbf{Q}_E(\mathbf{r}), \tag{223}$$

$$\mathbf{Q}_D(\mathbf{r}) = -\frac{1}{ik} \nabla \times \mathbf{Q}_H(\mathbf{r}). \tag{224}$$

Applying the equivalence relation between primary sources and scatterers, Eq. (214),

to each field vector equation, it follows that

$$\overleftrightarrow{\mathbf{F}}_E(\mathbf{r}) \cdot \mathbf{E}(\mathbf{r}) = \mathbf{Q}_E(\mathbf{r}), \tag{225}$$

$$\overleftrightarrow{\mathbf{F}}_H(\mathbf{r}) \cdot \mathbf{H}(\mathbf{r}) = \mathbf{Q}_H(\mathbf{r}), \tag{226}$$

$$\overleftrightarrow{\mathbf{F}}_B(\mathbf{r}) \cdot \mathbf{B}(\mathbf{r}) = \mathbf{Q}_B(\mathbf{r}), \tag{227}$$

$$\overleftrightarrow{\mathbf{F}}_D(\mathbf{r}) \cdot \mathbf{D}(\mathbf{r}) = \mathbf{Q}_D(\mathbf{r}), \tag{228}$$

where we introduce $\overleftrightarrow{\mathbf{F}}_B(\mathbf{r})$ and $\overleftrightarrow{\mathbf{F}}_D(\mathbf{r})$ as the scattering potential tensor operators for the vector wave equations for fields $\mathbf{B}(\mathbf{r})$ and $\mathbf{D}(\mathbf{r})$ to be defined. If we now apply the relations outlined by Eqs. (223) and (224) to Eqs. (225), (226), (227), and (228), we reveal a similar relationship between the scattering potential dyadics of each of the electromagnetic fields, given by

$$\overleftrightarrow{\mathbf{F}}_B(\mathbf{r}) \cdot \mathbf{B}(\mathbf{r}) = \frac{1}{ik} \nabla \times \left[\overleftrightarrow{\mathbf{F}}_E(\mathbf{r}) \cdot \mathbf{E}(\mathbf{r}) \right], \tag{229}$$

$$\overleftrightarrow{\mathbf{F}}_D(\mathbf{r}) \cdot \mathbf{D}(\mathbf{r}) = -\frac{1}{ik} \nabla \times \left[\overleftrightarrow{\mathbf{F}}_H(\mathbf{r}) \cdot \mathbf{H}(\mathbf{r}) \right], \tag{230}$$

where $\overleftrightarrow{\mathbf{F}}_B$ and $\overleftrightarrow{\mathbf{F}}_D$ are the scattering potential dyadic operators associated with the vector wave equations for $\mathbf{B}$ and $\mathbf{D}$, given by

$$\nabla \times [\nabla \times \mathbf{B}(\mathbf{r})] - k^2 \mathbf{B}(\mathbf{r}) = 4\pi \overleftrightarrow{\mathbf{F}}_B(\mathbf{r}) \cdot \mathbf{B}(\mathbf{r}), \tag{231}$$

$$\nabla \times [\nabla \times \mathbf{D}(\mathbf{r})] - k^2 \mathbf{D}(\mathbf{r}) = 4\pi \overleftrightarrow{\mathbf{F}}_D(\mathbf{r}) \cdot \mathbf{D}(\mathbf{r}). \tag{232}$$

The scattering potential tensor operators $\overleftrightarrow{\mathbf{F}}_E(\mathbf{r})$ and $\overleftrightarrow{\mathbf{F}}_H(\mathbf{r})$ given by Eqs. (185) and

(202) in Gaussian units are

$$\overleftrightarrow{\mathbf{F}}_E(\mathbf{r}) = \frac{k^2}{4\pi}\left\{\overleftrightarrow{\boldsymbol{\mu}}(\mathbf{r})\cdot\overleftrightarrow{\boldsymbol{\varepsilon}}(\mathbf{r}) - \overleftrightarrow{\mathbf{I}} + \frac{1}{k^2}\left[\nabla\times\overleftrightarrow{\boldsymbol{\mu}}(\mathbf{r})\right]\cdot\overleftrightarrow{\boldsymbol{\mu}}^{-1}(\mathbf{r})\cdot\nabla\times\right\}, \tag{233}$$

$$\overleftrightarrow{\mathbf{F}}_H(\mathbf{r}) = \frac{k^2}{4\pi}\left\{\overleftrightarrow{\boldsymbol{\varepsilon}}(\mathbf{r})\cdot\overleftrightarrow{\boldsymbol{\mu}}(\mathbf{r}) - \overleftrightarrow{\mathbf{I}} + \frac{1}{k^2}\left[\nabla\times\overleftrightarrow{\boldsymbol{\varepsilon}}(\mathbf{r})\right]\cdot\overleftrightarrow{\boldsymbol{\varepsilon}}^{-1}(\mathbf{r})\cdot\nabla\times\right\}. \tag{234}$$

First, let us evaluate Eq. (229),

$$\begin{aligned}\overleftrightarrow{\mathbf{F}}_B(\mathbf{r})\cdot\mathbf{B}(\mathbf{r}) &= \frac{1}{ik}\left\{\left[\nabla\times\overleftrightarrow{\mathbf{F}}_E(\mathbf{r})\right]\cdot\mathbf{E}(\mathbf{r}) + \overleftrightarrow{\mathbf{F}}_E(\mathbf{r})\cdot[\nabla\times\mathbf{E}(\mathbf{r})]\right\}\\ &= \frac{1}{ik}\left\{\left[\nabla\times\overleftrightarrow{\mathbf{F}}_E(\mathbf{r})\right]\cdot\mathbf{E}(\mathbf{r}) + \overleftrightarrow{\mathbf{F}}_E(\mathbf{r})\cdot ik\mathbf{B}(\mathbf{r})\right\},\end{aligned} \tag{235}$$

where we have substituted Eq. (30) in Chapter 2 to write as much as possible in terms of $\mathbf{B}$. Next we simplify the term $\nabla\times\overleftrightarrow{\mathbf{F}}_E(\mathbf{r})\cdot\mathbf{E}(\mathbf{r})$ by eliminating $\mathbf{E}(\mathbf{r})$ and writing it in terms of $\mathbf{B}(\mathbf{r})$. We rewrite Eq. (32) in terms of $\mathbf{B}$ and $\mathbf{E}$ by substituting the constitutive relations (Eqs. (101) and (102)) and obtain

$$\mathbf{E}(\mathbf{r}) = \frac{1}{ik}\overleftrightarrow{\boldsymbol{\varepsilon}}^{-1}(\mathbf{r})\cdot\nabla\times\left[\overleftrightarrow{\boldsymbol{\mu}}^{-1}(\mathbf{r})\cdot\mathbf{B}(\mathbf{r})\right]. \tag{236}$$

Now Eq. (235) may be rewritten as a function of $\mathbf{B}(\mathbf{r})$, given by

$$\begin{aligned}&\overleftrightarrow{\mathbf{F}}_B(\mathbf{r})\cdot\mathbf{B}(\mathbf{r})\\ &\quad= \frac{1}{ik}\left\{\overleftrightarrow{\mathbf{F}}_E(\mathbf{r})\cdot ik\mathbf{B}(\mathbf{r}) + \left[\nabla\times\overleftrightarrow{\mathbf{F}}_E(\mathbf{r})\right]\cdot\frac{1}{ik}\overleftrightarrow{\boldsymbol{\varepsilon}}^{-1}(\mathbf{r})\cdot\nabla\times\left[\overleftrightarrow{\boldsymbol{\mu}}^{-1}(\mathbf{r})\cdot\mathbf{B}(\mathbf{r})\right]\right\}\\ &\quad= \overleftrightarrow{\mathbf{F}}_E(\mathbf{r})\cdot\mathbf{B}(\mathbf{r}) + \frac{1}{k^2}\nabla\times\overleftrightarrow{\mathbf{F}}_E(\mathbf{r})\cdot\overleftrightarrow{\boldsymbol{\varepsilon}}^{-1}\left[\nabla\times\overleftrightarrow{\boldsymbol{\mu}}^{-1}(\mathbf{r}) + \overleftrightarrow{\boldsymbol{\mu}}^{-1}(\mathbf{r})\nabla\times\right]\mathbf{B}(\mathbf{r}),\end{aligned} \tag{237}$$

where the complete expression for scattering potential tensor operator $\overleftrightarrow{\mathbf{F}}_B(\mathbf{r})$ may be isolated, producing

$$\overleftrightarrow{\mathbf{F}}_B(\mathbf{r}) = \overleftrightarrow{\mathbf{F}}_E(\mathbf{r}) + \frac{1}{k^2}\nabla\times\overleftrightarrow{\mathbf{F}}_E(\mathbf{r})\cdot\overleftrightarrow{\boldsymbol{\varepsilon}}^{-1}(\mathbf{r})\left[\nabla\times\overleftrightarrow{\boldsymbol{\mu}}^{-1}(\mathbf{r}) + \overleftrightarrow{\boldsymbol{\mu}}^{-1}(\mathbf{r})\nabla\times\right]. \tag{238}$$

We may observe that this equation has a complex dependence on the permittivity, the permeability, and their inverse tensors. With this equation we have the flexibility of choosing $\overleftrightarrow{\boldsymbol{\mu}}$ and $\overleftrightarrow{\boldsymbol{\varepsilon}}$ independently of each other to satisfy the desired design objectives. For example, Eq. (238) may be simplified if we choose a scalar function for the permeability such that the inverse term $\frac{1}{\boldsymbol{\mu}(\mathbf{r})} = \nabla \ln \boldsymbol{\mu}(\mathbf{r}) \cdot [\nabla \boldsymbol{\mu}(\mathbf{r})]^{-1}$, while the permittivity remains a tensor. Eq. (238) reduces to

$$\begin{aligned}\overleftrightarrow{\mathbf{F}}_B(\mathbf{r}) = \overleftrightarrow{\mathbf{F}}_E(\mathbf{r}) + \frac{1}{k^2}\nabla\times\overleftrightarrow{\mathbf{F}}_E(\mathbf{r}) \cdot \overleftrightarrow{\boldsymbol{\varepsilon}}^{-1}(\mathbf{r})\cdot \\ \left\{\nabla\times\left[\nabla \ln \boldsymbol{\mu}(\mathbf{r}) \cdot [\nabla \boldsymbol{\mu}(\mathbf{r})]^{-1}\overleftrightarrow{\mathbf{I}}\right] + \nabla \ln \boldsymbol{\mu}(\mathbf{r}) \cdot [\nabla \boldsymbol{\mu}(\mathbf{r})]^{-1}\nabla\times\right\} \\ = \overleftrightarrow{\mathbf{F}}_E(\mathbf{r}),\end{aligned} \tag{239}$$

where we have employed the assumption that if $\boldsymbol{\mu}(\mathbf{r})$ varies more slowly than the wavelength, $\nabla \ln \boldsymbol{\mu}(\mathbf{r}) \approx 0$. However, recall that the scattering potential $\overleftrightarrow{\mathbf{F}}_E(\mathbf{r})$ in Eq. (239) for a scalar $\boldsymbol{\mu}(\mathbf{r})\overleftrightarrow{\mathbf{I}}$ reduces to

$$\overleftrightarrow{\mathbf{F}}_E(\mathbf{r}) = \frac{k^2}{4\pi}\left[\boldsymbol{\mu}(\mathbf{r}) \cdot \overleftrightarrow{\boldsymbol{\varepsilon}}(\mathbf{r}) - \overleftrightarrow{\mathbf{I}}\right]. \tag{240}$$

If we further assume that the permittivity is also a scalar function $\overleftrightarrow{\boldsymbol{\varepsilon}}(\mathbf{r}) = \boldsymbol{\varepsilon}(\mathbf{r})\overleftrightarrow{\mathbf{I}}$, Eq. (239) reduces to

$$\begin{aligned}\overleftrightarrow{\mathbf{F}}_B(\mathbf{r}) &= \overleftrightarrow{\mathbf{F}}_E(\mathbf{r}) \\ &= \frac{k^2}{4\pi}\left[\boldsymbol{\mu}(\mathbf{r}) \cdot \boldsymbol{\varepsilon}(\mathbf{r})\overleftrightarrow{\mathbf{I}} - \overleftrightarrow{\mathbf{I}}\right],\end{aligned} \tag{241}$$

where we have assumed that $\boldsymbol{\varepsilon}^{-1}(\mathbf{r}) = \nabla \ln \boldsymbol{\varepsilon} \cdot [\nabla \boldsymbol{\varepsilon}]^{-1}$ and $\nabla \ln \boldsymbol{\varepsilon} \approx 0$ when the permittivity varies slowly compared to the wavelength. This simplification may also be applied to the complete equation $\overleftrightarrow{\mathbf{F}}_B(\mathbf{r})$, Eq. (238). Let us assume that $\overleftrightarrow{\boldsymbol{\varepsilon}}(\mathbf{r}) = \boldsymbol{\varepsilon}(\mathbf{r})\overleftrightarrow{\mathbf{I}}$, the permittivity is a scalar function or $\mathbf{r}$, and that the permeability is a tensor.

The simplified equation is given by

$$\begin{aligned}\overleftrightarrow{\mathbf{F}}_B(\mathbf{r}) &= \overleftrightarrow{\mathbf{F}}_E(\mathbf{r}) \\ &= \frac{k^2}{4\pi}\left\{\boldsymbol{\varepsilon}(\mathbf{r})\overleftrightarrow{\boldsymbol{\mu}}(\mathbf{r}) - \overleftrightarrow{\mathbf{I}} + \frac{1}{k^2}\left[\nabla\times\overleftrightarrow{\boldsymbol{\mu}}(\mathbf{r})\right]\cdot\overleftrightarrow{\boldsymbol{\mu}}^{-1}(\mathbf{r})\cdot\nabla\times\right\},\end{aligned} \tag{242}$$

where we can see that the permeability plays a strong role in this scattering potential operator.

Following a very similar procedure used to derive $\overleftrightarrow{\mathbf{F}}_B(\mathbf{r})$, we now derive an expression for $\overleftrightarrow{\mathbf{F}}_D(\mathbf{r})$ by evaluating Eq. (230) and substituting Eqs. (32) and (30) to obtain

$$\begin{aligned}\overleftrightarrow{\mathbf{F}}_D(\mathbf{r})\cdot\mathbf{D}(\mathbf{r}) &= -\frac{1}{ik}\left\{[\nabla\times\overleftrightarrow{\mathbf{F}}_H(\mathbf{r})]\cdot\mathbf{H}(\mathbf{r}) + \overleftrightarrow{\mathbf{F}}_H(\mathbf{r})\cdot[\nabla\times\mathbf{H}(\mathbf{r})]\right\} \\ &= -\frac{1}{ik}\left\{\nabla\times\overleftrightarrow{\mathbf{F}}_H(\mathbf{r})\cdot\frac{1}{ik}\nabla\times\left[\overleftrightarrow{\boldsymbol{\varepsilon}}^{-1}(\mathbf{r})\cdot\mathbf{D}(\mathbf{r})\right] - ik\overleftrightarrow{\mathbf{F}}_H(\mathbf{r})\cdot\mathbf{D}(\mathbf{r})\right\} \\ &= \overleftrightarrow{\mathbf{F}}_H(\mathbf{r})\cdot\mathbf{D}(\mathbf{r}) + \frac{1}{k^2}\nabla\times\overleftrightarrow{\mathbf{F}}_H(\mathbf{r})\cdot\left[\nabla\times\overleftrightarrow{\boldsymbol{\varepsilon}}^{-1}(\mathbf{r})\cdot\mathbf{D}(\mathbf{r}) + \overleftrightarrow{\boldsymbol{\varepsilon}}^{-1}(\mathbf{r})\cdot\nabla\times\mathbf{D}\right].\end{aligned} \tag{243}$$

We may now isolate the scattering potential tensor operator $\overleftrightarrow{\mathbf{F}}_D(\mathbf{r})$, which is given by

$$\overleftrightarrow{\mathbf{F}}_D(\mathbf{r}) = \overleftrightarrow{\mathbf{F}}_H(\mathbf{r}) + \frac{1}{k^2}\nabla\times\overleftrightarrow{\mathbf{F}}_H(\mathbf{r})\cdot\left[\nabla\times\overleftrightarrow{\boldsymbol{\varepsilon}}^{-1}(\mathbf{r}) + \overleftrightarrow{\boldsymbol{\varepsilon}}^{-1}(\mathbf{r})\cdot\nabla\times\right], \tag{244}$$

where $\overleftrightarrow{\mathbf{F}}_H(\mathbf{r})$ is given by Eq. (234), repeated here for clarity

$$\overleftrightarrow{\mathbf{F}}_H(\mathbf{r}) = \frac{k^2}{4\pi}\left\{\overleftrightarrow{\boldsymbol{\varepsilon}}(\mathbf{r})\cdot\overleftrightarrow{\boldsymbol{\mu}}(\mathbf{r}) - \overleftrightarrow{\mathbf{I}} + \frac{1}{k^2}\left[\nabla\times\overleftrightarrow{\boldsymbol{\varepsilon}}(\mathbf{r})\right]\cdot\overleftrightarrow{\boldsymbol{\varepsilon}}^{-1}(\mathbf{r})\cdot\nabla\times\right\}, \tag{245}$$

where $\overleftrightarrow{\mathbf{F}}_D$ acts on the electric displacement $\mathbf{D}(\mathbf{r})$ in its corresponding wave equation (Eq. (232)) and represents the properties of the scatterer. These equations are valid as long as the determinants of $\overleftrightarrow{\boldsymbol{\mu}}$ and $\overleftrightarrow{\boldsymbol{\varepsilon}}$ are unequal to zero.

Whereas $\overleftrightarrow{\boldsymbol{\mu}}$ had the prominent role in Eq. (238) for $\overleftrightarrow{\mathbf{F}}_B(\mathbf{r})$, the permittivity tensor $\overleftrightarrow{\boldsymbol{\varepsilon}}$ has the strongest influence over reductions and simplifications in Eq. (244). For example, suppose the scatterer has a scalar permittivity given by $\overleftrightarrow{\boldsymbol{\varepsilon}} = \boldsymbol{\varepsilon}(\mathbf{r})\overleftrightarrow{\mathbf{I}}$ but a permeability tensor. Eq. (244) becomes

$$\begin{aligned}
\overleftrightarrow{\mathbf{F}}_D(\mathbf{r}) &= \overleftrightarrow{\mathbf{F}}_H(\mathbf{r}) + \frac{1}{k^2}\nabla\times\overleftrightarrow{\mathbf{F}}_H(\mathbf{r})\cdot\left[\nabla\times\boldsymbol{\varepsilon}^{-1}(\mathbf{r})\overleftrightarrow{\mathbf{I}} + \boldsymbol{\varepsilon}^{-1}(\mathbf{r})\cdot\nabla\times\right] \\
&= \overleftrightarrow{\mathbf{F}}_H(\mathbf{r}) \\
&+ \frac{1}{k^2}\nabla\times\overleftrightarrow{\mathbf{F}}_H(\mathbf{r})\cdot\left\{\nabla\times\left[\nabla\ln\boldsymbol{\varepsilon}(\mathbf{r})\cdot[\nabla\boldsymbol{\varepsilon}(\mathbf{r})]^{-1}\overleftrightarrow{\mathbf{I}}\right] + \nabla\ln\boldsymbol{\varepsilon}(\mathbf{r})\cdot[\nabla\boldsymbol{\varepsilon}(\mathbf{r})]^{-1}\nabla\times\right\} \\
&= \overleftrightarrow{\mathbf{F}}_H(\mathbf{r})
\end{aligned} \tag{246}$$

where we have substituted $\frac{1}{\boldsymbol{\varepsilon}(\mathbf{r})} = \nabla\ln\boldsymbol{\varepsilon}(\mathbf{r})\cdot[\nabla\boldsymbol{\varepsilon}(\mathbf{r})]^{-1}$, and it is assumed that $\boldsymbol{\varepsilon}(\mathbf{r})$ varies slowly compared to the wavelength, rendering $\nabla\ln\boldsymbol{\varepsilon}(\mathbf{r}) \approx 0$. Applying the same assumptions to Eq. (245), we obtain the reduced form

$$\begin{aligned}
\overleftrightarrow{\mathbf{F}}_H(\mathbf{r}) &= \frac{k^2}{4\pi}\left\{\boldsymbol{\varepsilon}(\mathbf{r})\cdot\overleftrightarrow{\boldsymbol{\mu}}(\mathbf{r}) - \overleftrightarrow{\mathbf{I}} + \frac{1}{k^2}\left\{\nabla\times\left[\boldsymbol{\varepsilon}(\mathbf{r})\overleftrightarrow{\mathbf{I}}\right]\right\}\cdot\boldsymbol{\varepsilon}^{-1}(\mathbf{r})\cdot\nabla\times\right\} \\
&= \frac{k^2}{4\pi}\left\{\boldsymbol{\varepsilon}(\mathbf{r})\cdot\overleftrightarrow{\boldsymbol{\mu}}(\mathbf{r}) - \overleftrightarrow{\mathbf{I}} + \frac{1}{k^2}\left\{\nabla\times\left[\boldsymbol{\varepsilon}(\mathbf{r})\overleftrightarrow{\mathbf{I}}\right]\right\}\cdot\nabla\ln\boldsymbol{\varepsilon}(\mathbf{r})\cdot[\nabla\boldsymbol{\varepsilon}(\mathbf{r})]^{-1}\nabla\times\right\} \\
&= \frac{k^2}{4\pi}\left[\boldsymbol{\varepsilon}(\mathbf{r})\cdot\overleftrightarrow{\boldsymbol{\mu}}(\mathbf{r}) - \overleftrightarrow{\mathbf{I}}\right].
\end{aligned} \tag{247}$$

On the other hand, suppose the scatterer has a permittivity tensor but the permeability is a scalar function of $\mathbf{r}$, $\overleftrightarrow{\boldsymbol{\mu}}(\mathbf{r}) = \boldsymbol{\mu}(\mathbf{r})\overleftrightarrow{\mathbf{I}}$. The equation for the scattering potential dyadic reduces to

$$\overleftrightarrow{\mathbf{F}}_D(\mathbf{r}) = \overleftrightarrow{\mathbf{F}}_H(\mathbf{r}) + \frac{1}{k^2}\nabla\times\overleftrightarrow{\mathbf{F}}_H(\mathbf{r})\cdot\left[\nabla\times\overleftrightarrow{\boldsymbol{\varepsilon}}^{-1}(\mathbf{r}) + \overleftrightarrow{\boldsymbol{\varepsilon}}^{-1}(\mathbf{r})\cdot\nabla\times\right], \tag{248}$$

where Eq. (245) is modified with $\overleftrightarrow{\boldsymbol{\mu}} = \boldsymbol{\mu}(\mathbf{r})\overleftrightarrow{\mathbf{I}}$, given by

$$\overleftrightarrow{\mathbf{F}}_H(\mathbf{r}) = \frac{k^2}{4\pi}\left\{\boldsymbol{\mu}(\mathbf{r})\cdot\overleftrightarrow{\boldsymbol{\varepsilon}}(\mathbf{r}) - \overleftrightarrow{\mathbf{I}} + \frac{1}{k^2}\left[\nabla\times\overleftrightarrow{\boldsymbol{\varepsilon}}(\mathbf{r})\right]\cdot\overleftrightarrow{\boldsymbol{\varepsilon}}^{-1}(\mathbf{r})\cdot\nabla\times\right\}. \tag{249}$$

In summary, for each of the four wave vector equations in terms of sources there are a complementary set of scattering wave equations, given by

$$\nabla\times[\nabla\times\mathbf{E}(\mathbf{r})] - k^2\mathbf{E}(\mathbf{r}) = 4\pi\overleftrightarrow{\mathbf{F}}_E\cdot\mathbf{E}, \tag{250}$$

$$\nabla\times[\nabla\times\mathbf{H}(\mathbf{r})] - k^2\mathbf{H}(\mathbf{r}) = 4\pi\overleftrightarrow{\mathbf{F}}_H\cdot\mathbf{H}, \tag{251}$$

$$\nabla\times[\nabla\times\mathbf{B}(\mathbf{r})] - k^2\mathbf{B}(\mathbf{r}) = 4\pi\overleftrightarrow{\mathbf{F}}_B\cdot\mathbf{B}, \tag{252}$$

$$\nabla\times[\nabla\times\mathbf{D}(\mathbf{r})] - k^2\mathbf{D}(\mathbf{r}) = 4\pi\overleftrightarrow{\mathbf{F}}_D\cdot\mathbf{D}, \tag{253}$$

each of which has a corresponding scattering potential dyadic, defined by

$$\overleftrightarrow{\mathbf{F}}_E(\mathbf{r}) = \frac{k^2}{4\pi}\left\{\overleftrightarrow{\boldsymbol{\mu}}(\mathbf{r})\cdot\overleftrightarrow{\boldsymbol{\varepsilon}}(\mathbf{r}) - \overleftrightarrow{\mathbf{I}} + \frac{1}{k^2}\left[\nabla\times\overleftrightarrow{\boldsymbol{\mu}}(\mathbf{r})\right]\cdot\overleftrightarrow{\boldsymbol{\mu}}^{-1}(\mathbf{r})\cdot\nabla\times\right\}, \tag{254}$$

$$\overleftrightarrow{\mathbf{F}}_H(\mathbf{r}) = \frac{k^2}{4\pi}\left\{\overleftrightarrow{\boldsymbol{\varepsilon}}(\mathbf{r})\cdot\overleftrightarrow{\boldsymbol{\mu}}(\mathbf{r}) - \overleftrightarrow{\mathbf{I}} + \frac{1}{k^2}\left[\nabla\times\overleftrightarrow{\boldsymbol{\varepsilon}}(\mathbf{r})\right]\cdot\overleftrightarrow{\boldsymbol{\varepsilon}}^{-1}(\mathbf{r})\cdot\nabla\times\right\}, \tag{255}$$

$$\overleftrightarrow{\mathbf{F}}_B(\mathbf{r}) = \overleftrightarrow{\mathbf{F}}_E(\mathbf{r}) + \frac{1}{k^2}\nabla\times\overleftrightarrow{\mathbf{F}}_E(\mathbf{r})\cdot\overleftrightarrow{\boldsymbol{\varepsilon}}^{-1}(\mathbf{r})\left[\nabla\times\overleftrightarrow{\boldsymbol{\mu}}^{-1}(\mathbf{r}) + \overleftrightarrow{\boldsymbol{\mu}}^{-1}(\mathbf{r})\nabla\times\right], \tag{256}$$

$$\overleftrightarrow{\mathbf{F}}_D(\mathbf{r}) = \overleftrightarrow{\mathbf{F}}_H(\mathbf{r}) + \frac{1}{k^2}\nabla\times\overleftrightarrow{\mathbf{F}}_H(\mathbf{r})\cdot\left[\nabla\times\overleftrightarrow{\boldsymbol{\varepsilon}}^{-1}(\mathbf{r}) + \overleftrightarrow{\boldsymbol{\varepsilon}}^{-1}(\mathbf{r})\cdot\nabla\times\right]. \tag{257}$$

Expressing the wave equations in terms of $\mathbf{B}$ and $\mathbf{D}$ as an inhomogeneous wave equation with homogeneous wave number and a scattering potential dependent on both the permittivity and the permeability increases the flexibility in designing scatterers. With these equations we now have two variables that we can independently manipulate to achieve the desired scattering behavior. For example, the equations could be greatly simplified by choosing either the permittivity or the permeability to be

a scalar function. In Chapter 6, it will be shown how this formulation of the equations is particularly advantageous to design directionally invisible objects, which are introduced in Chapter 4. Moreover, these equations can also demonstrate that it is possible to design invisible objects without the condition that the permittivity must be equal to the permeability, as is required by the transformation optics method. In addition, the existence of these equations also shows that there are solutions to the wave equation that do not require either the permittivity or the permeability to be the free space value.

3.4 Summary

This chapter began with the introduction of scalar scattering theory and its connection to the inverse problem. It was shown how to quantify the scattering behavior of an object through the optical cross-section theorem with the scattering, the extinction, and the absorption cross-sections. These figures of merit are used in the next chapter to characterize a variety of invisible objects. Finally, the vector wave equations for each of the electromagnetic fields was derived and restated in the form of an inhomogeneous equation with a scattering potential or tensor operator acting on the total field. The equations are also written so that a simple variable change would render them identical to the inverse source problem, and therefore solutions to the inverse source problem are applicable. The newly-derived equations also broaden the way in which scatterers may be designed and analyzed. Their particular usefulness in expanding the types of invisible objects that can exist beyond transformation optics is demonstrated in Chapter 6.

CHAPTER 4: DIRECTIONAL INVISIBILITY

In this chapter, we introduce a new method to design directionally invisible objects for an incident field with one direction of incidence, which we call the *field cloak method*. Unlike most approaches to invisibility, which involve manipulating the material parameters to guide light around a cloaked region, we begin by assuming the most basic requirement for invisibility: the scattered field outside of the domain must be zero. In order to achieve this, the scattered field must be subject to specific boundary conditions borrowed from a well-developed theory to design *nonradiating sources*. So essentially, here we work backwards from the fundamental assumption that the scattered field is absent, forcing the object to be perfectly invisible, and by solving the governing wave equation, we arrive at an expression for the scattering potential, which is directly related to the object's material parameters.

Upon simulating this class of invisible objects, we noticed that they were directionally invisible and, under certain conditions, displayed $\mathcal{PT}$ symmetry–a type of symmetry borrowed from quantum mechanics that in optics leads to balanced gain and loss and, therefore, perfect transmission of light. In optics, this was typically achieved by designing a material with a $\mathcal{PT}$-symmetric refractive index along one dimension, but we extended the theory by showing that a broader condition is requiring the scattering potential to be $\mathcal{PT}$ symmetric, which opened the possibility of designing two- and three-dimensional directionally invisible objects. Prior to the work

presented here, it was thought that $\mathcal{PT}$ symmetry was a necessary condition for directional invisibility, but here we demonstrate that it is possible to design directionally invisible objects without any particular symmetry.

In Section 4.1, we introduce the historical background of $\mathcal{PT}$ symmetry and its connection to optics, gain-loss devices, and directional invisibility. This is followed by a formal derivation of the field cloak method and demonstrating how it can result in two-dimensional $\mathcal{PT}$ symmetric directionally invisible objects in Section 4.2. Next, we derive the discrete forms of the equations and describe the simulation technique used to verify the theory (Section 4.3). Numerical simulation is then used to demonstrate and characterize both $\mathcal{PT}$-symmetric scatterers and asymmetric scatterers Section 4.4). To clarify the role of $\mathcal{PT}$ symmetry in directional invisibility, we formally prove that the boundary conditions applied to the scattered field and not $\mathcal{PT}$ symmetry account for the balanced gain loss, and their application to the wave equation in terms of the scattering potential determine the directionality (Section 4.5). We conclude this chapter with a summary of the highlights and their implications (Section 4.6).

4.1 Historical background

Physical systems, both classical and quantum-mechanical, are characterized by an operator called the Hamiltonian [5]. In quantum mechanics, we distinguish between two types of Hamiltonians. Hermitian Hamiltonians govern the behavior of isolated, idealized systems in equilibrium. In such systems, the total energy and probability are conserved, as represented by the Hamilitonian's real eigenvalues. In contrast,

non-Hermitian Hamiltonians govern the behavior of experimental systems which interact with the environment, involved in scattering or decay processes. Often these systems are not in equilibrium because they gain energy from or lose energy to the environment, often resulting in situations where the total energy and probability are not conserved. As a result, these types of systems exhibit complex energy eigenvalues. The imaginary part of the energy eigenvalue represents a quantity associated with the gain and loss. Consequently, it was assumed that the Hamiltonian of Schrödinger's equation was required to be Hermitian to guarantee that system's energy eigenvalues are real [4].

In 1998, the discovery that a wide class of non-Hermitian Hamiltonians can still possess entirely real energy spectra if they are parity-time ($\mathcal{PT}$)-symmetric therefore attracted much attention [3]. These $\mathcal{PT}$-symmetric Hamiltonians describe systems with balanced gain-loss and allow for constrained interaction with the environment, such that total energy and probability are conserved. Soon after, such systems were studied in many other areas of physics and eventually a connection was made to optics in 2007. In optics, it has been argued that the complex refractive index $n(\mathbf{r}) = n_R(\mathbf{r}) + in_I(\mathbf{r})$ is analogous to the quantum mechanical potential, where the real part of the refractive index must be a symmetric function of position $\mathbf{r}$, i.e. $n_R(\mathbf{r}) = n_R(-\mathbf{r})$, while the imaginary part of the $n(\mathbf{r})$ must be an anti-symmetric function of $\mathbf{r}$, i.e. $n_I(\mathbf{r}) = -n_I(-\mathbf{r})$, to achieve $\mathcal{PT}$-symmetric behavior [18, 48].

Around the same time, invisibility began to draw more attention when the first electromagnetic cloak was demonstrated via transformation optics and conformal mapping in 2006 [46, 55]. Then as of 2010 a variety of $\mathcal{PT}$-symmetric optical devices

that are unidirectionally invisible or exhibit perfect transmission and are reflectionless were demonstrated experimentally [58, 47, 21, 69]. A number of these $\mathcal{PT}$-symmetric systems have exhibited directional invisibility–they are perfectly reflectionless for one direction of illumination and strongly scattering in the opposite direction [58, 47], and this directional invisibility was attributed to their $\mathcal{PT}$-symmetry at that time. These systems have, however, almost entirely been investigated in layered, gain-loss, infinite slab geometries [21, 57], with the exception of two studies: One considers a specific localized $\mathcal{PT}$-symmetric scatterer designed using transformation optics [69], while the other explores a $\mathcal{PT}$-symmetric cylindrical cloak with a gain coating on the incident side and a loss coating on the exiting side for a microwave plane wave [64]. In 2015 Gbur introduced a method to design directionally invisible scatterers and cloaks from localized fields which exactly satisfy the governing wave equation [29]. It turns out that a subset of these directionally invisible scatterers and cloaks are $\mathcal{PT}$-symmetric, although directionally invisible scatterer without any symmetry were theoretically demonstrated as well [36]. In the next section, we formally derive this method and elucidate its relationship to $\mathcal{PT}$-symmetry.

4.2 $\mathcal{PT}$-symmetric directionally invisible scatterers

In this section, we explore the role $\mathcal{PT}$ symmetry plays in achieving directionally invisible scatterers using a newly-developed method for constructing directionally invisible objects. A directionally invisible object is invisible for an incident field with one or more directions of incidence. It is shown that $\mathcal{PT}$ symmetry is not a necessary condition for the scatterer to be directionally invisible or for the invisibility of

such objects in general. It is possible to design both $\mathcal{PT}$-symmetric and non-$\mathcal{PT}$-symmetric directionally invisible objects, and an example of each is presented. It is also shown that requiring the complex scattering potential, instead of the complex refractive index, to be $\mathcal{PT}$-symmetric reveals the complete set of $\mathcal{PT}$-symmetric optical structures. Consequently, if the scattering potential is $\mathcal{PT}$-symmetric, there are two distinct solutions for the complex refractive index. This implies that for every $\mathcal{PT}$-symmetric complex refractive index, there is a complementary non-$\mathcal{PT}$-symmetric refractive index that results in a $\mathcal{PT}$-symmetric scattering potential.

Recently, Gbur introduced a new technique [29] to design a wide variety of directionally invisible objects directly and without approximation from the governing wave equation, subject to a number of boundary conditions. The problem is framed in terms of classic scattering theory (Chapter 3, Section 3.1), in which the object or scatterer is described by its scattering potential instead of by its refractive index. Within this framework, the analogy between the time-independent Schrödinger equation, in terms of the quantum mechanical potential, and the Helmholtz equation, in terms of the scattering potential, evinces the relationship between $\mathcal{PT}$ symmetry in quantum mechanics and $\mathcal{PT}$ symmetry in optics. We show that this method, described below, naturally generates $\mathcal{PT}$-symmetric and more general invisible objects.

We begin by considering a scalar field scattered by an object of refractive index $n(\mathbf{r})$, illuminated by a monochromatic plane wave. The total field $U(\mathbf{r})$ satisfies the Helmholtz equation with an inhomogeneous wavenumber,

$$\left[\nabla^2 + n^2(\mathbf{r})k^2\right] U(\mathbf{r}) = 0, \tag{258}$$

where $k = \frac{\omega}{c} = \frac{2\pi}{\lambda}$, ω is the frequency, λ is the wavelength, and c is the vacuum speed of light. We again introduce the scattering potential $F(\mathbf{r})$ of the form,

$$F(\mathbf{r}) = \frac{k^2}{4\pi}\left[n^2(\mathbf{r}) - 1\right], \tag{259}$$

and write $U(\mathbf{r}) = U^{(i)}(\mathbf{r}) + U^{(s)}(\mathbf{r})$, where $U^{(i)}(\mathbf{r}) = e^{ik\hat{\mathbf{s}}_0\cdot\mathbf{r}}$ and $U^{(s)}(\mathbf{r})$ are the incident and scattered fields, respectively. We again have an inhomogeneous wave equation for the scattered field (Chapter 3, Section 3.1),

$$\left(\nabla^2 + k^2\right) U^{(s)}(\mathbf{r}) = -4\pi F(\mathbf{r})U(\mathbf{r}). \tag{260}$$

Because the scattered field is present on both sides of Eq. (260), it is generally not possible to solve this equation analytically. However, to find a nonscattering solution, we may define

$$U^{(s)}(\mathbf{r}) = U^{(i)}(\mathbf{r})U^{(loc)}(\mathbf{r}), \tag{261}$$

where $U^{(loc)}(\mathbf{r})$ is called the local scattered field of the inhomogeneous scatterer, representing the effect of the complex refractive index variation of the scatterer [29]. In essence, we treat the scattered field as a distortion of the incident field. Recall from Chapter 3, that there is an equivalence relation given by Eq. (118) between the Helmholtz equation describing a source and that describing a scatterer; this relation allows the solutions and theorems from the source equation to be applied to the scattering equation. A source distribution $q(\mathbf{r})$ generating a field $u(\mathbf{r})$ described by the Helmholtz equation, given by

$$\left(\nabla^2 + k^2\right)u(\mathbf{r}) = -4\pi q(\mathbf{r}), \tag{262}$$

is nonradiating if the field $u(\mathbf{r})$ satisfies the following boundary conditions [25],

$$u(\mathbf{r})|_S = 0, \text{ and } \left.\frac{\partial}{\partial n}u(\mathbf{r})\right|_S = 0, \tag{263}$$

where S is the boundary of source domain D and $\frac{\partial}{\partial n}$ denotes differentiation along the outward normal. The solution to Eq. (262) is

$$u(\mathbf{r}) = \int_D q(\mathbf{r}')\frac{e^{ik|\mathbf{r}-\mathbf{r}'|}}{|\mathbf{r}-\mathbf{r}'|}\,\mathrm{d}^3r'. \tag{264}$$

To find a source $q(\mathbf{r})$, we only have to solve Eq. (262) for $q(\mathbf{r})$, as follows

$$q(\mathbf{r}) = -\frac{1}{4\pi}\left(\nabla^2 + k^2\right)u(\mathbf{r}), \tag{265}$$

and choose a function $u(\mathbf{r})$ that satisfies the boundary conditions in Eq. (263) within domain D. The Green's function is symmetric and, therefore, only affects the value of $u(\mathbf{r})$ within the source, since the boundary conditions applied to the source distribution $q(\mathbf{r})$ causes the integral (Eq. (264)) to be zero outside of the domain D due to the symmetry imposed on the function $q(\mathbf{r})$ by the boundary conditions.

Comparing Eq. (260) and Eq. (262) we make the association $F(\mathbf{r})U(\mathbf{r}) = q(\mathbf{r})$ and $U^{(s)}(\mathbf{r}) = u(\mathbf{r})$. Consequently, we may apply the boundary conditions (Eq. (263), [25]) used to design *nonradiating sources* [27] to the scattered field $U^{(s)}(\mathbf{r})$ to design *non-scattering scatterers* [29]. The scattered field $U^{(s)}(\mathbf{r})$ must satisfy

$$U^{(s)}(\mathbf{r})\big|_S = 0, \text{ and } \left.\frac{\partial}{\partial n}U^{(s)}(\mathbf{r})\right|_S = 0, \tag{266}$$

where S is the surface of the domain D of the scatterer. Since we assume that the scattered field is given by Eq. (261) and $U^{(i)}(\mathbf{r})$ is a periodic function, for example,

a plane wave, the scattered field is limited to within the scatterer, only if $U^{(loc)}(\mathbf{r})$ is subject to the same boundary conditions,

$$U^{(loc)}(\mathbf{r})\big|_S = 0, \text{ and } \frac{\partial}{\partial n}U^{(loc)}(\mathbf{r})\bigg|_S = 0, \tag{267}$$

where $\frac{\partial}{\partial n}$ represents the derivative normal to the surface S, forming the boundary of the scatterer [29]. By limiting the local scattered field $U^{(loc)}(\mathbf{r})$, scattering outside of the domain of the scatterer is prevented. Writing the total field as

$$U(\mathbf{r}) = \left[1 + U^{(loc)}(\mathbf{r})\right] U^{(i)}(\mathbf{r}), \tag{268}$$

and substituting Eq. (268) and Eq. (261) into Eq. (259), we obtain the following expression

$$\left(\nabla^2 + k^2\right)U^{(i)}(\mathbf{r})U^{(loc)}(\mathbf{r}) = -4\pi F(\mathbf{r})\left[1 + U^{(loc)}(\mathbf{r})\right] U^{(i)}(\mathbf{r}). \tag{269}$$

First we evaluate the left side of Eq. (269) as follows

$$\begin{aligned}\left(\nabla^2 + k^2\right)U^{(i)}(\mathbf{r})U^{(loc)}(\mathbf{r}) &= \nabla^2[U^{(i)}(\mathbf{r})U^{(loc)}(\mathbf{r})] + k^2U^{(i)}(\mathbf{r})U^{(loc)}(\mathbf{r}) \\ &= \nabla^2[U^{(i)}(\mathbf{r})U^{(loc)}(\mathbf{r})] + k^2U^{(i)}(\mathbf{r})U^{(loc)}(\mathbf{r}) \\ &= \nabla\cdot\nabla[U^{(i)}(\mathbf{r})U^{(loc)}(\mathbf{r})] + k^2U^{(i)}(\mathbf{r})U^{(loc)}(\mathbf{r}).\end{aligned} \tag{270}$$

If we now simplify the first term of the last line,

$$\begin{aligned}\nabla\cdot\nabla[U^{(i)}(\mathbf{r})U^{(loc)}(\mathbf{r})] &= \nabla\cdot[ik\hat{\mathbf{s}}_0U^{(i)}(\mathbf{r})U^{(loc)}(\mathbf{r}) + U^{(i)}(\mathbf{r})\nabla U^{(loc)}(\mathbf{r})] \\ &- k^2U^{(i)}(\mathbf{r})U^{(loc)}(\mathbf{r}) + 2ik\hat{\mathbf{s}}_0U^{(i)}(\mathbf{r})\cdot\nabla U^{(loc)}(\mathbf{r}) + U^{(i)}(\mathbf{r})\nabla^2U^{(loc)}(\mathbf{r}),\end{aligned} \tag{271}$$

where we have evaluated $\nabla U^{(i)}(\mathbf{r}) = ik\hat{\mathbf{s}}_0e^{ik\hat{\mathbf{s}}_0\cdot\mathbf{r}}$ and $(ik)\hat{\mathbf{s}}_0\cdot(ik)\hat{\mathbf{s}}_0 = -k^2$. Combining

Eqs. (270) and (271) we find that the left side of Eq. (269) is given by

$$\left(\nabla^2 + k^2\right)U^{(i)}(\mathbf{r})U^{(loc)}(\mathbf{r}) = \nabla^2 U^{(loc)}(\mathbf{r})U^{(i)}(\mathbf{r}) + 2ik\hat{\mathbf{s}}_0 \cdot \nabla U^{(loc)}(\mathbf{r})U^{(i)}(\mathbf{r}). \quad (272)$$

Comparing the result for the left side in Eq. (272) with the right side of Eq. (269), as follows,

$$\nabla^2 U^{(loc)}(\mathbf{r})U^{(i)}(\mathbf{r}) + 2ik\hat{\mathbf{s}}_0 \cdot \nabla U^{(loc)}(\mathbf{r})U^{(i)}(\mathbf{r}) = -4\pi F(\mathbf{r})\left[1 + U^{(loc)}(\mathbf{r})\right]U^{(i)}(\mathbf{r}), \quad (273)$$

we see that after dividing by the incident field $U^{(i)}(\mathbf{r})$ on both sides, it is possible to derive an exact expression for the scattering potential $F(\mathbf{r})$ that produces the scattered field, given by

$$F(\mathbf{r}) = -\frac{1}{4\pi}\frac{\nabla^2 U^{(loc)}(\mathbf{r}) + 2ik\hat{\mathbf{s}}_0 \cdot \nabla U^{(loc)}(\mathbf{r})}{1 + U^{(loc)}(\mathbf{r})}, \quad (274)$$

which only is a function of the local scattered field $U^{(loc)}(\mathbf{r})$, as was originally derived by Gbur in [29]. We now note that a remarkable effect of this construction is that any real, mirror symmetric $U^{(loc)}$ will result in a localized $\mathcal{PT}$-symmetric, directionally invisible object. This occurs because the numerator of Eq. (274) consists of a real, symmetric operation on $U^{(loc)}(\mathbf{r})$ and an imaginary, anti-symmetric operation on $U^{(loc)}(\mathbf{r})$, while the denominator is a function of $U^{(loc)}(\mathbf{r})$. If we take the complex conjugate of the scattering potential defined by Eq. (274), we obtain

$$F^{\star}(\mathbf{r}) = -\frac{1}{4\pi}\frac{\nabla^2 U^{(loc)\star}(\mathbf{r}) - 2ik\hat{\mathbf{s}}_0 \cdot \nabla U^{(loc)\star}(\mathbf{r})}{1 + U^{(loc)\star}(\mathbf{r})}. \quad (275)$$

If we further assume that $U^{(loc)}(\mathbf{r})$ is real and symmetric and substitute $U^{(loc)}(\mathbf{r}) =$

$U^{(loc)}(-\mathbf{r})$ into Eq. (275), then we may see that

$$\begin{aligned} F^{\star}(\mathbf{r}) &= -\frac{1}{4\pi}\frac{\nabla^2 U^{(loc)}(-\mathbf{r}) - 2ik\hat{\mathbf{s}}_0 \cdot \nabla[U^{(loc)}(-\mathbf{r})]}{1+U^{(loc)}(-\mathbf{r})} \\ &= -\frac{1}{4\pi}\frac{\nabla^2 U^{(loc)}(-\mathbf{r}) - 2ik\hat{\mathbf{s}}_0 \cdot \left[-\nabla U^{(loc)}(-\mathbf{r})\right]}{1+U^{(loc)}(-\mathbf{r})} \\ &= -\frac{1}{4\pi}\frac{\nabla^2 U^{(loc)}(-\mathbf{r}) + 2ik\hat{\mathbf{s}}_0 \cdot \nabla U^{(loc)}(-\mathbf{r})}{1+U^{(loc)}(-\mathbf{r})} \\ &= F(-\mathbf{r}), \end{aligned} \tag{276}$$

where we take advantage of the relation that if $U^{(loc)}(\mathbf{r})$ is real and symmetric its derivative is antisymmetric and $\nabla U^{(loc)}(\mathbf{r}) = -\nabla[U^{(loc)}(-\mathbf{r})]$ and the expression $\nabla^2 U^{(loc)}(-\mathbf{r}) = \nabla^2 U^{(loc)}(\mathbf{r})$ is symmetric with respect to $\mathbf{r}$. Therefore, the scattering potential satisfies the condition $F^{(\star)}(\mathbf{r}) = F(-\mathbf{r})$ and is, consequently, $\mathcal{PT}$ symmetric. With this framework, we may provide some examples of directionally invisible objects after explaining the simulation technique.

4.3 Simulations of Directionally Invisible Scatterers

To demonstrate these types of invisible objects, we apply a Green's function method [49] to calculate response of the scatterer to the incident field. Recall that the solution to the scattered field $U^{(s)}$ associated with the governing wave equation (Eq. (260)),

$$[\nabla^2 + k^2]U^{(s)}(\mathbf{r}) = -4\pi F(\mathbf{r})U(\mathbf{r}), \tag{277}$$

is given by the integral (Chapter 3, Section 3.1),

$$U^{(s)}(\mathbf{r}) = \int G(\mathbf{r},\mathbf{r}')F(\mathbf{r}')U(\mathbf{r}')\,\mathrm{d}^2 r', \tag{278}$$

where $G(\mathbf{r},\mathbf{r}')$ is the Green's function. Although the equations are valid for three dimensional objects, here for all practical purposes, we use the two-dimensional forms

for the simulations to model two-dimensional objects. The first step is to discretize the scatterer into small regions and a limited region surrounding the scatterer. A Cartesian coordinate and grid system is used with spacing a along both the vertical and horizontal axes. This way, any type of scatterer that satisfies the boundary conditions can be studied by this method. To reflect the discretization of the scatterer in the simulation, we derive the discrete form of the scattered field from its continuous counterpart. In terms of the discrete regions labeled i, j with respective volumes labeled V_i and V_j, and the scattered field (Eq. (278)) is written as

$$U^{(s)}(\mathbf{r}_i) = \sum_j \int_{V_j} G(\mathbf{r}_i, \mathbf{r}') F(\mathbf{r}') U(\mathbf{r}') \, \mathrm{d}^2 r' \tag{279}$$

This equation is also known as the self-consistency equation. For $j \neq i$ all terms are approximately constant, and the integrand is simply a constant multiplied by the area $\Delta A = a^2$, but for $j = i$ the elements of $U^{(s)}(\mathbf{r}_i)$ must be treated separately. Therefore, we divide Eq. (279) into two components,

$$U^{(s)}(\mathbf{r}_i) = \sum_{j \neq i} G(\mathbf{r}_i, \mathbf{r}_j) F(\mathbf{r}_j) U(\mathbf{r}_j) \Delta A + F(\mathbf{r}_i) U(\mathbf{r}_i) \int_{V_i} G(\mathbf{r}_i, \mathbf{r}') \, \mathrm{d}^2 r', \tag{280}$$

where $\Delta A = a^2$ is the area of the discrete region V_j. Next, we need to figure out how to solve Green's function integral in (280). Let Q be the Green's function integral per unit area a^2, given by

$$Q \equiv \frac{1}{a^2} \int_{V_i} G(\mathbf{r}_i, \mathbf{r}') \, \mathrm{d}^2 r' \tag{281}$$

The two-dimensional Green's function is

$$G = i\pi H_0^{(1)}(kr) \tag{282}$$

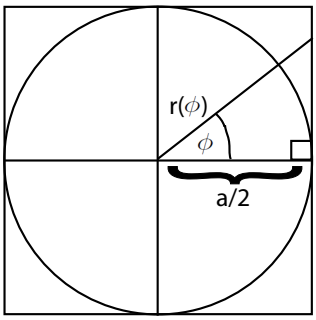

Figure 12: The relationship between the discrete unit length a, the angle ϕ with respect to the $\hat{\mathbf{x}}$ axis, and the radius r.

The Hankel function is composed of the Bessel and Neumann functions and for small r the zeroth order Bessel function goes to 1, and consequently the Hankel function may be rewritten as follows:

$$\begin{aligned} H_0^{(1)}(kr) &= J_0(kr) + iN_0(x) \\ &\approx J_0(kr)\left[1 + i\frac{2}{\pi}\ln\left(\frac{kr}{2}\right)\right] \\ &\approx 1 + i\frac{2}{\pi}\log\left(\frac{kr}{2}\right). \end{aligned} \tag{283}$$

By substituting Eq. (283) into Eq. (282) and Eq. (282) into Eq. (281), we obtain

$$\begin{aligned} Q &= \frac{i\pi}{a^2}\int_0^r\int_0^{2\pi}\left(1 + i\frac{2}{\pi}\ln\frac{kr'}{2}\right)r'\,\mathrm{d}r'\,\mathrm{d}\phi \\ &= \frac{i\pi}{a^2}\int_0^{2\pi}\left[\frac{r^2}{2} + i\frac{r^2}{2\pi}\left(\ln\frac{kr}{2} - 1\right)\right]\mathrm{d}\phi, \end{aligned} \tag{284}$$

where r in terms of ϕ shown in Fig. 12 is defined as

$$r = \frac{a}{2\cos\phi}. \tag{285}$$

Then Eq. (284) in terms of ϕ is given by

$$\begin{aligned} Q &= \frac{i\pi}{2a^2} \int_0^{2\pi} \left[\frac{a^2}{4\cos^2\phi} + i\frac{a^2}{4\pi\cos^2\phi} \left(\ln \frac{ka}{4\cos\phi} - 1 \right) \right] \mathrm{d}\phi \\ &= \frac{i\pi}{8} \int_0^{2\pi} \left[\frac{1}{\cos^2\phi} + \frac{i}{\pi\cos^2\phi} \left(\ln ka - \ln\left(4\cos\phi\right) - 1 \right) \right] \mathrm{d}\phi. \end{aligned} \tag{286}$$

Using four-fold symmetry and separating the integral in Eq. (286),

$$\begin{aligned} Q &= \frac{i\pi}{2} \int_{-\frac{\pi}{4}}^{\frac{\pi}{4}} \left[\frac{1}{\cos^2\phi} + \frac{i(\ln ka - 1)}{\pi\cos^2\phi} \right] \mathrm{d}\phi - \frac{i\pi}{2} \int_{-\frac{\pi}{4}}^{\frac{\pi}{4}} \frac{i}{\pi\cos^2\phi} \ln\left(4\cos\phi\right) \mathrm{d}\phi \\ &= \frac{i\pi - \ln ka + 1}{2} \int_{-\frac{\pi}{4}}^{\frac{\pi}{4}} \frac{1}{\cos^2\phi}\, \mathrm{d}\phi + \frac{1}{2} \int_{-\frac{\pi}{4}}^{\frac{\pi}{4}} \frac{\ln\left(4\cos\phi\right)}{\cos^2\phi}\, \mathrm{d}\phi \end{aligned} \tag{287}$$

Numerical integration in Mathematica gives 2 and 2.50685 for the first and second integral in Eq. (287), resulting in the following simplified expression for Q,

$$\begin{aligned} Q &= i\pi - \ln ka + 1 + \frac{2.50865}{2} \\ &= 2.25432 - \ln ka + i\pi. \end{aligned} \tag{288}$$

This is the value of the Q or the Green's function integral when $i = j$ in Eq. (290), i.e. the diagonal element, as a function of the discrete length a and the wavenumber k. The next step is to set up a coordinate system and map the matrix of discrete spatial positions (m, n) onto a vector of positions with a single index i (Fig.13). Suppose the square matrix that includes the scatterer has rows and columns of length N, the values from a vector with index i are mapped into matrix by the following conversion

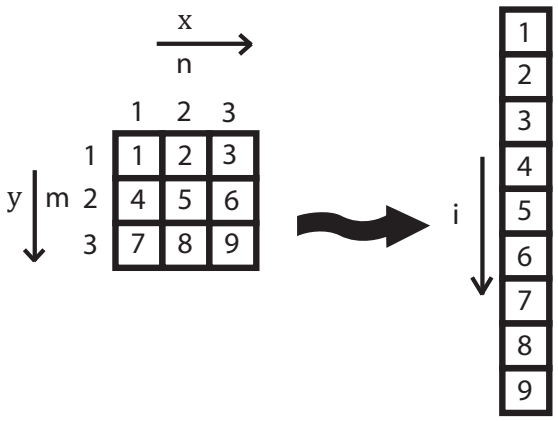

Figure 13: This shows the elements of the two-dimensional array are mapped onto a one-dimensional vector.

to indices m and n:

$$m = \text{floor}\left(\frac{i-1}{N}\right) + 1,$$
$$n = \quad \text{mod}\left(\frac{i-1}{N}\right) + 1.$$

Now Eq. (280) may be rewritten in a discretized form with the differential area, $\Delta A = a^2$, given by

$$U^{(s)}(\mathbf{r}_i) = \sum_{j \neq i} G(\mathbf{r}_i, \mathbf{r}_j) F(\mathbf{r}_j) U(\mathbf{r}_j) a^2 + F(\mathbf{r}_j) U(\mathbf{r}_j) a^2 Q \tag{289}$$

where where the array elements of the Green's function are defined as

$$\overline{G}(\mathbf{r}_i, \mathbf{r}_j) = \begin{cases} G(\mathbf{r}_i, \mathbf{r}_j) & i \neq j \\ Q & i = j \end{cases} \tag{290}$$

If we add $U^{(i)}$ to each side and recall that $U = U^{(s)} + U^{(i)}$, the total field is defined as

$$U(\mathbf{r}_i) = \sum_j \overline{G}(\mathbf{r}_i, \mathbf{r}_j) F(\mathbf{r}_j) U(\mathbf{r}_j) a^2 + U^{(i)}(\mathbf{r}_i) \tag{291}$$

This permits us to rewrite the incident field $U^{(i)}$ in terms of the total field U, given

by

$$U^{(i)}(\mathbf{r}_i) = [\delta_{ij} - a^2\overline{G}(\mathbf{r}_i, \mathbf{r}_j)F(\mathbf{r}_j)]U(\mathbf{r}_j), \tag{292}$$

where the expression in square brackets represents a matrix. Solving for the total field now is easily accomplished by multiplying both sides by the inverted matrix, resulting in the following expression for the total field

$$U(\mathbf{r}_j) = [\delta_{ij} - a^2\overline{G}(\mathbf{r}_i, \mathbf{r}_j)F(\mathbf{r}_j)]^{-1}U^{(i)}(\mathbf{r}_i). \tag{293}$$

This expression is used to calculate the total field within a small square region enclosing the scatterer. Then the total field outside of the scatter is calculated by using Eq. (291), where the total field resulting from Eq. (293) is substituted for $U(\mathbf{r}_j)$ in the integral.

To compute the total and scattered fields given by these equations in Matlab, we create a number of variables. First, the size of the scattering region is given by the length L of one side of the square. The square has N number of cells on each side, and consequently each cell's size is $a = \frac{L}{N}$. The remaining variables are defined in

terms of the dimensions of the region, including

$$\mathrm{x} = -\frac{L}{2} + \frac{a}{2} < m < \frac{L}{2} - \frac{a}{2} \tag{294}$$

$$\mathrm{y} = -\frac{L}{2} + \frac{a}{2} < n < \frac{L}{2} - \frac{a}{2} \tag{295}$$

$$\mathrm{xy}|_i = \{\mathrm{x}(m); \mathrm{y}(n)\} \tag{296}$$

$$\mathrm{potential}|_i = F[\mathrm{xy}(1,i), \mathrm{xy}(2,i)] \tag{297}$$

$$\mathrm{diff}|_{ij} = \sqrt{(\mathrm{xy}(1,i) - \mathrm{xy}(1,j))^2 + (\mathrm{xy}(2,i) - \mathrm{xy}(2,j))^2} \tag{298}$$

$$\mathrm{gbar}|_{ij} = \begin{cases} G(\mathbf{r}_i, \mathbf{r}_j) & i \neq j \\ Q & i = j \end{cases} \tag{299}$$

$$A|_{ij} = \delta_{ij} - \mathrm{a}^2 \mathrm{gbar}|_{ij} \mathrm{potential}|_j \tag{300}$$

$$U^{(i)}|_i = U^{(i)}(\mathrm{xy}(1,i), \mathrm{xy}(2,i)) \tag{301}$$

where Eqs. (294) and (295) define the x- and y-positions, which are incorporated into a two-dimensional position matrix in Eq. (296). This position matrix is used to define the scattering potential F in Eq. (297). To calculate the Green's function when $i \neq j$, it is necessary to define a difference matrix, as shown in Eq. (298). Eq. (299) computationally defines $\overline{G}$ as described by above in Eq. (290), where Q is defined in Eq. (288). The full matrix $A|_{ij}$ in Eq. (300) represents the left factor in Eq. (292) which multiplies the total field U. The matrix $U^{(i)}|_i$ in Eq. (301) stores the incident field as it is computed. Once we have established these variables we can proceed to compute the total field.

We recall that Eq. (291) allows us to compute the total field U from the incident field, the Green's function (Eq. (290)), and the scattering function within the

scatterer. But now we need to modify it to also account for points outside of the scatterer. Therefore a new set of indices is created in terms of p and q, which include the ranges by m and n. Whereas m and n are used to traverse an area of size L^2 and reach a maximum index N, p and q traverse an area of size $L_{tot}^2 = (2L)^2$ and reach a maximum index $N_{tot} = 2N$. The area L^2 is centered within L_{tot}^2. This allows us to maintain the same unit area a^2 across the entire region. To calculate the total field outside of the scatterer, the following equation must be discretized (Chapter 3):

$$U(\mathbf{r}) = U^{(i)}(\mathbf{r}) + \int G(\mathbf{r}, \mathbf{r}')F(\mathbf{r}')U(\mathbf{r}')\,\mathrm{d}^2 r'. \tag{302}$$

For points outside of the scatterer at $\mathbf{r}_{mn}$, the discrete equation is given by

$$U(\mathbf{r}_{mn}) = U^{(i)}(\mathbf{r}_{mn}) + a^2 \sum_{p,q} G(\mathbf{r}_{mn}, \mathbf{r}_{pq})F(\mathbf{r}_{pq})U(\mathbf{r}_{pq}). \tag{303}$$

We calculate the total field using Eq. (303) through the entire region indexed by m and n, where the total field for points outside the scatterer is calculated with Eq. (303) and $U(\mathbf{r}_{pq})$ is the result for the total field from Eq. (293). In the end, $U(\mathbf{r}_{mn})$ includes $U(\mathbf{r}_{pq})$ in addition the total field for points outside of the scatterer. The scattered field is easily obtained by subtracting the incident field from the total field. The local field for the invisibility direction is then calculated by dividing the scattered field by the incident field. This technique enables the numerical simulation of a scatterer with an incident plane wave from any direction. The fields are then used to calculate the extinction and scattering cross-sections.

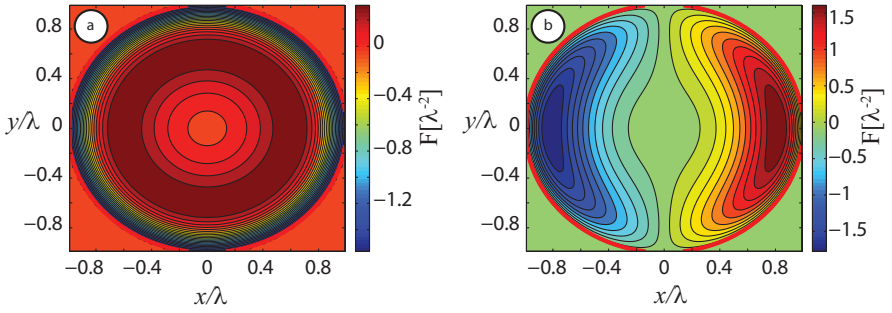

Figure 14: The real part (a) and the imaginary part (b) of the scattering potential $F(\mathbf{r})$ associated with Eq. (304), ($a = 1$).

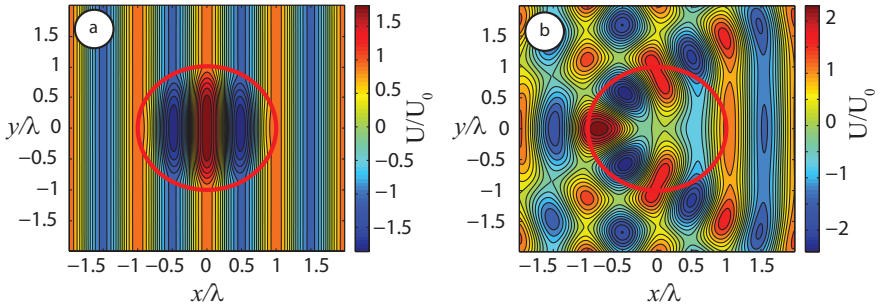

Figure 15: The real part of the total field (incident + scattered) when the incident plane wave ($\lambda = 1$) propagates in the positive $\hat{\mathbf{x}}$-direction ($\theta = 0°$) (a) and when the incident plane wave propagates in the negative $\hat{\mathbf{x}}$-direction ($\theta = 180°$) (b). The circles indicate the domain of the scatterer, which has a radius $a = 1$. U_0 is the incident field amplitude.

4.4 Examples of directionally invisible objects

To demonstrate such a $\mathcal{PT}$-symmetric invisible scatterer, we consider a system with $\hat{\mathbf{s}}_0 = \hat{\mathbf{x}}$ and $U^{(loc)}$ given by

$$U^{(loc)}(\mathbf{r}) = \cos^2\left(\frac{\pi r^2}{2a^2}\right), \ |r| \leq a, \tag{304}$$

where $r = \sqrt{x^2 + y^2}$ and a is the radius of the scatterer. The scatterer is designed by substituting Eq. (304) into Eq. (274). The calculated real and imaginary parts of the scattering potential are symmetric and anti-symmetric, respectively, with respect to position along the $\hat{\mathbf{x}}$-axis, as shown in Fig. 14. When a plane wave is incident from

the left (the invisibility direction), there is no scattered field (Fig. 15(a)), whereas there is strong scattering when a plane wave is incident from the opposite direction (Fig. 15(b)).

Unidirectional perfect transmission has been observed in other $\mathcal{PT}$-symmetric structures, for example, in optically coupled fibers [58] and in a unidirectional reflectionless fiber [47]. The absence of reflection for one direction in those cases was demonstrated by calculating and measuring the transmission and reflection coefficients for both directions. Perfect transmission is evidently achieved by balancing gain and loss for one direction of propagation. In a slab structure, this is easily achieved by calculating the transmission and reflection coefficients for each direction by measuring the incident power before the slab and power transmitted by the slab.

However, there is a more general approach to understanding the energy exchange between the medium of any shape and the incident field. Instead of calculating transmission and reflection coefficients for each direction, the extinction cross-section, which describes energy removed from the incident wave, and the scattering cross-section of the scatterer may be calculated. Since light can be scattered in many directions simultaneously by a scatterer, the scattering cross-section, which is calculated from the scattered field at a surface enclosing the scatterer, quantifies all of the scattered energy in all directions with respect to the scatterer regardless of its geometry. It can then be said that perfect transmission takes place when the incident field passes through the scatterer undistorted. In this case both the scattering cross-section and the extinction cross-section are zero.

In 1975 during the study of dielectric spheres of varying sizes and one or more

layers, Kerker discovered that the invisible spheres had a zero scattering cross-section, while the other spheres exhibited a high scattering cross-section although all of the spheres were non-absorbing [41]. These non-absorbing dielectric spheres with a high scattering cross-section are examples of pure gain objects. These findings led him to postulate that non-absorbing objects with a scattering cross-section of zero are invisible. Alexopoulos and Uzunoglu subsequently observed that when the extinction cross-section is zero the particles were invisible [1]. Consequently, they stated that a zero extinction cross-section was a less stringent, necessary condition for invisibility. Then Kerker studied the the implications of a an extinction cross-section equal to zero in active (gain-loss) media and came to the conclusion that an object with an extinction cross-section equal to zero was insufficient for true invisibility [42]. There existed objects with zero extinction cross-section with balanced absorption and scattering cross-sections which were highly visible. Therefore, Kerker concluded that for true invisibility an object must have both zero extinction cross-section and zero-scattering cross-section.

From the derivation of these cross-sections in Chapter 3, Section 3.2 the relevant equations leading up to and the expressions for the extinction and scattering cross-sections for two dimensional scatterers are repeated here. Far from the object, the scattered field approximates cylindrical waves of the form $i\pi H_0^1(kr)$. However, these cylindrical waves are distorted by the scattering amplitude $f(\hat{\mathbf{s}}, \hat{\mathbf{s}}_0)$ associated with the scatterer, defined as scattered amplitude in direction $\hat{\mathbf{s}}$ in response to an incident field of unit amplitude propagating in direction $\hat{\mathbf{s}}_0$. Far from the object ($r \to \infty$) in direction $\hat{\mathbf{s}}$, the scattered field as a function of the scattering amplitude $f(\hat{\mathbf{s}}, \hat{\mathbf{s}}_0)$ is

mathematically defined as

$$U^{(s)}(r\hat{\mathbf{s}}) = f(\hat{\mathbf{s}}, \hat{\mathbf{s}}_0) i\pi H_0^{(1)}(kr), \tag{305}$$

where the function H_0^1 is the zeroeth order Hankel function of the first kind. The extinction cross-section $Q^{(ext)}$, the energy per unit area (or length in two dimensional objects) removed from the incident field by the scattering object, in terms of the forward scattering amplitude $f(\hat{\mathbf{s}}_0, \hat{\mathbf{s}}_0)$ is

$$Q^{(ext)} = Q^{(abs)} + Q^{(sca)} = \frac{4\pi}{k} \mathrm{Im}\left\{ f(\hat{\mathbf{s}}_0, \hat{\mathbf{s}}_0) \right\}, \tag{306}$$

where $Q^{(abs)}$ is the absorption cross-section, the energy absorbed per unit area, and $Q^{(sca)}$ is the scattering cross-section, the energy scattered per unit area, as defined in Chapter 3, Section 3.2. When the scattering direction, the first direction vector in $f(\hat{\mathbf{s}}, \hat{\mathbf{s}}_0)$, and the incident field direction $\hat{\mathbf{s}}_0$, the second direction vector in $f(\hat{\mathbf{s}}, \hat{\mathbf{s}}_0)$, are identical, the scattering amplitude $f(\hat{\mathbf{s}}_0, \hat{\mathbf{s}}_0)$ is called the *forward scattering amplitude*, since it represents the part of the scattered field in the incident direction (forward direction). The scattering cross-section $Q^{(sca)}$ may also be written in terms of the scattering amplitude, as follows

$$Q^{(sca)} = \int_L |f(\hat{\mathbf{s}}, \hat{\mathbf{s}}_0)|^2 \, \mathrm{d}l, \tag{307}$$

where L is the boundary outside of the scatterer. Alternatively, the scattering cross-section, combining Eqs. (307) and (305), may be written as

$$Q^{(sca)} = \int_L \frac{|U^{(s)}|^2}{|i\pi H_0^{(1)}(kr)|^2} \, \mathrm{d}l, \tag{308}$$

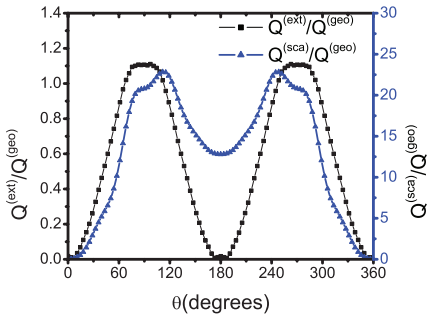

Figure 16: The ratios of extinction and scattering cross-sections over the scatterers geometric cross-section as a function of incident angle ($\mathcal{PT}$-symmetric example, Eq. (304)).

enabling its calculation directly from the scattered field. Eq. (308) facilitates calculation of the scattering cross-section in the simulations to verify the invisibility of a scatterer.

We calculated the extinction and scattering cross-sections for all directions of incidence $\hat{\mathbf{s}}_0$. A nonzero extinction cross-section $Q^{(ext)}$ with $Q^{(sca)} = 0$, therefore, indicates loss, while a nonzero scattering cross-section $Q^{(sca)}$ with $Q^{(ext)} = 0$ indicates gain. Dividing the extinction and scattering cross-sections by the geometric cross-section of the scatterer, $Q^{(geo)} = 2\lambda$, connects the cross-section of the energy extinguished or scattered to the size of the object. In the invisibility direction ($\theta = 0°$), both $Q^{(ext)}$ and $Q^{(sca)}$ are equal to zero. In the opposite direction ($\theta = 180°$), there is strong scattering, and, consequently, $Q^{(sca)} \neq 0$ (Fig. 16). Nevertheless, for the opposite direction $Q^{(ext)} \approx 0$: due to the presence of the gain medium, it is possible to have strong scattering and no extinction of the illuminating wave. This phenomenon is analogous to that observed in Ref. [21] for a $\mathcal{PT}$-symmetric layered scatterer. Taking a closer look at Fig. 15 (b) reveals that, when the wave is incident in the scattering direction, the wave preferentially scatters in specific directions. It may be of note

that these preferred scattering directions coincide with the peaks of the scattering cross-section (Fig. 16).

A question of some interest is the robustness of the invisibility when the object is not perfect, for example, when errors in manufacturing occur. There are many ways to simulate such imperfections, such as adding spherical harmonic terms or periodic linear distributions to the scattering potential. To estimate the effect of manufacturing error, a periodic error of the form $c \cdot \%error \cdot \max|F(\mathbf{r})| \cos 2\pi f x$ was added to the scattering potential $F(\mathbf{r})$ and a Monte Carlo simulation was performed for the invisibility direction of the scatterer. The spatial frequency was arbitrarily set to $f = 6k$. The amplitude c representing the percent error was chosen from a Gaussian distribution of values between 0 and 1. The $\max|F(\mathbf{r})|$ value is the maximum value of the absolute value of the $F(\mathbf{r})$ over its entire domain without any error introduced. The simulation was run 10 times for each percentage of error ranging from zero to 10% increments of 1%. At 10% error $Q^{(ext)}/Q^{(geo)} = 0.03679 \pm 0.02911$ and $Q^{(sca)}/Q^{(geo)} = 0.07734 \pm 0.03388$. These numbers are only slightly larger than the values for the perfect scatterer, $Q^{(ext)}/Q^{(geo)} = 0.01775$ and $Q^{(sca)}/Q^{(geo)} = 0.02431$, which are only due to computational effects.

We may also use the method to design invisible objects that are gain/loss but not $\mathcal{PT}$-symmetric and this was not found in the literature before [36]. It turns out that they share many properties with their $\mathcal{PT}$-symmetric counterparts. An example of a simple local function that results in a non-$\mathcal{PT}$-symmetric scattering potential is given

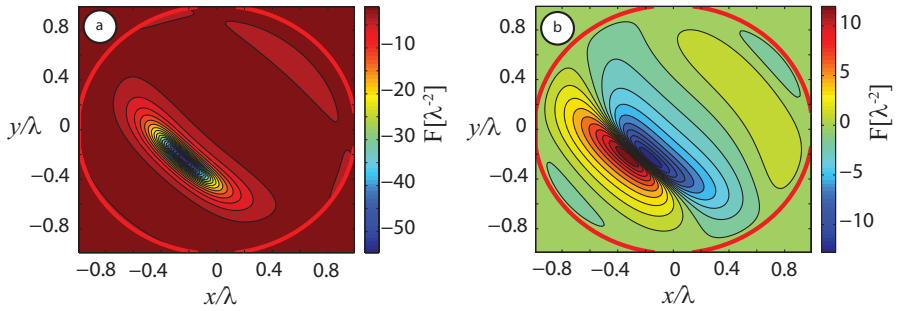

Figure 17: The real (a) and imaginary (b) parts of the scattering potential for a non $\mathcal{PT}$-symmetric nonscattering scatterer ($a = 1$).

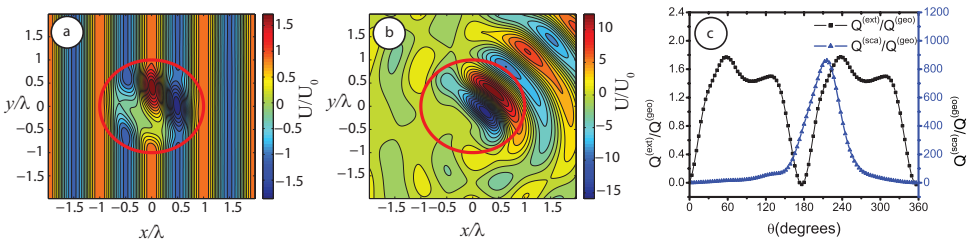

Figure 18: The real part of the total field (incident + scattered) when the incident plane wave propagates in the positive $\hat{\mathbf{x}}$-direction ($\theta = 0°$) (a) and when the incident plane wave propagates in the negative $\hat{\mathbf{x}}$-direction ($\theta = 180°$)(b). The fields are scaled to the incident field amplitude U_0. The circles indicate the domain of the scatterer, which has a radius of $a = 1$. The extinction and scattering cross-sections are shown in (c) for all angles θ or incidence.

by

$$U^{(loc)}(\mathbf{r}) = \sin \pi(x + y) \cos^2 \left(\frac{\pi r^2}{2a^2} \right), \ |r| \leq a. \tag{309}$$

The real and imaginary parts of the scattering potential associated with the $U^{(loc)}$ in Eq. (309) are shown in Fig. 17. Neither one has any particular symmetry with respect to the horizontal $\hat{\mathbf{x}}$-axis or, in fact, any axis.

Nevertheless, when the wave is incident on the scatterer in the invisibility direction ($+\hat{\mathbf{x}}$ direction) the field around the scatterer is not perturbed (Fig. 18 (a)), while when the wave is incident on the scatterer in the opposite direction, the object scatters strongly (Fig. 18 (b)). This is the first time a scatterer with an asymmetric

scattering potential demonstrates directional invisibility [36] and demonstrates that $\mathcal{PT}$ symmetry is not the ultimate condition for directional invisibility. Again, in the invisibility direction both the extinction and the scattering cross-sections are equal to zero, but in the opposite direction only the extinction cross-section is equal to zero (Fig. 18 (c)). Here the preferred scattering directions again appear to coincide with the peak of the scattering cross-sections (Fig. 18(b) and (c)). In contrast to the $\mathcal{PT}$-symmetric case, where both the scattering and extinction cross-sections are symmetric (Fig. 16 (c)), in this case the extinction and scattering cross-sections are asymmetric (Fig. 18(c)).

The initial connection between $\mathcal{PT}$ symmetry and optics was made by setting an equivalence between the refractive index in the inhomogeneous wave equation and the quantum potential in the Schrödinger equation. Before this work, it was thought that to design a $\mathcal{PT}$-symmetric scatterer, the only way to achieve this in optics was with a $\mathcal{PT}$-symmetric refractive index. Here, we discover an alternative condition by closely examining the relationships between the real and complex components of the scattering potential $F(\mathbf{r})$ and the real and complex components of the refractive index $n(\mathbf{r})$. To explore the role of the symmetries of each component, we substitute the complex definitions of refractive index $n(\mathbf{r}) = n_R(\mathbf{r}) + in_I(\mathbf{r})$ and the scattering potential $F(\mathbf{r}) = F_R(\mathbf{r}) + iF_I(\mathbf{r})$ into Eq. (259), and obtain for the real and imaginary parts of the scattering potential

$$F_R(\mathbf{r}) = \frac{k^2}{4\pi}\left(n_R^2(\mathbf{r}) - n_I^2(\mathbf{r}) - 1\right), \tag{310a}$$

$$F_I(\mathbf{r}) = \frac{k^2}{4\pi} 2n_I(\mathbf{r})n_R(\mathbf{r}). \tag{310b}$$

If $\mathcal{PT}$ symmetry is defined by a symmetric $F_R(\mathbf{r})$ and an anti-symmetric $F_I(\mathbf{r})$ with respect to the position $\mathbf{r}$, then there are at least two ways to choose the refractive index to satisfy these conditions. We may choose n_R to be symmetric and n_I anti-symmetric with respect to position. Alternatively, we may choose n_I to be symmetric and n_R to be anti-symmetric with respect to position. This means that requiring the refractive index to be $\mathcal{PT}$-symmetric is not the ultimate condition for $\mathcal{PT}$ symmetry, and misses half of the possible solutions for the refractive index. Therefore, requiring that the refractive index be $\mathcal{PT}$-symmetric forces the scattering potential to be $\mathcal{PT}$-symmetric but the converse does not hold true. Here, we were the first to show that a broader requirement for $\mathcal{PT}$ symmetry is the requirement that the scattering potential, the mathematical equivalent of the quantum potential, be $\mathcal{PT}$-symmetric [36].

4.5 Origin of directional invisibility with balanced gain and loss

In this section, we explore the origin of directional invisibility and $\mathcal{PT}$-symmetry. This is achieved by designing a general directionally invisible scatterer, using the method presented in Section 4.2, and calculating the scattering amplitude which is directly connected to the extinction and scattering cross-sections for several directions of incidence and scattering. Here two types of scatterers are examined. The first is a scatterer with a $\mathcal{PT}$-symmetric scattering potential, and the second is scatterer which does not possess any particular symmetry at all. By exploring these two scatterer, we elucidate the determining condition for directional invisibility, and as our simulations have shown, it is not $\mathcal{PT}$-symmetry.

Rather than selecting a $\mathcal{PT}$-symmetric refractive index, we choose a more general

condition: We require the scattering potential to be $\mathcal{PT}$-symmetric. We start with the most general definition of the extinction and scattering cross-sections and calculate them for two directions, with the following assumptions: (1) The scattering potential is $\mathcal{PT}$-symmetric, (2) the scattering potential is a function of localized field, and (3) the local field $U^{(loc)}$ satisfies the nonradiating source boundary conditions (Eq. (267)).

The extinction cross-section of the scattering object (Chapter 3, Section 3.2) is defined as the ratio between the rate of energy dissipation and the rate at which energy is incident on a unit cross-sectional area of the scatterer perpendicular to the direction of incidence $\hat{\mathbf{s}}_0$. In terms of the forward scattering amplitude $f(\hat{\mathbf{s}}_0, \hat{\mathbf{s}}_0)$, it is given by Eq. (306). The scattering amplitude is given by:

$$f(\hat{\mathbf{s}}, \hat{\mathbf{s}}_0) = \int_V F(\mathbf{r}')U(\mathbf{r}')e^{ik\hat{\mathbf{s}}\cdot\mathbf{r}'}\,\mathrm{d}^3r', \tag{311}$$

where $\hat{\mathbf{s}}$ is the scattering direction, $\hat{\mathbf{s}}_0$ is the direction of the incident wave, V is the volume of the scatterer, $F(\mathbf{r})$ is the scattering potential of the medium, and $U(\mathbf{r})$ is the total field. The total field is given by

$$U(\mathbf{r}) = U^{(s)}(\mathbf{r}) + U^{(i)}(\mathbf{r}), \tag{312}$$

where $U^{(i)}$ is the incident field of the form

$$U^{(i)}(\mathbf{r}, \omega) = e^{ik\hat{\mathbf{s}}_0\cdot\mathbf{r}} \tag{313}$$

and $U^{(s)}$ is the scattered field, which may be rewritten for the invisibility direction $\hat{\mathbf{s}}_0$ (Eq. (261)) as

$$U^{(s)}(\mathbf{r}) = U^{(i)}(\mathbf{r})U^{(loc)}(\mathbf{r}), \tag{314}$$

which is limited to the volume V of the scatterer because $U^{(loc)}(\mathbf{r})$ satisfies the boundary conditions in Eq. (267). The total field may then be expressed as

$$U(\mathbf{r}) = e^{ik\hat{\mathbf{s}}_0\cdot\mathbf{r}}\left[1 + U^{(loc)}(\mathbf{r})\right] \tag{315}$$

The scattering potential $F(\mathbf{r})$ in terms of $U^{(loc)}(\mathbf{r})$ again is given by Eq. (274)

$$F(\mathbf{r}) = -\frac{1}{4\pi}\frac{\nabla^2 U^{(loc)}(\mathbf{r}) + 2ik\hat{\mathbf{s}}_0\cdot\nabla U^{(loc)}(\mathbf{r})}{1 + U^{(loc)}(\mathbf{r})}. \tag{316}$$

Now we may evaluate the forward scattering amplitude $f(\hat{\mathbf{s}}_0, \hat{\mathbf{s}}_0)$ given by Eq. (311) where we set $\hat{\mathbf{s}} = \hat{\mathbf{s}}_0$ and by substituting Eqs. (314), (315), and (274), and obtain

$$\begin{aligned} f(\hat{\mathbf{s}}_0, \hat{\mathbf{s}}_0) &= \int_V -\frac{1}{4\pi}\frac{\nabla^2 U^{(loc)}(\mathbf{r}') + 2ik\hat{\mathbf{s}}_0\cdot\nabla U^{(loc)}(\mathbf{r}')}{1 + U^{(loc)}(\mathbf{r}')} e^{ik\hat{\mathbf{s}}_0\cdot\mathbf{r}'}[1 + U^{(loc)}(\mathbf{r}')]e^{ik\hat{\mathbf{s}}_0\cdot\mathbf{r}'}\,\mathrm{d}^3r' \\ &= -\frac{1}{4\pi}\int_V \left(\nabla^2 U^{(loc)}(\mathbf{r}') + 2ik\hat{\mathbf{s}}_0\cdot\nabla U^{(loc)}(\mathbf{r}')\right) e^{2ik\hat{\mathbf{s}}_0\cdot\mathbf{r}'}\,\mathrm{d}^3r'. \end{aligned} \tag{317}$$

By using the divergence theorem and applying the boundary conditions (Eqs. (267)),

$$\begin{aligned} f(\hat{\mathbf{s}}_0, \hat{\mathbf{s}}_0) &= -\frac{1}{4\pi}\int_V \nabla\cdot\left(\nabla U^{(loc)}(\mathbf{r}')e^{2ik\hat{\mathbf{s}}_0\cdot\mathbf{r}'}\right)\,\mathrm{d}^3r' \\ &= -\frac{1}{4\pi}\int_S \nabla U^{(loc)}(\mathbf{r}')e^{2ik\hat{\mathbf{s}}_0\cdot\mathbf{r}'}\cdot\hat{\mathbf{n}}\,\mathrm{d}^2r' \\ &= 0, \end{aligned} \tag{318}$$

we see that the forward scattering amplitude is zero. Since both the real and imaginary parts of the forward scattering amplitude are identically zero, it implies that both $Q^{(ext)}$ and $Q^{(sca)}$ are also zero for the direction $\hat{\mathbf{s}}_0$ and that the object is indeed invisible for an incident field in the designated invisibility direction.

We may also verify that the reflected scattered field is also zero by calculating $f(-\hat{\mathbf{s}}_0, \hat{\mathbf{s}}_0)$, where $\hat{\mathbf{s}} = -\hat{\mathbf{s}}_0$. The scattering amplitude reflected direction for the same

incident field is

$$f(-\hat{\mathbf{s}}_0,\hat{\mathbf{s}}_0) = \int_V -\frac{1}{4\pi}\frac{\nabla^2 U^{(loc)}(\mathbf{r}') + 2ik\hat{\mathbf{s}}_0\cdot\nabla U^{(loc)}(\mathbf{r}')}{1+U^{(loc)}(\mathbf{r}')} e^{ik\hat{\mathbf{s}}_0\cdot\mathbf{r}'}(1+U^{(loc)}(\mathbf{r}'))e^{-ik\hat{\mathbf{s}}_0\cdot\mathbf{r}'}\,\mathrm{d}^3r'$$
$$= -\frac{1}{4\pi}\int_V \left[\nabla^2 U^{(loc)}(\mathbf{r}') + 2ik\hat{\mathbf{s}}_0\cdot\nabla U^{(loc)}(\mathbf{r}')\right]\,\mathrm{d}^3r', \tag{319}$$

We may rewrite the integrand and apply the divergence theorem as follows

$$\begin{aligned} f(-\hat{\mathbf{s}}_0,\hat{\mathbf{s}}_0) &= -\frac{1}{4\pi}\int_V \nabla\cdot\left(\nabla U^{(loc)}(\mathbf{r}')\right)\,\mathrm{d}^3r' - \frac{2ik\hat{\mathbf{s}}_0}{4\pi}\cdot\int_V \nabla U^{(loc)}(\mathbf{r}')\,\mathrm{d}^3r' \\ &= -\frac{1}{4\pi}\int_S \nabla U^{(loc)}(\mathbf{r}')\cdot\hat{\mathbf{n}}\,\mathrm{d}^2r' - \frac{2ik\hat{\mathbf{s}}_0}{4\pi}\cdot\int_S U^{(loc)}(\mathbf{r}')\cdot\hat{\mathbf{n}}\,\mathrm{d}^2r' \\ &= 0, \end{aligned} \tag{320}$$

where we have applied the boundary conditions, demonstrating that the scattering amplitude for the reflection is also equal to zero. This shows that this class of invisible scatterer is directionally invisible and reflectionless, because of the boundary conditions imposed on the local scattered field as it was not necessary to use any symmetry arguments. The boundary conditions ensure balanced gain and loss, while the fact that it is applied to the scattered field in the scattering equation determines the directionality according to the incident field, as shown in the derivation of the scattering potential(Section 4.2). It has been observed in $\mathcal{PT}$ symmetric slab structures that if the incident field is incident upon the scatterer opposite to the invisibility direction, the extinction cross-section is still zero and that the object is reflectionless. To verify this, we may calculate the scattering amplitude with both a scattering and

incident field direction $-\hat{\mathbf{s}}_0$, given by

$$\begin{aligned} f(-\hat{\mathbf{s}}_0, -\hat{\mathbf{s}}_0) &= \int_V F(\mathbf{r}') e^{-2ik\hat{\mathbf{s}}_0\cdot\mathbf{r}'} \,\mathrm{d}^3 r' + \int_V F(\mathbf{r}') U^{(s)}(\mathbf{r}') e^{-ik\hat{\mathbf{s}}_0\cdot\mathbf{r}'} \,\mathrm{d}^3 r' \\ &= \Re\{f(-\hat{\mathbf{s}}_0, -\hat{\mathbf{s}}_0)\} + i\mathrm{Im}\{f(-\hat{\mathbf{s}}_0, -\hat{\mathbf{s}}_0)\}, \end{aligned} \tag{321}$$

where it is important to remember that when the wave is not incident in the invisibility direction $U^{(s)} \neq U^{(i)}U^{(loc)}$ but the scattering potential $F(\mathbf{r})$ remains the same. Assuming that each function within the integral has a real and an imaginary part, the real and imaginary parts of the $f(-\hat{\mathbf{s}}_0, -\hat{\mathbf{s}}_0)$ may be rewritten as follows

$$\begin{aligned} \Re\{f(-\hat{\mathbf{s}}_0, -\hat{\mathbf{s}}_0)\} &= \int_V \left(F_R(\mathbf{r}')\cos\left(2k\hat{\mathbf{s}}_0\cdot\mathbf{r}'\right) + F_I(\mathbf{r}')\sin\left(2k\hat{\mathbf{s}}_0\cdot\mathbf{r}'\right)\right) \mathrm{d}^3 r' \\ &\quad + \int_V \Big(F_R(\mathbf{r}')U_R^{(s)}(\mathbf{r}') - F_I(\mathbf{r}')U_I^{(s)}(\mathbf{r}')\Big)\cos\left(k\hat{\mathbf{s}}_0\cdot\mathbf{r}'\right)\mathrm{d}^3 r' \\ &\quad + \int_V \Big(F_R(\mathbf{r}')U_I^{(s)}(\mathbf{r}') + F_I(\mathbf{r}')U_R^{(s)}(\mathbf{r}')\Big)\sin\left(k\hat{\mathbf{s}}_0\cdot\mathbf{r}'\right)\mathrm{d}^3 r', \end{aligned} \tag{322}$$

$$\begin{aligned} \mathrm{Im}\{f(-\hat{\mathbf{s}}_0, -\hat{\mathbf{s}}_0)\} &= \int_V \left(F_I(\mathbf{r}')\cos\left(2k\hat{\mathbf{s}}_0\cdot\mathbf{r}'\right) - F_R(\mathbf{r}')\sin\left(2k\hat{\mathbf{s}}_0\cdot\mathbf{r}'\right)\right) \mathrm{d}^3 r' \\ &\quad - \int_V \Big(F_R(\mathbf{r}')U_R^{(s)}(\mathbf{r}') + F_I(\mathbf{r}')U_I^{(s)}(\mathbf{r}')\Big)\sin\left(k\hat{\mathbf{s}}_0\cdot\mathbf{r}'\right)\mathrm{d}^3 r' \\ &\quad + \int_V \Big(F_R(\mathbf{r}')U_I^{(s)}(\mathbf{r}') + F_I(\mathbf{r}')U_R^{(s)}(\mathbf{r}')\Big)\cos\left(k\hat{\mathbf{s}}_0\cdot\mathbf{r}'\right)\mathrm{d}^3 r', \end{aligned} \tag{323}$$

For the extinction cross-section $Q^{(ext)}$ to be zero, the imaginary part of the forward scattering amplitude in the $-\hat{\mathbf{s}}_0$ direction must be zero. Since the scattering potential is bounded by the volume of the scatterer, it limits the domain of the other function by which it is multiplied to this domain of the scatterer. In addition it is important to remember that because of the boundary conditions, the scattering potential evaluated at the surface of the domain of the scatterer is equal to zero. By examining the symmetries of the functions within the integral, we can show that it is in fact equal

to zero. If the local function $U^{(loc)}$ is chosen so that the scattering potential is $\mathcal{PT}$-symmetric, i.e. the real part is symmetric and the imaginary part is antisymmetric with respect to position, and satisfies Eq. (274), then the first integral in Eq. (323) must be equal to zero. The next two integrals depend on the symmetry of the real and imaginary parts of the scattering function the scattering potential and the components of the incident field. Since in any direction for which the scatterer is not invisible, $U^{(s)} \neq U^{(i)}U^{(loc)}$, and must be calculated with the Green's function integral, which is a function of the Green's function, the scattering potential and the total field. Since the Green's function is symmetric and scattering potential is assumed to be $\mathcal{PT}$-symmetric, it is safe to assume that within the scatterer it may weakly mirror that of the scattering potential, such $U_R^{(s)}$ is symmetric and $U_I^{(s)}$ is anti-symmetric. In this case, the second two integrals of the imaginary component are also zero because of the combined anti-symmetry of the functions. As a consequence, the extinction cross-section when the incident field is in the opposite direction of the scatterer is zero. As a result of the same symmetry arguments, it can be seen that the real part of the forward scattering amplitude in the $-\hat{\mathbf{s}}_0$ is not zero, and therefore at least for one direction the scattering cross-section is not zero. Recall that the scattering cross-section is a function of the magnitude of the scattered field outside of the scatterer. Since the scattered field is nonzero outside of the scatterer, the evaluation of the integral is a positive value.

4.6 Summary

We introduced a method to design directionally invisible scatterers for an incident field with one direction of incidence exploiting a technique originally used to design nonradiating sources developed by Gbur. In the derivation, it was shown that under certain conditions the scattering potential was $\mathcal{PT}$-symmetric, resulting in directionally invisible $\mathcal{PT}$ symmetric objects. In that context, we also demonstrated that $\mathcal{PT}$-symmetric scattering potentials could be constructed with either a $\mathcal{PT}$ symmetric refractive index or a refractive index without $\mathcal{PT}$ symmetry. Therefore, requiring the scattering potential to be $\mathcal{PT}$ symmetric is a broader condition for $\mathcal{PT}$ symmetry. The technique was used to design $\mathcal{PT}$-symmetric and asymmetric directionally invisible scatterers, demonstrating that $\mathcal{PT}$ symmetry is not the ultimate condition for directional invisibility. Moreover, the origin of directionally invisible objects is studied by calculating the scattering amplitudes associated with the extinction cross-section and the scattering cross-section for specific directions of incidence. This proved that boundary conditions applied to scattered field are responsible for the balanced gain and loss, and that the directionality is a function of incident field for which the scattering potential is designed to be invisible.

CHAPTER 5: OPTICALLY SWITCHABLE INVISIBILITY

In this chapter, we generalize the theoretical framework of directional invisibility introduced in Chapter 4 to construct objects that are only invisible when simultaneously illuminated by multiple plane waves from given directions. With these results, it is suggested that such devices could be used to design novel couplers, switches, and other optical sensors. The following derivations were previously published in Optics Letters [37].

5.1 Derivation of a simultaneously N-directional scattering potential

Consider an object of refractive index $n(\mathbf{r})$ bounded by a finite surface S and volume V, illuminated by a scalar monochromatic incident field $U^{(i)}(\mathbf{r})$, which may now consist of one or more plane waves $U_n(\mathbf{r})$ of different amplitudes,

$$U^{(i)}(\mathbf{r}) = \sum_{n=1}^{N} U_n(\mathbf{r}), \tag{324}$$

where $U_n(\mathbf{r})$ is defined by

$$U_n(\mathbf{r}) = A_n e^{ik\hat{\mathbf{s}}_n \cdot \mathbf{r}}, \tag{325}$$

with A_n representing the amplitude and $\hat{\mathbf{s}}_n$ the direction of the nth plane wave, and $k = \frac{\omega}{c} = \frac{2\pi}{\lambda}$, ω the angular frequency, λ the wavelength, and c representing the vacuum speed of light. The total field $U(\mathbf{r}) = U^{(i)}(\mathbf{r}) + U^{(s)}(\mathbf{r})$, where $U^{(i)}(\mathbf{r})$ and $U^{(s)}(\mathbf{r})$ are the incident and scattered fields, respectively, again satisfies the Helmholtz

equation with an inhomogeneous wave number,

$$\left[\nabla^2 + n^2(\mathbf{r})k^2\right] U(\mathbf{r}) = 0. \tag{326}$$

Introducing the scattering potential $F(\mathbf{r})$ of the form,

$$F(\mathbf{r}) = \frac{k^2}{4\pi}\left[n^2(\mathbf{r}) - 1\right], \tag{327}$$

it is possible to write an inhomogeneous wave equation for the scattered field [9],

$$\left[\nabla^2 + k^2\right] U^{(s)}(\mathbf{r}) = -4\pi F(\mathbf{r})U(\mathbf{r}). \tag{328}$$

As the scattered field is present on both sides of Eq. (328), it is not possible to solve this equation analytically. However, we may use it to construct a nonscattering object by following the procedure first presented in [29]. First, we write

$$U^{(s)}(\mathbf{r}) = U^{(i)}(\mathbf{r})U^{(loc)}(\mathbf{r}), \tag{329}$$

where $U^{(loc)}(\mathbf{r})$ is the *local scattered field* of the inhomogeneous scatterer; it is the scattered field with the oscillations of the incident field removed [29]. Next, we apply techniques promulgated to create *nonradiating sources* [27] to design invisible objects. To this end, the boundary conditions typically employed for nonradiating sources [25] are applied to the local field $U^{(loc)}(\mathbf{r})$ that defines the invisible object, namely,

$$U^{(loc)}(\mathbf{r})\big|_S = 0, \text{ and } \left.\frac{\partial}{\partial n}U^{(loc)}(\mathbf{r})\right|_S = 0, \tag{330}$$

where $\frac{\partial}{\partial n}$ represents the derivative normal to the surface S which forms the boundary of the scatterer. The scattered field $U^{(loc)}(\mathbf{r}) = 0$ outside of the scatterer. Writing

the total field as $U(\mathbf{r}) = \left[1 + U^{(loc)}(\mathbf{r})\right] U^{(i)}(\mathbf{r})$, where $U^{(i)}(\mathbf{r})$ is defined by Eq. (324), and substituting it with Eq. (329) into Eq. (328), results in the scattering potential $F(\mathbf{r})$ that produces the scattered field, i.e.

$$F(\mathbf{r}) = -\frac{1}{4\pi[1 + U^{(loc)}(\mathbf{r})]} \times \left[\nabla^2 U^{(loc)}(\mathbf{r}) + \frac{2ik \sum_{n=1}^{N} U_n(\mathbf{r}) \hat{\mathbf{s}}_n \cdot \nabla U^{(loc)}(\mathbf{r})}{\sum_{n=1}^{N} U_n(\mathbf{r})} \right]. \tag{331}$$

For only one incident wave ($N = 1$), the scattering potential is

$$F(\mathbf{r}) = -\frac{1}{4\pi} \frac{\nabla^2 U^{(loc)}(\mathbf{r}) + 2ik\hat{\mathbf{s}}_1 \cdot \nabla U^{(loc)}(\mathbf{r})}{1 + U^{(loc)}(\mathbf{r})}, \tag{332}$$

which is the original equation for a directionally invisible scatterer, derived and studied in Chapter 4. We now demonstrate how this equation may be used to design objects that are directionally invisible for a sum of simultaneously incident plane waves and how they might be used to make optically switchable invisible objects.

5.2 Examples of N-directionally optically switchable invisible scatterers

Here we demonstrate by applying the general equation how to design two- and three-directionally invisible objects. The simulations are performed using the same method described in Chapter 4, Section 4.3. The general equation (Eq. (331)) for N discrete directions facilitates the design of a scatterer that is invisible for an incident field consisting of multiple plane waves. For two incident waves of different

amplitudes, i.e. $N = 2$, the scattering potential is defined by

$$F(\mathbf{r}) = -\frac{1}{4\pi[1+U^{(loc)}(\mathbf{r})]}\times \left[\nabla^2 U^{(loc)}(\mathbf{r}) + \frac{2ik\hat{\mathbf{s}}_1\cdot\nabla U^{(loc)}(\mathbf{r})}{1+\frac{A_2}{A_1}e^{ik(\hat{\mathbf{s}}_2-\hat{\mathbf{s}}_1)\cdot\mathbf{r}}} + \frac{2ik\hat{\mathbf{s}}_2\cdot\nabla U^{(loc)}(\mathbf{r})}{1+\frac{A_1}{A_2}e^{ik(\hat{\mathbf{s}}_1-\hat{\mathbf{s}}_2)\cdot\mathbf{r}}}\right], \tag{333}$$

where A_1 and A_2 are the amplitudes and $\hat{\mathbf{s}}_1$ and $\hat{\mathbf{s}}_2$ are the directions of incidence of the two plane waves. An appropriate ratio of A_1/A_2 must be chosen so that neither of the denominators are equal to zero to avoid producing a singularity. By choosing $U^{(loc)}(\mathbf{r})$ with appropriate boundary conditions and the amplitudes and directions of incidence for the plane waves, we uniquely specify the form of $F(\mathbf{r})$ with the desired invisibility properties. For example, let us choose a circular object of radius a with

$$U^{(loc)}(\mathbf{r}) = \cos^2\left(\frac{\pi r^2}{2a^2}\right), \tag{334}$$

where $r = \sqrt{x^2+y^2}$, $a = 1$, $A_1 = 1$, $A_2 = 20$, $\hat{\mathbf{s}}_1 = \hat{\mathbf{x}}$, and $\hat{\mathbf{s}}_2 = \hat{\mathbf{y}}$. This choice of $U^{(loc)}$ provides a simple example, but any $U^{(loc)}$ that satisfies Eq. (330) may be chosen. The incident field is defined by Eq. (324) with $N = 2$ such that

$$U^{(i)}(\mathbf{r}) = A_1 e^{ik\hat{\mathbf{s}}_1\cdot\mathbf{r}} + A_2 e^{ik\hat{\mathbf{s}}_2\cdot\mathbf{r}}. \tag{335}$$

Numerical simulations of waves interacting with this directionally invisible object were performed using a Green's function method [49] for two cases. First, the fields were calculated when both components of the incident field given by Eq. (335) were present. Then the total and scattered fields were calculated when only one of the components of the incident field was present. The scattering potential is found by substituting Eq. (334) into Eq. (333). While the real part has a more balanced

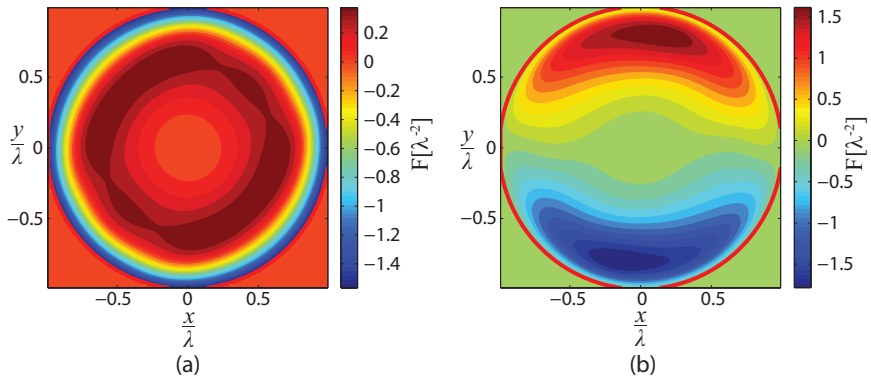

Figure 19: The real (a) and imaginary (b) parts of $F(\mathbf{r})$ (Eq. (333)) with $U^{(loc)}(\mathbf{r})$ (Eq. (334)) with $a = 1$, $A_1 = 1$, $A_2 = 20$, $\hat{\mathbf{s}}_1 = \hat{\mathbf{x}}$, and $\hat{\mathbf{s}}_2 = \hat{\mathbf{y}}$.

amplitude in both the $\hat{\mathbf{x}}$ and $\hat{\mathbf{y}}$ directions, the imaginary part, associated with gain and loss, is roughly antisymmetric along the $\hat{\mathbf{y}}$ axis and has an amplitude range roughly twice as large as the real component (Fig. 19). Therefore gain and loss contributes significantly to the invisibility of these objects. Because the local scattered field $U^{(loc)}(\mathbf{r})$ was taken to be real and symmetric, the scattering potential possesses the conjugate inversion symmetry $F(\mathbf{r}) = F^{\star}(-\mathbf{r})$. This is a very general example of $\mathcal{PT}$ symmetry; most examples of $\mathcal{PT}$ symmetry that have been studied to date focus on structures that only have this conjugate symmetry with respect to a single axis, i.e. $F(x, y, z) = F^{\star}(-x, y, z)$, which our structure does not have. More generally, by choosing a $U^{(loc)}$ which is not real and symmetric, it is possible to produce structures that do not possess any symmetry in their potential. These directionally invisible objects are active gain-loss scatterers with balanced gain and loss.

When both of the components of the incident fields are present, the nonscattering scatterer is invisible (Fig. 20). The incident fields appear undisturbed outside of the scatterer (Fig. 20 (a)). This is further confirmed in that the scattered field outside of the scatterer is identically zero (Fig. 20 (b)). However, if one of the components of

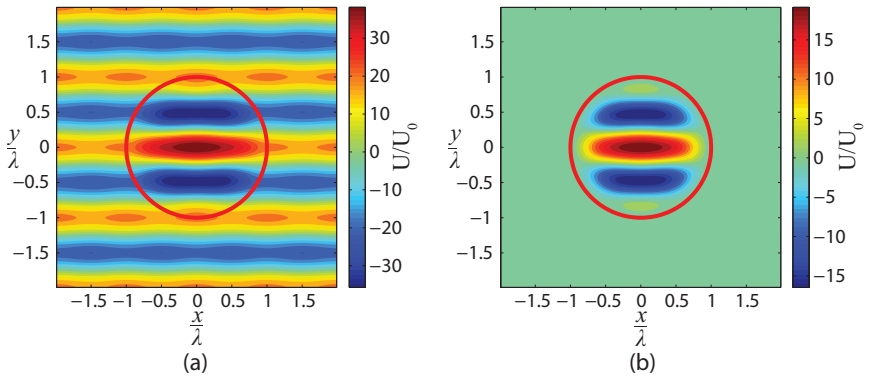

Figure 20: The real parts of the $U(\mathbf{r})$ (a) and $U^{(s)}(\mathbf{r})$ (b) invisible to $U^{(i)}(\mathbf{r})$ (Eq. (335)) with $F(\mathbf{r})$ (Eq. (333)) with $a = 1$, $A_1 = 1$, $A_2 = 20$, $\hat{\mathbf{s}}_1 = \hat{\mathbf{x}}$, and $\hat{\mathbf{s}}_2 = \hat{\mathbf{y}}$.

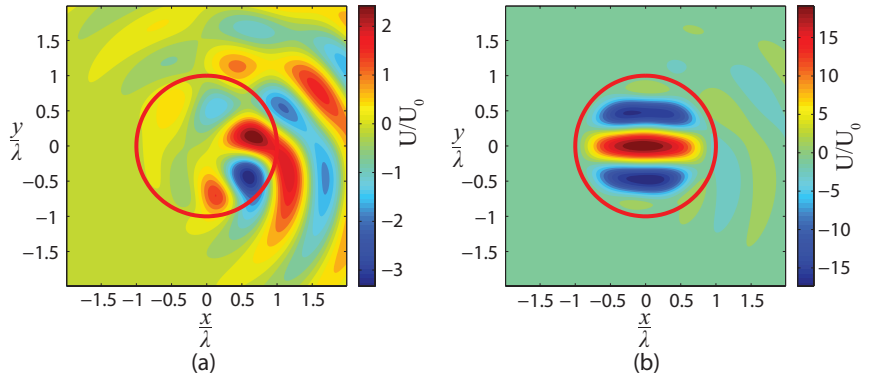

Figure 21: The real part of $U^{(s)}(\mathbf{r})$ when $U^{(i)}(\mathbf{r})$ is incident in either (a) $\hat{\mathbf{x}}$ or (b) $\hat{\mathbf{y}}$, for an object invisible to $U^{(i)}(\mathbf{r})$ (Eq. (335)). $F(\mathbf{r})$ (Eq. (333)) has $a = 1$, $A_1 = 1$, $A_2 = 20$, $\hat{\mathbf{s}}_1 = \hat{\mathbf{x}}$, and $\hat{\mathbf{s}}_2 = \hat{\mathbf{y}}$.

the incident field is removed, or incident from a different direction, there is significant scattering, as we will now illustrate. Fig. 21 (a) shows the scattered field when a field is only incident in the $\hat{\mathbf{x}}$-direction. Fig. 21 (b) shows the scattered field when an incident field only propagates in the $\hat{\mathbf{y}}$-direction. In both cases, there is a strong scattered field. Therefore, this kind of scatterer is only invisible when both waves are incident in their respective directions simultaneously with the proper amplitudes. Because this nonscattering scatterer is only invisible if the incident field comprises specific plane waves with designated directions and amplitudes, one could imagine building

an optically switchable coupler with this device, where one field is the "pump" and the other field is the "probe." While the pump is held at the designed magnitude and direction, the probe might be varied. The device only transmits both fields perfectly when the probe is also set to the correct amplitude and direction.

To explore this switching effect further, we consider the power extinguished and scattered by the object as the amplitude of the probe is varied. In the previous chapter, invisibility was verified by calculating the extinction and scattering cross-sections, both of which should be zero when the incident field is incident in the invisibility direction. However, these cross-sections are derived as a function of the forward scattering amplitude from one incident plane wave with one direction $\hat{\mathbf{s}}_0$. As the incident fields in these examples are the sum of several plane waves, each of which possessing unique direction and amplitude, we may quantify the energy exchange between the object and the incident field by the more general extinguished and scattered powers. The extinguished power $P^{(ext)}$ is defined as the power removed from the incident field by the scatterer [11, Chapter 2] (and can also be derived from [9]), and is given by

$$P^{(ext)} = -\frac{1}{2ik}\int_L \left(U^{(i)\star}\nabla U^{(s)} + U^{(s)\star}\nabla U^{(i)} - c.c.\right)\cdot\hat{\mathbf{n}}\,\mathrm{d}l, \tag{336}$$

where $c.c.$ refers to the complex conjugate and $\mathrm{d}l$ is the differential unit length of the boundary L of the two-dimensional object. The scattered power $P^{(sca)}$ is defined as the total integrated power scattered by the object [11, 9, Chapter 2], and is given by

$$P^{(sca)} = \frac{1}{2ik}\int_L \left(U^{(s)\star}\nabla U^{(s)} - U^{(s)}\nabla U^{(s)\star}\right)\cdot\hat{\mathbf{n}}\,\mathrm{d}l. \tag{337}$$

We may also introduce the power absorbed by the object as $P^{(abs)}$ [9]; it is related to $P^{(ext)}$ and $P^{(sca)}$ by

$$P^{(ext)} = P^{(sca)} + P^{(abs)}. \tag{338}$$

In the presence of gain, $P^{(abs)}$ may be negative, since, when there is gain, energy is scattered by an object ($P^{(sca)} > 0$) but is not removed from the incident field ($P^{(ext)} = 0$), as shown by Kerker [42]; it is therefore possible to have a gain object with zero extinguished power, but nonzero scattered power. This is the case when one of the incident field components is omitted (Fig. 21); $P^{(sca)} = 6.66$ when only the $\hat{\mathbf{x}}$ component was present and $P^{(sca)} = 6.53$ when only the $\hat{\mathbf{y}}$ component was present, while $P^{(ext)} = 0$ in the presence of both components of the incident field.

True invisibility only occurs when $P^{(abs)}$ and $P^{(ext)}$ are simultaneously zero [1]. Normalized versions of these quantities are shown in Fig. 22 as a function of the ratio A/A_2, where A is the probe field amplitude and A_2 is the value of the probe field amplitude at which it has been designed to be invisible. $P^{(sca)}$ and $P^{(ext)}$ have been normalized by $A_1^2+A^2$, which is the average power per unit length of the incident field. It can be seen that both quantities are simultaneously zero only when $A/A_2 = 1$.

To study the effect of relative phase between the incident field components on invisibility, a phase between 0 and $\pi/2$ was added to one of the components, and $P^{(ext)}$ and $P^{(sca)}$ were calculated normalized by $A_1^2 + A_2^2$. All of the calculated values were below 10%, indicating that this type of scatterer is resilient in the presence of a relative phase change.

A scatterer can also be designed for a field with three or more directions of incidence.

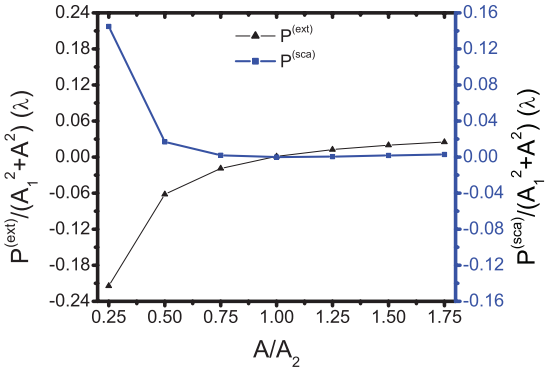

Figure 22: $P^{(ext)}$ and $P^{(sca)}$ vs. the ratio A/A_2. $A = A_2$ is the value of the probe field at which the object is invisible.

For example, if $N = 3$ in Eq. (331), the scattering potential is given by

$$\begin{aligned} F(\mathbf{r}) = -\frac{1}{4\pi[1+U^{(loc)}(\mathbf{r})]} \times \Big[& \nabla^2 U^{(loc)}(\mathbf{r}) \\ & + \frac{2ik\hat{\mathbf{s}}_1 \cdot \nabla U^{(loc)}(\mathbf{r})}{1 + \frac{A_2}{A_1} e^{ik(\hat{\mathbf{s}}_2 - \hat{\mathbf{s}}_1)\cdot\mathbf{r}} + \frac{A_3}{A_1} e^{ik(\hat{\mathbf{s}}_3 - \hat{\mathbf{s}}_1)\cdot\mathbf{r}}} \\ & + \frac{2ik\hat{\mathbf{s}}_2 \cdot \nabla U^{(loc)}(\mathbf{r})}{1 + \frac{A_1}{A_2} e^{ik(\hat{\mathbf{s}}_1 - \hat{\mathbf{s}}_2)\cdot\mathbf{r}} + \frac{A_3}{A_2} e^{ik(\hat{\mathbf{s}}_3 - \hat{\mathbf{s}}_2)\cdot\mathbf{r}}} \\ & + \frac{2ik\hat{\mathbf{s}}_3 \cdot \nabla U^{(loc)}(\mathbf{r})}{1 + \frac{A_1}{A_3} e^{ik(\hat{\mathbf{s}}_1 - \hat{\mathbf{s}}_3)\cdot\mathbf{r}} + \frac{A_2}{A_3} e^{ik(\hat{\mathbf{s}}_2 - \hat{\mathbf{s}}_3)\cdot\mathbf{r}}} \Big], \end{aligned} \tag{339}$$

where A_1, A_2, A_3 are the amplitudes and $\hat{\mathbf{s}}_1$, $\hat{\mathbf{s}}_2$, $\hat{\mathbf{s}}_3$, are the directions of incidence of the incident field $U^{(i)}(\mathbf{r})$, given by,

$$U^{(i)}(\mathbf{r}) = A_1 e^{ik\hat{\mathbf{s}}_1\cdot\mathbf{r}} + A_2 e^{ik\hat{\mathbf{s}}_2\cdot\mathbf{r}} + A_3 e^{ik\hat{\mathbf{s}}_3\cdot\mathbf{r}}. \tag{340}$$

Two tri-directional scatterers were designed using the local scattered field given by Eq. (334). The first one is invisible for fields simultaneously incident in the $\hat{\mathbf{s}}_1 = \hat{\mathbf{x}}$, $\hat{\mathbf{s}}_2 = \hat{\mathbf{y}}$, and in the $\hat{\mathbf{s}}_3 = \hat{\mathbf{x}} - \hat{\mathbf{y}}$ directions. The following values were used for the incident fields: $A_1 = 1$, $A_2 = 1$, and $A_3 = 5$. Again, the real part of the scattering potential exhibits inversion symmetry, while its imaginary part has inversion anti-symmetry (Fig. 23). The scattered field for this tri-directionally invisible scatterer is

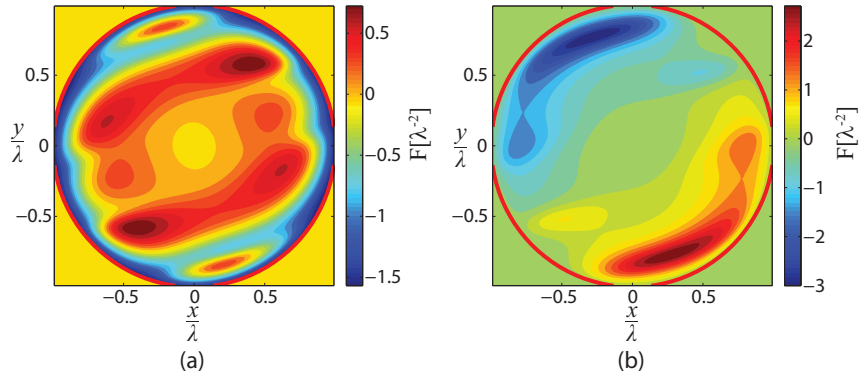

Figure 23: The real (a) and imaginary (b) parts of $F(\mathbf{r})$ (Eq. (339)) with $U^{(loc)}(\mathbf{r})$ (Eq. (334)) with $a = 1$, and $A_1 = 1$, $A_2 = 1$, $A_3 = 5$, $\hat{\mathbf{s}}_1 = \hat{\mathbf{x}}$, $\hat{\mathbf{s}}_2 = \hat{\mathbf{y}}$, and $\hat{\mathbf{s}}_3 = \hat{\mathbf{x}} - \hat{\mathbf{y}}$.

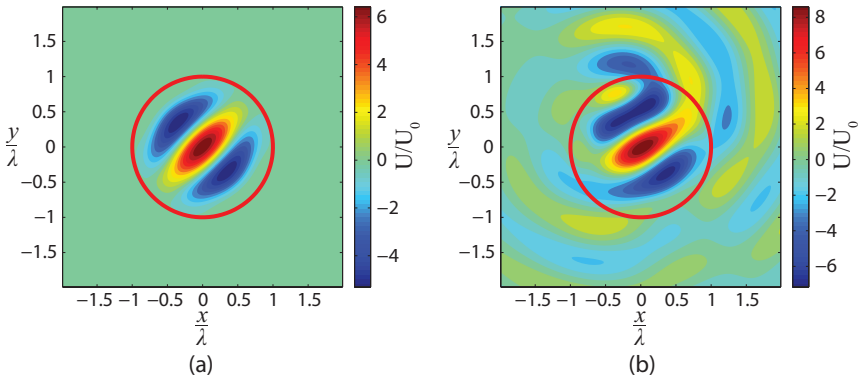

Figure 24: The real part of $U^{(s)}(\mathbf{r})$ with $U^{(i)}(\mathbf{r})$ (Eq. (340)) and (a) $\hat{\mathbf{s}}_2 = \hat{\mathbf{y}}$ (invisibility) or (b) $\hat{\mathbf{s}}_2 = -\hat{\mathbf{y}}$. $F(\mathbf{r})$ is given by Eq. (339) with $a = 1$, $A_1 = 1$, $A_2 = 1$, $A_3 = 5$, $\hat{\mathbf{s}}_1 = \hat{\mathbf{x}}$, $\hat{\mathbf{s}}_2 = \hat{\mathbf{y}}$, and $\hat{\mathbf{s}}_3 = \hat{\mathbf{x}} - \hat{\mathbf{y}}$.

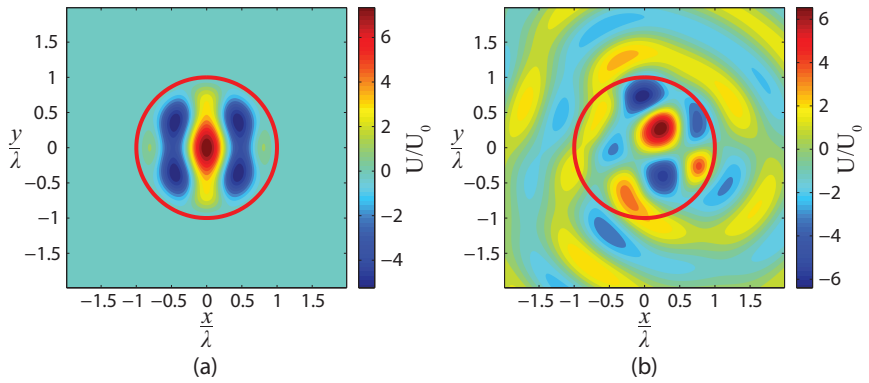

Figure 25: The real part of $U^{(s)}(\mathbf{r})$ for $U^{(i)}(\mathbf{r})$ (Eq. (340)) and (a) $\hat{\mathbf{s}}_3 = -\hat{\mathbf{x}}$ (invisibility) or (b) with $\hat{\mathbf{s}}_3 = -\hat{\mathbf{x}} + \hat{\mathbf{y}}$. $F(\mathbf{r})$ (Eq. (339)) has $a = 1$, $A_1 = 1$, $A_2 = 2$, $A_3 = 5$, $\hat{\mathbf{s}}_1 = \hat{\mathbf{x}}$, $\hat{\mathbf{s}}_2 = \hat{\mathbf{y}}$, and $\hat{\mathbf{s}}_3 = -\hat{\mathbf{x}}$.

shown for when the incident fields are propagating in the invisibility directions (Fig. 24 (a)). When the field in the $\hat{\mathbf{y}}$ direction instead propagates in the $-\hat{\mathbf{y}}$ direction, the scatterer is no longer invisible (Fig. 24 (b)). Such a scatterer can also be designed with counter-propagating pump fields. The second tri-directional nonscattering scatterer is invisible for fields simultaneously incident in the $\hat{\mathbf{s}}_1 = \hat{\mathbf{x}}$, $\hat{\mathbf{s}}_2 = \hat{\mathbf{y}}$, and in the $\hat{\mathbf{s}}_3 = -\hat{\mathbf{x}}$ directions with amplitudes $A_1 = 1$, $A_2 = 2$, and $A_3 = 5$. It is of note that the scattering potential in this case has also the aforementioned inversion symmetry. The real part of the scattered field for this tri-directionally invisible scatterer is shown in Fig. 25 (a) for the case when the incident fields all propagate in the invisibility direction. This shows that it is possible to design directionally invisible scatterers using this method with unequal amplitudes in opposite directions. If the third incident field $\hat{\mathbf{s}}_3 = -\hat{\mathbf{x}} + \hat{\mathbf{y}}$ instead of its given direction, the scatterer no longer is invisible and scatters in response to the incident field (Fig. 25 (b)).

5.3 Summary

Though we have focused in this section on the scalar wave equation for simplicity, the same methods may be applied to electromagnetic waves, as was shown in [29] and as is explored further in Chapter 6. For a non-magnetic material, one uses the vector wave equation for the electric field $\mathbf{E}$,

$$\nabla \times (\nabla \times \mathbf{E}^{(s)}) - k^2 \mathbf{E}^{(s)} = 4\pi \mathbf{F} \cdot \mathbf{E}, \tag{341}$$

where $\mathbf{F}$ is a generally anisotropic scattering potential based on the permittivity. The same conditions for the scalar field in Eq. (330) may be used for the electric field $\mathbf{E}$ to make an invisible object.

The examples given here have a scattering potential that varies continuously in space, something that in practice will be difficult to fabricate. However, because Eq. (331) for the scattering potential depends in a simple way upon the derivatives of the chosen local field, it should be possible to make a more sophisticated choice of $U^{(loc)}$ that will provide a simpler, even piecewise constant, potential. The only conditions that $U^{(loc)}$ must satisfy are continuity of the field and its derivative throughout the volume and Eq. (330) on the boundary, which provides much freedom.

This method could be used to design a variety of novel, directional optical devices, for example, an optically switchable, directionally invisible, optical coupler. It is also possible to imagine an optical lock or switch which will only transmit at the right power and direction if all beams are present at the same time. Such a device might also be combined with an optical detector, designed to detect only a specific incident

field composed of the sum of plane waves. These kinds of devices could also be used to improve efficiency of solar cells and thermophotovoltaic cells, where light incident in a number of directions simultaneously will be transmitted with minimal reflection.

CHAPTER 6: ELECTROMAGNETIC CASE: MAXWELL'S EQUATIONS AND INVISIBILITY

Up to this point, we have only considered scalar nonscattering scatterers. It is possible to make simple devices from one-dimensional models, for example, the unidirectional fiber coupler based on a one-dimensional quantum mechanical model exploiting $\mathcal{PT}$ symmetry applied to optics [58]. However to make the theory more practical, now we extend the "field cloak method" to the electromagnetic vector case to make invisible objects with a wider variety of properties, and thus enable the development of a new class of optical devices. For example, it may be possible to make a device invisible to light of a specific wavelength and polarization. As such a device would have balanced gain/loss, it may be possible to design a whole new class of lossless devices. In this chapter, we demonstrate how to design directionally invisible objects within the framework of the electromagnetic wave equation. Simple examples of directionally invisible objects are shown and verified by numerical simulation. This model may be used to determine the material parameters necessary to realize an invisible object and allows for greater flexibility in selecting which and how many fields may be transmitted perfectly through the object.

6.1 The vector field cloak equation

To apply the field cloak method [29] to the electromagnetic scattering equation, we will assume that the scattered field $\mathbf{E}^{(s)}(\mathbf{r})$ is a function of the incident field $\mathbf{E}^{(i)}(\mathbf{r})$

given by

$$\mathbf{E}^{(s)}(\mathbf{r}) = \overset{\leftrightarrow}{\mathbf{X}}{}^{(loc)}(\mathbf{r}) \cdot \mathbf{E}^{(i)}(\mathbf{r}), \tag{342}$$

where the tensor/dyadic $\overset{\leftrightarrow}{\mathbf{X}}{}^{(loc)}(\mathbf{r})$ is termed the $\mathbf{X}$-factor and each of its spatially varying elements represents a *locally scattered field* with spatially varying elements, each of which must satisfy the nonradiating source conditions at the surface of the scatterer as follows,

$$X_{ij}^{(loc)}(\mathbf{r})\Big|_S = 0, \text{ and } \frac{\partial}{\partial n} X_{ij}^{(loc)}(\mathbf{r})\Big|_S = 0, \text{ where } i,j = x,y,z. \tag{343}$$

Then we can write the total field $\mathbf{E}(\mathbf{r}) = \mathbf{E}^{(i)}(\mathbf{r}) + \mathbf{E}^{(s)}(\mathbf{r})$ in terms of $\overset{\leftrightarrow}{\mathbf{X}}{}^{(loc)}(\mathbf{r})$ given by

$$\mathbf{E}(\mathbf{r}) = \left[\overset{\leftrightarrow}{\mathbf{I}} + \overset{\leftrightarrow}{\mathbf{X}}{}^{(loc)}(\mathbf{r})\right] \cdot \mathbf{E}^{(i)}(\mathbf{r}), \tag{344}$$

where $\overset{\leftrightarrow}{\mathbf{I}}$ is the identity tensor. Substituting Eqs. (342) and (344) into Eq. (177) we obtain

$$\begin{aligned} \nabla \times \left\{ \nabla \times \left[\overset{\leftrightarrow}{\mathbf{X}}{}^{(loc)}(\mathbf{r}) \cdot \mathbf{E}^{(i)}(\mathbf{r}) \right] \right\} - k^2 \overset{\leftrightarrow}{\mathbf{X}}{}^{(loc)}(\mathbf{r}) \cdot \mathbf{E}^{(i)}(\mathbf{r}) \\ = 4\pi \overset{\leftrightarrow}{\mathbf{F}}(\mathbf{r}) \cdot \left\{ \left[\overset{\leftrightarrow}{\mathbf{I}} + \overset{\leftrightarrow}{\mathbf{X}}{}^{(loc)}(\mathbf{r}) \right] \cdot \mathbf{E}^{(i)}(\mathbf{r}) \right\}. \end{aligned} \tag{345}$$

Now we apply $\nabla \times [\nabla \times \mathbf{A}] = \nabla(\nabla \cdot \mathbf{A}) - \nabla^2 \mathbf{A}$ to the left side of Eq. (345) yielding

$$\begin{aligned} \nabla \left\{ \nabla \cdot \left[\overset{\leftrightarrow}{\mathbf{X}}{}^{(loc)}(\mathbf{r}) \cdot \mathbf{E}^{(i)}(\mathbf{r}) \right] \right\} - (\nabla^2 + k^2) \left[\overset{\leftrightarrow}{\mathbf{X}}{}^{(loc)}(\mathbf{r}) \cdot \mathbf{E}^{(i)}(\mathbf{r}) \right] \\ = 4\pi \overset{\leftrightarrow}{\mathbf{F}}(\mathbf{r}) \cdot \left\{ \left[\overset{\leftrightarrow}{\mathbf{I}} + \overset{\leftrightarrow}{\mathbf{X}}{}^{(loc)}(\mathbf{r}) \right] \cdot \mathbf{E}^{(i)}(\mathbf{r}) \right\}. \end{aligned} \tag{346}$$

If we assume the most general case, in which the locally scattered field dyadic

$\overleftrightarrow{\mathbf{X}}^{(loc)}(\mathbf{r})$ has the form

$$\overleftrightarrow{\mathbf{X}}^{(loc)}(\mathbf{r}) = \begin{bmatrix} X_{xx}^{(loc)}(\mathbf{r}) & X_{xy}^{(loc)}(\mathbf{r}) & X_{xz}^{(loc)}(\mathbf{r}) \\ X_{yx}^{(loc)}(\mathbf{r}) & X_{yy}^{(loc)}(\mathbf{r}) & X_{yz}^{(loc)}(\mathbf{r}) \\ X_{zx}^{(loc)}(\mathbf{r}) & X_{zy}^{(loc)}(\mathbf{r}) & X_{zz}^{(loc)}(\mathbf{r}) \end{bmatrix}, \tag{347}$$

and the scattering potential dyadic $\mathbf{F}(\mathbf{r})$ has the form

$$\overleftrightarrow{\mathbf{F}}(\mathbf{r}) = \begin{bmatrix} F_{xx}(\mathbf{r}) & F_{xy}(\mathbf{r}) & F_{xz}(\mathbf{r}) \\ F_{yx}(\mathbf{r}) & F_{yy}(\mathbf{r}) & F_{yz}(\mathbf{r}) \\ F_{zx}(\mathbf{r}) & F_{zy}(\mathbf{r}) & F_{zz}(\mathbf{r}) \end{bmatrix}, \tag{348}$$

it is possible to substitute Eqs. (347) and (348) into Eq. (346) and separate the resulting equation into its vector components. The expression for the $\hat{\mathbf{x}}$ component of the Eq. (346) is

$$\begin{aligned} &\partial_x\partial_y\left(X_{yx}^{(loc)}E_x^{(i)} + X_{yy}^{(loc)}E_y^{(i)} + X_{yz}^{(loc)}E_z^{(i)}\right) \\ &+ \partial_x\partial_z\left(X_{zx}^{(loc)}E_x^{(i)} + X_{zy}^{(loc)}E_y^{(i)} + X_{zz}^{(loc)}E_z^{(i)}\right) \\ &- \left(\partial_y^2 + \partial_z^2 + k^2\right)\left(X_{xx}^{(loc)}E_x^{(i)} + X_{xy}^{(loc)}E_y^{(i)} + X_{xz}^{(loc)}E_z^{(i)}\right) \\ &\qquad = 4\pi\left\{F_{xx}\left[\left(1 + X_{xx}^{(loc)}\right)E_x^{(i)} + X_{xy}^{(loc)}E_y^{(i)} + X_{xz}^{(loc)}E_z^{(i)}\right]\right. \\ &\qquad\quad + F_{xy}\left[X_{yx}^{(loc)}E_x^{(i)} + \left(1 + X_{yy}^{(loc)}\right)E_y^{(i)} + X_{yz}^{(loc)}E_z^{(i)}\right] \\ &\qquad\quad \left. + F_{xz}\left[X_{zx}^{(loc)}E_x^{(i)} + X_{zy}^{(loc)}E_y^{(i)} + \left(1 + X_{zz}^{(loc)}\right)E_z^{(i)}\right]\right\}. \end{aligned} \tag{349}$$

The expression for the $\hat{\mathbf{y}}$ component is given by

$$\begin{aligned}
&\partial_y\partial_x\left(X_{xx}^{(loc)}E_x^{(i)}+X_{xy}^{(loc)}E_y^{(i)}+X_{xz}^{(loc)}E_z^{(i)}\right)\\
&+\partial_y\partial_z\left(X_{zx}^{(loc)}E_x^{(i)}+X_{zy}^{(loc)}E_y^{(i)}+X_{zz}^{(loc)}E_z^{(i)}\right)\\
&-\left(\partial_x^2+\partial_z^2+k^2\right)\left(X_{yx}^{(loc)}E_x^{(i)}+X_{yy}^{(loc)}E_y^{(i)}+X_{yz}^{(loc)}E_z^{(i)}\right)\\
&\qquad=4\pi\left\{F_{yx}\left[\left(1+X_{xx}^{(loc)}\right)E_x^{(i)}+X_{xy}^{(loc)}E_y^{(i)}+X_{xz}^{(loc)}E_z^{(i)}\right]\right.\\
&\qquad\quad+F_{yy}\left[X_{yx}^{(loc)}E_x^{(i)}+\left(1+X_{yy}^{(loc)}\right)E_y^{(i)}+X_{yz}^{(loc)}E_z^{(i)}\right]\\
&\qquad\quad\left.+F_{yz}\left[X_{zx}^{(loc)}E_x^{(i)}+X_{zy}^{(loc)}E_y^{(i)}+\left(1+X_{zz}^{(loc)}\right)E_z^{(i)}\right]\right\}. \qquad (350)
\end{aligned}$$

The expression for the $\hat{\mathbf{z}}$ component is given by

$$\begin{aligned}
&\partial_z\partial_x\left(X_{xx}^{(loc)}E_x^{(i)}+X_{xy}^{(loc)}E_y^{(i)}+X_{xz}^{(loc)}E_z^{(i)}\right)\\
&+\partial_z\partial_y\left(X_{yx}^{(loc)}E_x^{(i)}+X_{yy}^{(loc)}E_y^{(i)}+X_{yz}^{(loc)}E_z^{(i)}\right)\\
&-\left(\partial_x^2+\partial_y^2+k^2\right)\left(X_{zx}^{(loc)}E_x^{(i)}+X_{zy}^{(loc)}E_y^{(i)}+X_{zz}^{(loc)}E_z^{(i)}\right)\\
&\qquad=4\pi\left\{F_{zx}\left[\left(1+X_{xx}^{(loc)}\right)E_x^{(i)}+X_{xy}^{(loc)}E_y^{(i)}+X_{xz}^{(loc)}E_z^{(i)}\right]\right.\\
&\qquad\quad+F_{zy}\left[X_{yx}^{(loc)}E_x^{(i)}+\left(1+X_{yy}^{(loc)}\right)E_y^{(i)}+X_{yz}^{(loc)}E_z^{(i)}\right]\\
&\qquad\quad\left.+F_{zz}\left[X_{zx}^{(loc)}E_x^{(i)}+X_{zy}^{(loc)}E_y^{(i)}+\left(1+X_{zz}^{(loc)}\right)E_z^{(i)}\right]\right\}. \qquad (351)
\end{aligned}$$

As these expressions are fairly complex, let us simplify them by making some assumptions about the scattered and incident field. Once the assumptions are applied, it is possible to break the equations down further by writing them as a set of simultaneous equations. First, let us examine the simpler cases, for example, when the incident field has a single polarization.

Suppose the incident field $\mathbf{E}^{(i)}=E_x^{(i)}\hat{\mathbf{x}}$ (TM), where $E_x^{(i)}=E_{0x}^{(i)}e^{ikz}$ and $E_{0x}^{(i)}$ is a

constant amplitude linearly polarized wave propagating in the $\hat{\mathbf{z}}$ direction and that the domain of the scatterer is in the (x, z) plane. The components of the scattering potential dyadic which are governed by these constraints are given by

$$F_{xx} = -\frac{1}{4\pi}\frac{\partial_z^2 X_{xx}^{(loc)} + 2ik\partial_z X_{xx}^{(loc)}}{1 + X_{xx}^{(loc)}}, \tag{352}$$

$$F_{xy} = 0, \tag{353}$$

$$F_{xz} = \frac{1}{4\pi}\frac{\partial_x\partial_z X_{zx}^{(loc)} + ik\partial_x X_{xz}^{(loc)}}{X_{xz}^{(loc)}}, \tag{354}$$

$$F_{yx} = 0, \tag{355}$$

$$F_{yy} = -\frac{1}{4\pi}\frac{\partial_x^2 X_{yx}^{(loc)} + \partial_z^2 X_{yx}^{(loc)} + 2ik\partial_z X_{yx}^{(loc)}}{X_{yx}^{(loc)}}, \tag{356}$$

$$F_{yz} = 0, \tag{357}$$

$$F_{zx} = \frac{1}{4\pi}\frac{\partial_z\partial_x X_{xx}^{(loc)} + ik\partial_x X_{xx}^{(loc)}}{1 + X_{xx}^{(loc)}}, \tag{358}$$

$$F_{zy} = 0, \tag{359}$$

$$F_{zz} = -\frac{1}{4\pi}\frac{\partial_x^2 X_{zx}^{(loc)} + k^2 X_{zx}^{(loc)}}{X_{zx}^{(loc)}}, \tag{360}$$

and have the same property demonstrated in the scalar case, that they do not depend on the incident field $E_x^{(i)}$ at all. However, with this framework the field can scatter in any direction even if the field is a monochromatic, linearly polarized plane wave. To use this framework for invisibility, it is now necessary to impose conditions on the scattered field. If we assume that the $\mathbf{E}^{(s)}(\mathbf{r})$ obeys Eq. (342) and is $\hat{\mathbf{x}}$-polarized, then several other terms fall out since the scattered field is then defined by $\mathbf{E}^{(s)}(\mathbf{r}) = X_{xx}^{(loc)}(\mathbf{r})E_x^{(i)}(\mathbf{r})$, and therefore only the following elements of the

scattering dyadic would define the scattered field.

$$F_{xx} = -\frac{1}{4\pi}\frac{\partial_z^2 X_{xx}^{(loc)} + 2ik\partial_z X_{xx}^{(loc)}}{1 + X_{xx}^{(loc)}}, \tag{361}$$

$$F_{xy} = 0, \tag{362}$$

$$F_{zx} = \frac{1}{4\pi}\frac{\partial_z\partial_x X_{xx}^{(loc)} + ik\partial_x X_{xx}^{(loc)}}{1 + X_{xx}^{(loc)}}, \tag{363}$$

and the rest of the scattering potential dyadic elements would either be equal to zero or not interact with the incident field. If the local scattered field dyadic elements are subject to the nonradiating source boundary conditions, the scatterer will be invisible for the prescribed direction of incidence.

Suppose the same exercise is performed for an incident field $\mathbf{E}^{(i)}(\mathbf{r}) = E_y^{(i)}\hat{\mathbf{y}} = E_{0y}^{(i)}e^{ikz}\hat{\mathbf{y}}$ (TE). The scatterer exists still in the (x, z) domain. The components of the scattering dyadic which obey these constraints are

$$F_{xx} = -\frac{1}{4\pi}\frac{\partial_z^2 X_{xy}^{(loc)} + 2ikX_{xy}^{(loc)}}{X_{xy}^{(loc)}}, \tag{364}$$

$$F_{xy} = 0, \tag{365}$$

$$F_{xz} = \frac{1}{4\pi}\frac{\partial_x\partial_z X_{zy}^{(loc)} + ik\partial_x X_{zy}^{(loc)}}{X_{zy}^{(loc)}}, \tag{366}$$

$$F_{yx} = 0, \tag{367}$$

$$F_{yy} = -\frac{1}{4\pi}\frac{\left(\partial_x^2 + \partial_z^2\right) X_{yy}^{(loc)} + 2ik\partial_z X_{yy}^{(loc)}}{1 + X_{yy}^{(loc)}}, \tag{368}$$

$$F_{yz} = 0, \tag{369}$$

$$F_{zx} = \frac{1}{4\pi} \frac{\partial_z \partial_x X_{xy}^{(loc)} + ik\partial_x X_{xy}^{(loc)}}{X_{xy}^{(loc)}}, \tag{370}$$

$$F_{zy} = 0, \tag{371}$$

$$F_{zz} = -\frac{1}{4\pi} \frac{\left(\partial_x^2 + k^2\right) X_{zy}^{(loc)}}{X_{zy}^{(loc)}}, \tag{372}$$

and also do not depend on the incident field. The result for F_{yy} is identical to the scalar case (see [29]). Let us further assume that the scattered field is also $\hat{\mathbf{y}}$ polarized (only $X_{yy}^{(loc)} \neq 0$). The components determined by this constraint are

$$F_{yx} = 0, \tag{373}$$

$$F_{yy} = -\frac{1}{4\pi} \frac{(\partial_x^2 + \partial_z^2) X_{yy}^{(loc)} + 2ik\partial_z X_{yy}^{(loc)}}{1 + X_{yy}^{(loc)}}, \tag{374}$$

$$F_{yz} = 0, \tag{375}$$

The other elements of the scattering dyadic are not determined by these constraints and can be arbitrarily chosen.

Since we know how the scattering dyadic is defined when the incident field is composed of one polarization, it is of interest to explore the situation when the incident field consists of two polarizations. For example, suppose that $\mathbf{E}^{(i)}(\mathbf{r}) = E_x^{(i)}\hat{\mathbf{x}} + E_y^{(i)}\hat{\mathbf{y}}$, where $E_x^{(i)} = E_{0x}^{(i)} e^{ikz}$ and $E_y^{(i)} = E_{0y}^{(i)} e^{ikz}$ and that the scatterer exists in the (x, z) plane. The components of the scattering dyadic governed by these

constraints are

$$F_{xx} = -\frac{1}{4\pi}\frac{(\partial_z^2 + k^2)\left(X_{xx}^{(loc)}E_x^{(i)} + X_{xy}^{(loc)}E_y^{(i)}\right)}{\left(1 + X_{xx}^{(loc)}\right)E_x^{(i)} + X_{xy}^{(loc)}E_y^{(i)}}, \tag{376}$$

$$F_{xy} = 0, \tag{377}$$

$$F_{xz} = \frac{1}{4\pi}\frac{\partial_x\partial_z\left(X_{zx}^{(loc)}E_x^{(i)} + X_{xy}^{(loc)}E_y^{(i)}\right)}{X_{zx}^{(loc)}E_x^{(i)} + X_{zy}^{(loc)}E_y^{(i)}}, \tag{378}$$

$$F_{yx} = 0, \tag{379}$$

$$F_{yy} = -\frac{1}{4\pi}\frac{(\partial_x^2 + \partial_z^2 + 2ik\partial_z)\left(X_{yx}^{(loc)}E_x^{(i)} + X_{yy}^{(loc)}E_y^{(i)}\right)}{X_{yx}^{(loc)}E_x^{(i)} + \left(1 + X_{yy}^{(loc)}\right)E_y^{(i)}}, \tag{380}$$

$$F_{yz} = 0, \tag{381}$$

$$F_{zx} = \frac{1}{4\pi}\frac{\partial_z\partial_x\left(X_{xx}^{(loc)}E_x^{(i)} + X_{xy}^{(loc)}E_y^{(i)}\right)}{\left(1 + X_{xx}^{(loc)}\right)E_x^{(i)} + X_{xy}^{(loc)}E_y^{(i)}}, \tag{382}$$

$$F_{zy} = 0, \tag{383}$$

$$F_{zz} = -\frac{1}{4\pi}\frac{(\partial_x^2 + k^2)\left(X_{zx}^{(loc)}E_x^{(i)} + X_{zy}^{(loc)}E_y^{(i)}\right)}{X_{zx}^{(loc)}E_x^{(i)} + X_{zy}^{(loc)}E_y^{(i)}}, \tag{384}$$

Now that we have the general definitions of the scattering potential dyadic elements, we can explore special cases for the scattered field. The special case of invisibility occurs when the the scattered field is zero. Following the previous examples, it is natural to investigate which elements remain if $\mathbf{E}^{(s)}(\mathbf{r}) = X_{xx}^{(loc)}E_x^{(i)}\hat{\mathbf{x}} + X_{yy}^{(loc)}E_y^{(i)}\hat{\mathbf{y}}$. At this point, we may choose which elements the scattering potential or $\overleftrightarrow{\mathbf{X}}^{(loc)}$ should be set to zero to achieve the desired scattered field.

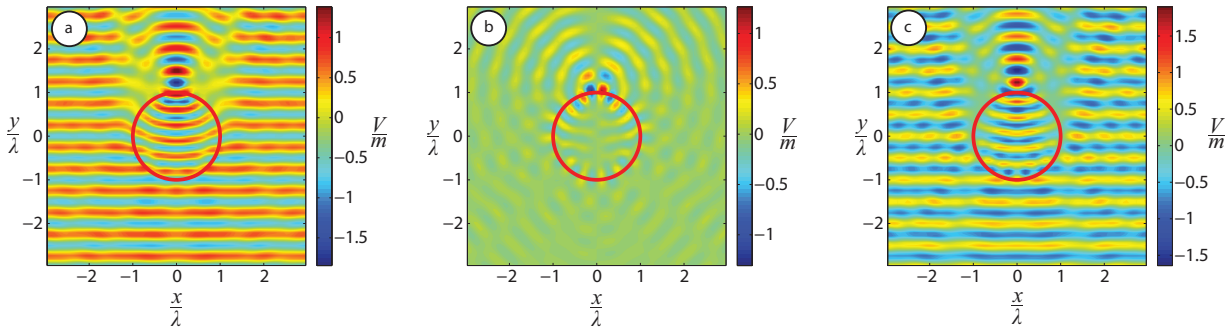

Figure 26: The real parts of the (a) $\hat{\mathbf{x}}$, (b) $\hat{\mathbf{y}}$, and (c) $\hat{\mathbf{z}}$ components of the electric field for a Mie scattering example, where a unit plane wave propagates through a spherical lens with an isotropic dielectric constant $\varepsilon = 2$.

6.2 Example Scatterers

The equations were simulated using a Green's function method similar to the one described in Chapter 4, extended to the electromagnetic case in two dimensions. Simulations in three dimensions did not produce any added information, but the matrix size increases significantly, reducing the resolution of the images. To test the simulation, a circular scatterer with an isotropic constant permittivity of $\overleftrightarrow{\boldsymbol{\varepsilon}} = 2\overleftrightarrow{\mathbf{I}}$ with a diameter equal to four wavelengths of the incident plane wave. The results are shown in Fig. 26. As expected, the ball focuses the light to a spot on the opposite side of the lens and shows the typical cylindrical scattered waves, where the light is not focused.

Next, a scatterer was simulated for the vector case in which one plane wave oriented in the $\hat{\mathbf{z}}$ direction is propagating towards a scatterer located in the xy-plane (Fig. 27). This produced the same fields as in the first example in Chapter 4, Section 4.4. All of the relevant components of $\overleftrightarrow{\mathbf{X}}^{(loc)}(\mathbf{r})$ were the same cosine function used for the

scalar local field in previous examples, $\cos^2\left(\frac{\pi r^2}{2a^2}\right)$. The incident field is

$$\mathbf{E}^{(i)} = E_{0z}^{(i)} e^{ikx} \hat{\mathbf{z}}, \tag{385}$$

and we assume that $\partial_z = 0$ since the field is constant along the $\hat{\mathbf{z}}$ axis. The equations governing the scattering potential are

$$F_{xx} = -\frac{(\partial_y^2 + k^2)(X_{xz}^{(loc)} E_z^{(i)})}{4\pi X_{xz}^{(loc)} E_z^{(i)}}, \tag{386}$$

$$F_{xy} = \frac{\partial_x \partial_y X_{yz}^{(loc)} E_z^{(i)}}{X_{yz}^{(loc)} E_z^{(i)}}, \tag{387}$$

$$F_{xz} = 0, \tag{388}$$

$$F_{yx} = \frac{\partial_y \partial_x (X_{xz}^{(loc)} E_z^{(i)})}{4\pi X_{xz}^{(loc)} E_z^{(i)}}, \tag{389}$$

$$F_{yy} = -\frac{(\partial_x^2 + k^2)(X_{yz}^{(loc)} E_z^{(i)})}{4\pi X_{yz}^{(loc)} E_z^{(i)}}, \tag{390}$$

$$F_{yz} = 0, \tag{391}$$

$$F_{zx} = 0, \tag{392}$$

$$F_{zy} = 0, \tag{393}$$

$$F_{zz} = -\frac{1}{4\pi} \frac{(\partial_x^2 + \partial_y^2 + k^2)(X_{zz}^{(loc)} E_z^{(i)})}{(1 + X_{zz}^{(loc)}) E_z^{(i)}} \tag{394}$$

The last component of the scattering potential is identical to the expression for the scalar case. Since the scattered field in Fig. 27(b) is confined to the domain of the scatterer and the total field is a plane wave outside of the scatterer, this scatterer is indeed invisible for that direction of incidence.

Another example of a scatterer with an incident field propagating in the plane of

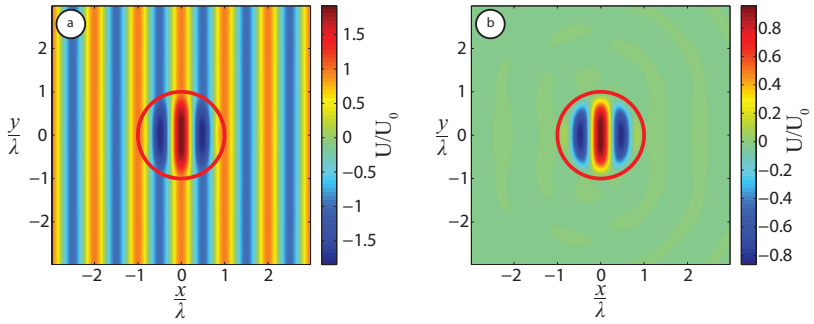

Figure 27: The real parts of the $\hat{\mathbf{z}}$ component of the (a) total electric field and (b) scattered field when the object is invisible to an incident field in the $\hat{\mathbf{y}}$ direction.

the scatterer was also demonstrated. The incident field is

$$\mathbf{E}^{(i)} = E_{0y}^{(i)} e^{ikx} \hat{\mathbf{y}}. \tag{395}$$

The scattering potential is

$$F_{xx} = -\frac{1}{4\pi} \frac{(\partial_y^2 + k^2) X_{xy}^{(loc)}}{X_{xy}^{(loc)}}, \tag{396}$$

$$F_{xy} = \frac{\partial_x \partial_y X_{yy}^{(loc)} + ik\partial_y X_{yy}^{(loc)}}{4\pi(1 + X_{yy}^{(loc)})}, \tag{397}$$

$$F_{xz} = 0, \tag{398}$$

$$F_{yx} = \frac{\partial_y \partial_x X_{xy}^{(loc)} + ik\partial_y X_{xy}^{(loc)}}{4\pi X_{xy}^{(loc)}}, \tag{399}$$

$$F_{yy} = -\frac{1}{4\pi} \frac{\partial_x^2 X_{yy}^{(loc)} + 2ik\partial_x X_{yy}^{(loc)}}{1 + X_{yy}^{(loc)}}, \tag{400}$$

$$F_{yz} = 0, \tag{401}$$

$$F_{zx} = 0, \tag{402}$$

$$F_{zy} = 0, \tag{403}$$

$$F_{zz} = irrelevant. \tag{404}$$

The in-plane scattering is shown in Fig. 28. The scattered field is confined to the

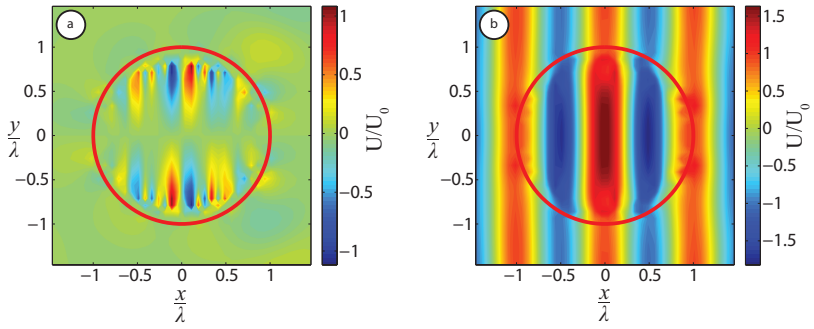

Figure 28: The real part of the (a) $\hat{\mathbf{x}}$ component and (b) $\hat{\mathbf{y}}$ component of the total electric field is shown for an incident field propagating in the horizontal direction $\hat{\mathbf{x}}$ direction.

domain of the scatterer. Therefore this scatterer is invisible to that field.

6.3 The connection between EM nonradiating sources and directional scatterers

The field cloak method may be applied to any of the wave equations derived in Chapter 3. In Chapter 2 if one field was designed to be a null-field, the remaining fields would not be capable of propagating outside of the scatterer. Therefore, it follows that if any of the scattering equations satisfy the conditions of the field cloak method, the other fields should also be invisible. Since it is an exact solution to the vector wave equation, there is the possibility that such scatterers could be realized. Fortunately, the values of the refractive index fluctuate around $n = 1$, which is equivalent to air, and is therefore within the realm of possibility. The almost perfectly transparent $\mathcal{PT}$-symmetric optical fiber (Chapter 4) [58] had an imaginary part that was approximately 4% of the real part of the refractive index and was designed with scalar theory. Design of materials to implement this theoretical approach involves three logical steps. First, a scattering potential is chosen that satisfies the invisibility conditions, $\overleftrightarrow{\mathbf{F}}(\overleftrightarrow{\mathbf{X}}^{(loc)}(\mathbf{r}))$. Next, the scattering potential as a function of the locally

scattered field tensor is equated with the scattering potential as a function of the material parameters, for example

$$\overleftrightarrow{\mathbf{F}}(\overleftrightarrow{\mathbf{X}}^{(loc)}(\mathbf{r})) = \frac{k^2}{4\pi}\left[\overleftrightarrow{\boldsymbol{\varepsilon}}(\mathbf{r}) - \overleftrightarrow{\mathbf{I}}\right]. \tag{405}$$

Finally, a new set of equations may be derived to solve for the functions determining the permittivity (and/or permeability with another scattering potential) that the elements must satisfy. There is also a lot of flexibility regarding which form the material parameters may take–for example, whether they are scalar or in tensor form, isotropic or anisotropic. Furthermore, these directionally invisible objects may be designed to be invisible for any type or number of incident fields, and a sum of incident fields, as illustrated in Chapter 5, could just as easily be put into this framework to derive a different scattering potential.

CHAPTER 7: CONCLUSION

There are two classes of invisible objects, nonradiating sources and nonscattering scatterers. Nonradiating sources are primary radiation sources that do not radiate outside of their domain of support. Nonscattering scatterers neither scatter nor absorb radiation and behave as if no object were present. In this work, we have extended the theory of monochromatic, invisible objects. We have developed a few different ways of constructing invisible objects, beginning with the earliest form of a nonradiating source and ending with the extension of the field cloak method to design a directionally invisible scatterer.

The earliest prescription for a nonradiating source by Paul Ehrenfest showed that if the magnetic field $\mathbf{H}$ is set to zero, the radiation of the source is confined to its domain of support. Therefore it does not radiate and is invisible. Here we extended this theory and demonstrated that any of the other fields may be selectively set to zero (null), resulting in a null-field nonradiating source. This was achieved by rewriting Maxwell's equations in terms of the polarization and magnetization and setting the resulting wave equations equal to zero. By framing the problem in this manner, we may draw a parallel between nonradiating sources and directionally invisible scatterers.

A primary source of polarization and magnetization is mathematically equivalent to a scattering object with spatially-varying permittivity and permeability excited by an electromagnetic wave; the fields produced by the primary source are equivalent to

the scattered fields produced by the interaction. A null-field radiationless source is then equivalent to a scattering object that produces no scattered field. We exploit this equivalence between null-field nonradiating sources and nonscattering scatterers to derive wave equations for each of the four macroscopic fields, **E**, **H**, **B**, and **D**, in terms of a scattering potential or tensor operator and the permittivity and permeability, expanding the ways in which the scattering problem may be expressed and, consequently, solved in different ways. These equations are valid for scatterers whether or not they are invisible.

The field cloak method, applying to the scalar scattering equation the nonradiating source boundary conditions to the scattered field, provides for the first time a path to design directionally invisible objects without any approximation, which we have demonstrated. Scatterers with both $\mathcal{PT}$-symmetric scattering potentials and those without any symmetry whatsoever were designed and examined. The resulting scattering potentials had the remarkable property that they only depend on the locally scattered field and are independent of the incident field. First, it was shown that the ultimate condition for a scatterer to be $\mathcal{PT}$-symmetric is that only the scattering potential be $\mathcal{PT}$ symmetric and not the refractive index, as was previously thought. We also demonstrated that it is possible to design directionally invisible objects with scattering potentials that possess no symmetry at all, which was a controversial result at the time.

When $\mathcal{PT}$ symmetry was first applied to optics, it was thought that a necessary condition for the directional invisibility of an object was $\mathcal{PT}$ symmetry. Consequently, it became unclear what the origin of directional invisibility is in these scatterers. Here,

we answer that question definitively by proving that the boundary conditions applied to the scattering equation are responsible for the directional invisibility of the object and not the symmetry of the scattering potential. This is because the application of the boundary conditions to the integral defining the scattering and extinction cross-sections causes that integral to be zero.

The field cloak method was then extended within the scalar wave equation to account for an incident field composed of a sum of plane waves, each with its own direction and amplitude. This resulted in the design of scatterers that are simultaneously invisible to multiple plane waves. Under certain conditions, the scattering potential is inversion symmetric, and $\mathcal{PT}$-symmetry is the special case of that for a uni-directionally invisible object. This enables a whole new host of optically switchable, directionally invisible scatterers and devices, such as couplers, switches, and sensors, which may be controlled by adjusting the amplitude or the direction of one of the incident plane waves.

Finally, the field cloak method was extended to the electromagnetic wave equation by creating a tensor of locally scattered fields, each of which may be arbitrarily chosen and is subject to same boundary conditions. The resulting directionally invisible objects could be designed to be invisible for $\hat{\mathbf{x}}$ or $\hat{\mathbf{y}}$ polarized incident fields. It turns out that the expressions or $\hat{\mathbf{x}}$ and $\hat{\mathbf{y}}$ are independent of each other, so that these objects may be directionally invisible to incident fields with both polarizations simultaneously present. In other words, they are polarization independent. These directionally invisible scatterers may be designed to be two or three-dimensional, although here only the two-dimensional versions were demonstrated. In our examples,

we applied the field cloak method to electric field **E**, however this method may be applied to cancel any of the other macroscopic fields. Essentially, if one of the fields is canceled, the others collapse because of their interdependence.

Another pathway for future research could entail matching material permitivity and permeability to satisfy the functions chosen for the locally scattered field tensor. It is also straightforward to design electromagnetic scatterers that are directionally invisible for multiple plane waves simultaneously. The field cloak method applied to the electromagnetic vector wave equation offers unprecedented flexibility in types of invisible objects that may be theoretically designed. Because the boundary conditions guarantee balanced gain and loss, this technique enables the design of a whole new class of theoretically lossless devices, in which both the incident field and the scattered field may be chosen, as long as the set of simultaneous equations are satisfied.

It seems unlikely that null-field scattering objects can be produced by the techniques of transformation optics for the following reason. To design an invisible object using transformation optics or conformal mapping, the material parameters are expanded from a line or a point into a cloaked space through a coordinate-transformation, resulting in an invisible object with a cloaked region (within which the fields are zero). Therefore it would be very difficult to selectively render one or more of the fields zero. In contrast, with this approach we work with the field equations to selectively render one or more of the fields zero, and then we may calculate the material parameters. It is important to note that rendering one of the fields zero, confines the other fields to the domain of the nonradiating source, if so desired.

The existence of null-field sources, therefore, indicates that the class of invisible

and cloaked objects is broader than previously realized. In addition, the invisibility solutions in transformation optics require the permittivity to be equal to the permeability and for both to be equal to zero. This is not the case for our directionally invisible objects. When the refractive index or the permittivity is calculated from the scattering potential, it fluctuates around unity, the value of air in free space. Recently, a material with a permittivity of 1.025 has been experimentally realized [68], and therefore it is not outside the realm of possibility that such directionally invisible objects might also be experimentally realized. Moreover, depending on the definition of the scattering potential, the permittivity and the permeability do not need to be equal. In our example, the permeability is unity and only the permittivity is defined according the vector wave equation used to the derive the scattering potential tensor. Therefore, this technique broadens the types of invisible objects that may exist and provides a pathway for the design of novel balanced gain/loss optical devices.

REFERENCES

[1] N. G. Alexopoulos and N. K. Uzunoglu. Electromagnetic scattering from active objects: invisible scatterers. *Appl. Opt.*, 17(2):235–239, Jan 1978.

[2] B. Baker and E. T. Copson. *The Mathematical Theory of Huygens' Principle.* Chelsea Publishing Co., New York, NY, 2 edition, 1987.

[3] C. Bender and S. Boettcher. Real spectra in Non-Hermitian Hamiltonians Having $\mathscr{P}\mathscr{T}$ symmetry. *Phys. Rev. Lett.*, 80:5243–5246, Jun 1998.

[4] C. M. Bender. Introduction to $\mathcal{PT}$-symmetric quantum theory. *Contemp. Phys.*, 46(4):277–292, 2005.

[5] C. M. Bender. $\mathcal{PT}$-symmetric quantum theory. *Journal of Physics: Conference Series*, 631(1):012002, 2015.

[6] J. V. Bladel. On the equivalence of electric and magnetic currents. *Archiv für Elektronik und Übertragungstechnik*, 42:314–315, 1988.

[7] N. Bleistein and J. K. Cohen. Nonuniqueness in the inverse source problem in acoustics and electromagnetics. *Journal of Mathematical Physics*, 18(2):194–201, 1977.

[8] D. Bohm and M. Weinstein. The self-oscillations of a charged particle. *Phys. Rev.*, 74:1789–1798, Dec 1948.

[9] M. Born and E. Wolf. *Principles of Optics.* Cambridge University Press, 7 edition, 1999.

[10] Bricard, J. Lumire diffuse en avant par une goutte d'eau sphrique. *J. Phys. Radium*, 4(4):57–66, 1943.

[11] S. Carney. *Optical Theorems in Statistical Wavefields with Applications.* PhD thesis, The University of Rochester, Rochester, New York, 1999.

[12] L. DeBroglie. Recherches sur la théorie des quanta. *Annales de la Physique*, 3:22–128, 1925.

[13] A. Devaney. The inverse problem for random sources. *Journal of Mathematical Physics*, 20:1687–1691, 1979.

[14] A. Devaney and E. Wolf. Nonradiating stochastic scalar sources. In L. Mandel and E. Wolf, editors, *Coherence and Quantum Optics V*, pages 417–421. New York: Plenum Press, 1984.

[15] A. J. Devaney. Nonuniqueness in the inverse scattering problem. *Journal of Mathematical Physics*, 19(7):1526–1531, 1978.

[16] A. J. Devaney and E. Wolf. Radiating and nonradiating classical current distributions and the fields they generate. *Phys. Rev. D*, 8:1044–1047, Aug 1973.

[17] P. Ehrenfest. Ungleichförmige elektrizitätsbewegungen ohne magnet- und strahlungsfeld. *Physik unserer Zeit*, 11:708–709, 1910.

[18] R. El-Ganainy, K. G. Makris, D. N. Christodoulides, and Z. H. Musslimani. Theory of coupled optical PT-symmetric structures. *Opt. Lett.*, 32(17):2632–2634, Sep 2007.

[19] K. M. Evenson, J. S. Wells, F. R. Petersen, B. L. Danielson, G. W. Day, R. L. Barger, and J. L. Hall. Speed of light from direct frequency and wavelength measurements of the methane-stabilized laser. *Phys. Rev. Lett.*, 29:1346–1349, Nov 1972.

[20] E. Feenberg. The scattering of slow electrons by neutral atoms. *Phys. Rev.*, 40:40–54, Apr 1932.

[21] L. Feng, Y.-L. Xu, W. Fegadolli, M.-H. Lu, J. Oliveira, V. Almeida, Y.-F. Chen, and A. Scherer. Experimental demonstration of a unidirectional reflectionless parity-time metamaterial at optical frequencies. *Nature Materials*, 12:108–113, 2013.

[22] F. Friedlander. An inverse problem for radiation fields. *Proc. London Math. Soc.*, s3-27:551–576, October 1973.

[23] G. S. F.R.S. Lix. the electromagnetic field of a moving uniformly and rigidly electrified sphere and its radiationless orbits. *The London, Edinburgh, and Dublin Philosophical Magazine and Journal of Science*, 15(100):752–761, 1933.

[24] G. S. F.R.S. The uniform circular motion with invariable normal spin of a rigidly and uniformly electrified sphere, iv. *Proceedings of the Royal Society of London A: Mathematical, Physical and Engineering Sciences*, 159(899):570–591, 1937.

[25] A. Gamliel, K. Kim, A. I. Nachman, and E. Wolf. A new method for specifying nonradiating, monochromatic, scalar sources and their fields. *J. Opt. Soc. Am. A*, 6(9):1388–1393, Sep 1989.

[26] G. Gbur. Uniqueness of the solution to the inverse source problem for quasi-homogeneous problems. *Optical Communications*, 187:301–309, 2001.

[27] G. Gbur. Chapter 5 nonradiating sources and other ?invisible? objects. In E. Wolf, editor, *Progress in Optics*, volume 45, pages 273–315. Elsevier, 2003.

[28] G. Gbur. Invisibility physics: Past, present, and future. In E. Wolf, editor, *Progress in Optics*, volume 58 of *Progress in Optics*, pages 65 – 114. Elsevier, 2013.

[29] G. Gbur. Designing directional cloaks from localized fields. *Opt. Lett.*, 40(6):986–989, Mar 2015.

[30] G. J. Gbur. *Mathematical Methods for Optical Physics and Engineering*. Cambridge University Press, 1 edition, 2011.

[31] G. H. Goedecke. Classically radiationless motions and possible implications for quantum theory. *Phys. Rev.*, 135:B281–B288, Jul 1964.

[32] D. J. Griffiths. *Introduction to Electrodynamics*. Pearson, 4 edition, 2013.

[33] B. Hoenders and H. Baltes. The scalar theory of nonradiating partially coherent sources. *Lettere al Nuovo Cimento*, 23(7):206–208, 1979.

[34] H. V. D. Hulst. On the attenuation of plane waves by obstacles of arbitrary size and form. *Physica*, 15(8):740 – 746, 1949.

[35] E. Hurwitz and G. Gbur. Null-field radiationless sources. *Opt. Lett.*, 39(22):6529–6532, Nov 2014.

[36] E. Hurwitz and G. Gbur. Localized $\mathcal{PT}$-symmetric directionally invisible scatterers. *Phys. Rev. A*, 93:041803, Apr 2016.

[37] E. Hurwitz and G. Gbur. Optically switchable directional invisibility. *Opt. Lett.*, 42(7):1301–1304, Apr 2017.

[38] J. D. Jackson. *Classical Electrodynamics*. John Wiley & Sons, Inc, 2 edition, 1975.

[39] J. Jeans. On the constitution of the atom. *Philosophical Magazine*, 11:604–607, 1906.

[40] T. Jevremovic. *Atomic Theory*, chapter 2. Springer Science+Business Media, 2 edition, 2009.

[41] M. Kerker. Invisible bodies. *J. Opt. Soc. Am.*, 65(4):376–379, Apr 1975.

[42] M. Kerker. Electromagnetic scattering from active objects. *Appl. Opt.*, 17(21):3337–3339, Nov 1978.

[43] I. J. LaHaie. Inverse source problem for three-dimensional partially coherent sources and fields. *J. Opt. Soc. Am. A*, 2(1):35–45, Jan 1985.

[44] S.-W. Lee, J. Boersma, C.-L. Law, and G. A. Deschamps. Singularity in green's function and its numerical evaluation. *Antennas and Propagation, IEEE Transactions on*, 28(3):311–317, May 1980.

[45] P. Lenard. Über die absorption der kathodenstrahlen verschiedener geschwindigkeit. *Annale der Physik*, 12:714–744, 1904.

[46] U. Leonhardt. Optical conformal mapping. *Science*, 312(5781):1777–1780, 2006.

[47] Z. Lin, H. Ramezani, T. Eichelkraut, T. Kottos, H. Cao, and D. N. Christodoulides. Unidirectional invisibility induced by $\mathcal{PT}$-symmetric periodic structures. *Phys. Rev. Lett.*, 106:213901, May 2011.

[48] K. G. Makris, R. El-Ganainy, D. N. Christodoulides, and Z. H. Musslimani. Beam dynamics in $\mathcal{PT}$ symmetric optical lattices. *Phys. Rev. Lett.*, 100:103904, Mar 2008.

[49] O. J. F. Martin and N. B. Piller. Electromagnetic scattering in polarizable backgrounds. *Phys. Rev. E*, 58:3909–3915, Sep 1998.

[50] F. Monticone and A. Alù. Embedded photonic eigenvalues in 3d nanostructures. *Phys. Rev. Lett.*, 112:213903, May 2014.

[51] H. Nagaoka. Kinetics of a system of particles illustrating the line and the band spectrum and the phenomenon of radioactivity. *Philosophical Magazine*, 7:445–455, 1904.

[52] N. K. Nikolova and Y. S. Rickard. Nonradiating electromagnetic sources in a nonuniform medium. *Phys. Rev. E*, 71:016617, Jan 2005.

[53] J. Pendry, D. Smith, and D. Schurig. Electromagnetic cloaking method, July 2006. US11459728.

[54] J. B. Pendry. Negative refraction makes a perfect lens. *Phys. Rev. Lett.*, 85:3966–3969, Oct 2000.

[55] J. B. Pendry, D. Schurig, and D. R. Smith. Controlling electromagnetic fields. *Science*, 312(5781):1780–1782, 2006.

[56] N. B. D. phil. Xxxvii. on the constitution of atoms and molecules. *Philosophical Magazine Series 6*, 26(153):476–502, 1913.

[57] A. Regensburger, C. Bersch, M.-A. Miri, G. Onishchukov, D. N. Christodoulides, and U. Peschel. Parity-time synthetic photonic lattices. *Nature*, 488:167–171, 2012.

[58] C. Rüter, K. Makris, R. El-Ganainy, D. Christodoulides, M. Segev, and D. Kip. Observation of parity-time symmetry in optics. *Nature Physics*, 6(3):192–195, 2010.

[59] E. Rutherford. Scattering of α and β particles by matter. *Philosophical Magazine*, 21:669–688, 1911.

[60] E. Schroedinger. An undulatory theory of the mechanics of atoms and molecules. *The Physical Review*, 28(6):1049–1070, 1926.

[61] M. G. Silveirinha. Trapping light in open plasmonic nanostructures. *Phys. Rev. A*, 89:023813, Feb 2014.

[62] A. Sommerfeld. Zur elektronentheorie. i. allgemeine untersuchung des feldes eines belibig bewegten elektrons. *Nachrichten von der Gesellschaft der Wissenschaften zu Göttingen, Mathematisch-Physikalische Klasse*, 1904:99–130, 1904.

[63] A. Sommerfeld. Zur elektronentheorie. ii. grundlagen für eine allgemeine dynamik des elektrons. *Nachrichten von der Gesellschaft der Wissenschaften zu Göttingen, Mathematisch-Physikalische Klasse*, 1904:363–439, 1904.

[64] D. L. Sounas, R. Fleury, and A. Alù. Unidirectional cloaking based on metasurfaces with balanced loss and gain. *Phys. Rev. Applied*, 4:014005, Jul 2015.

[65] J. Thomson. On the structure of the atom: an investigation of the stability and periods of oscillation of a number of corpuscles arranged at equal intervals around the circumference of a circle; with application of the results to the theory of atomic structure. *Philosophical Magazine*, 7:237–265, 1904.

[66] V. G. Veselago. The electrodynamics of substances with simultaneously negative values of ε and μ. *Soviet Physics Uspekhi*, 10(4):509, 1968.

[67] E. Wolf and T. Habashy. Invisible bodies and uniqueness of the inverse scattering problem. *Journal of Modern Optics*, 40(5):785–792, 1993.

[68] X. A. Zhang, A. Bagal, E. C. Dandley, J. Zhao, C. J. Oldham, B.-I. Wu, G. N. Parsons, and C.-H. Chang. Ordered 3d thin-shell nanolattice materials with near-unity refractive indices. *Advanced Functional Materials*, 25(42):6644–6649, 2015.

[69] X. Zhu, L. Feng, P. Zhang, X. Yin, and X. Zhang. One-way invisible cloak using parity-time symmetric transformation optics. *Opt. Lett.*, 38(15):2821–2824, Aug 2013.